NASA Tech Briefs

National Aeronautics and
Space Administration
January 1987
Volume 11 Number 1

Marshall Space Flight Center:
Propelling NASA into the Future

In space: looking back to look forward.

What can the nature and origin of the universe tell us about the future of Earth? To help answer that question, we make craft and instruments for traveling billions of miles in space and seeing as far as 15 billion years back in time. Martin Marietta was the integrator and builder of two Viking landers, which sent back remarkable photos of the surface of Mars, examined soil samples, and studied Martian weather and seismic activity. For the Voyagers we provided instrumentation that reported on electromagnetic activity near Jupiter and Saturn–Voyager 2 went on to Uranus, some 2 billion miles from Earth. That was nine years after launch; next destination, Neptune, in 1989. These are but a few results of Martin Marietta's ability to create survivable, mystery-solving craft and their instruments–from concept through mission completion.

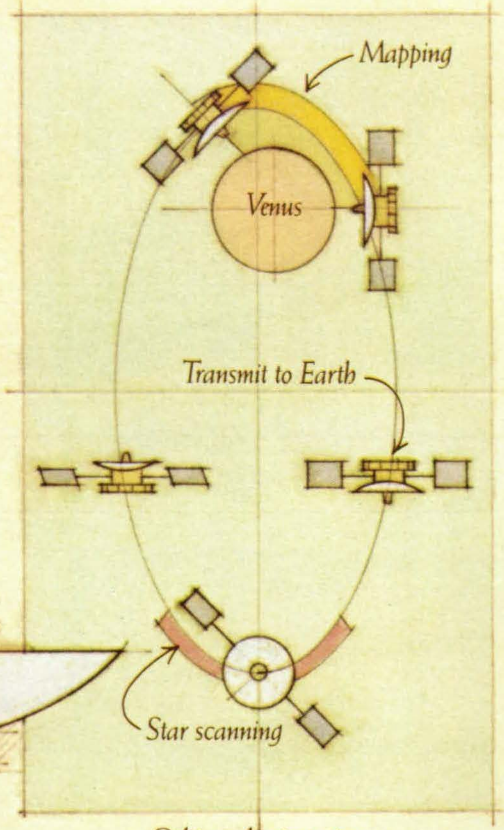

Orbit and orientation

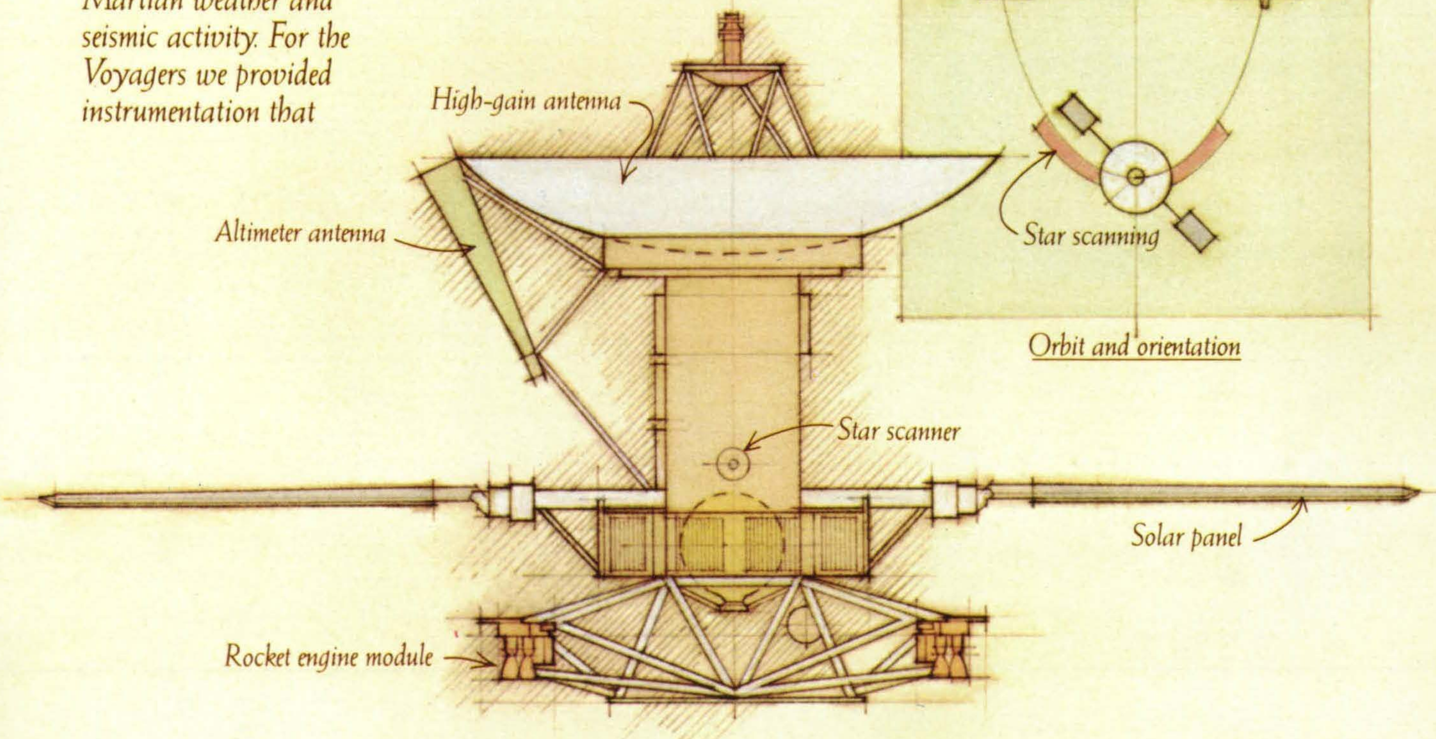

Magellan Spacecraft

Mission: map Venus.

From orbit, Magellan's radar will penetrate the planet's thick, gaseous cloud cover and send back photo-like images of nearly 90% of its surface. Our role: design, integrate, build and test the craft.

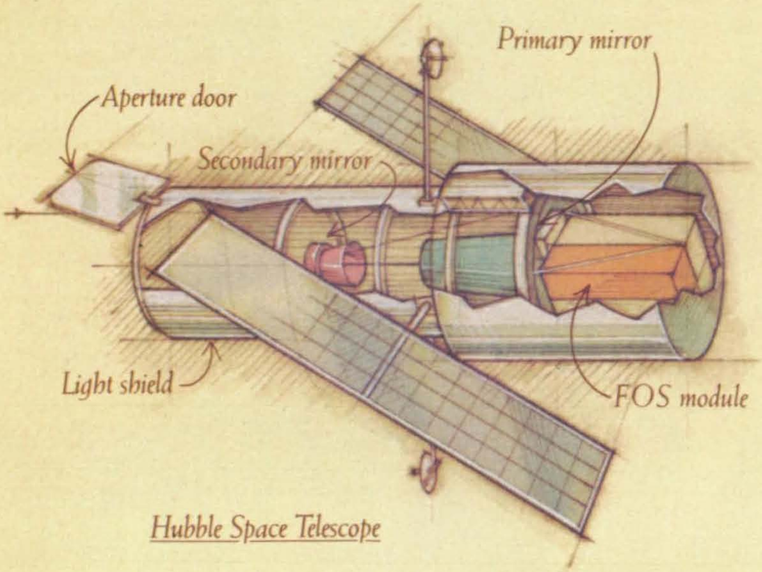

Hubble Space Telescope

Viewing the infant universe.

For the Hubble Space Telescope we are providing the Faint Object Spectrograph (FOS), which will see objects up to 15 billion light-years away. Since the universe is estimated to be 18-20 billion years old, astronomers will witness events close to its birth.

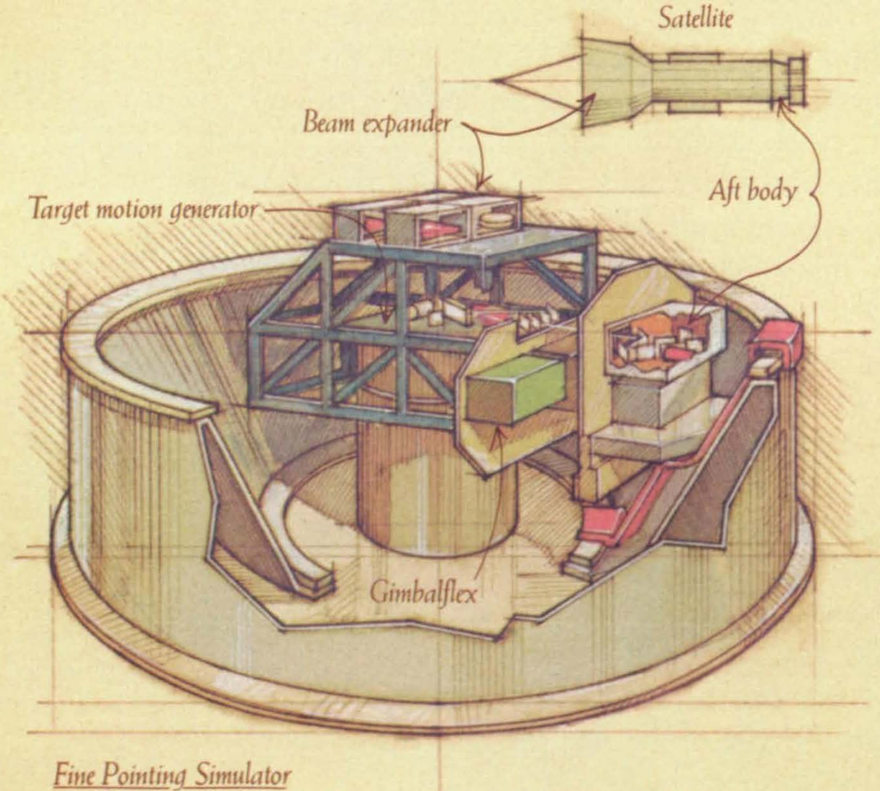

Fine Pointing Simulator

The fine points of fine pointing.

Precisely controlled, space-spanning energy delivery and collection systems create difficult pointing and retargeting challenges, which we can now simulate. This new lab is working toward the precision to zero in on a football-size object 3,000 miles away, in support of the Strategic Defense Initiative research program.

NASA Tech Briefs

National Aeronautics and
Space Administration

JANUARY 1987
Volume 11 Number 1

ABP BPA

Special Features and Departments

Before thermal vacuum tests, the Hubble Space Telescope was surrounded by a Lockheed-built solar simulator. 1800 quartz lamps were divided into computer controlled zones to simulate nighttime, daytime, hot and cold orbits. Information on other programs managed by Marshall begins on page 10.

Color coded by brightness level, the sun's corona was photographed by the Skylab space station's Apollo Telescope Mount. NASA's Marshall Space Flight Center coordinated the eight instrument solar observatory, which collected more than 150,000 exposures of the sun during its nine month operation.

Technical Section Thumb Index

Thumb Index Technical Section

NASA Tech Briefs, ISSN 0145-319X, copyright © 1987 in U.S., is published monthly except July/August and November/December (10x per year) by Associated Business Publications Co., 41 E. 42nd St., New York, NY 10017-5391. The copyrighted information does not include the individual Tech Briefs which are supplied by NASA. Editorial, sales, production and circulation offices at 41 E. 42nd Street, New York, NY 10017-5391. Subscriptions for non-qualified subscribers in the U.S., Panama Canal Zone, and Puerto Rico, $75.00 for 1 year; $125.00 for 2 years; $200 for 3 years. Single copies $15.00. Remit by check, draft, postal or express orders. Other remittances at sender's risk. Address all communications for subscriptions or circulation to NASA Tech Briefs, 41 E. 42nd Street, New York, NY 10017-5391. Application to mail at second-class postage rates is pending at New York, NY 10017 and additional mailing offices.

POSTMASTER: please send address changes to NASA Tech Briefs, 41 E. 42nd Street, Suite 921, New York, NY 10017-5391.

NASA Tech Briefs

National Aeronautics and Space Administration

NASA Tech Briefs:

Published by .... **Associated Business Publications**
Editor-in-Chief/Publisher .... **Bill Schnirring**
Associate Publisher .... **Frank Nothaft**
Managing Editor .... **R.J. Laer**
Associate Editor .... **Leo D. Kluger**
Technical Advisor .... **Dr. Robert E. Waterman**
Art Director .... **Melanie Gottlieb**
Assistant Art Director .... **Michelle Schmitz**
Production Manager .... **Rita Nothaft**
Traffic Manager .... **J.T. Pramberger**
Circulation Manager .... **Anita Weissman**
Fulfillment Manager .... **Elizabeth Kuzio**
Controller .... **Neil B. Rose**

Technical Staff:

Briefs prepared for National Aeronautics and Space Administration by **Logical Technical Services Corp.**, NY, NY
Technical Editor .... **Ted Selinsky**
Art Director .... **Ernest Gillespie**
Managing Editor .... **Theron Cole, Jr.**
Administrator .... **Elizabeth Texeira**
Chief Copy Editor .... **Joe Renzler**
Staff Editors .... **James Boyd, Larry Grunberger, Jordan Randjelovich, George Watson**
Graphics .... **Luis Martinez, Huburn Profitt**
Editorial & Production .... **Lorne Bullen, Bill Little, Frank Ponce, Ivonne Valdes**

NASA:

NASA Tech Briefs are provided by the National Aeronautics and Space Administration, Technology Transfer Division, Washington, DC:
Administrator .... **Dr. James C. Fletcher**
Assistant Administrator for Commercial Programs ... **Isaac T. Gillam IV**
Director Technology Utilization Division ... **Henry J. Clarks**
Publications Manager .... **Leonard A. Ault**

Associated Business Publications
41 East 42nd Street, Suite 921
New York, NY 10017-5391
(212) 490-3999
President .... **Bill Schnirring**
Executive Vice President .... **Frank Nothaft**
Vice President .... **John K. Abely**

Advertising:

New York Office: (212) 490-3999
Sales Manager .... **Robin DuCharme**
Account Executive .... **Dick Soule**
Account Executive .... **Carol-Lynne Cox**
Account Executive .... **Fred Bousquet**
Advertising Assistant .... **Erving Dockery, Jr.**

Los Angeles Office: (213) 477-5866

ABP

BPA

Circle Reader Action No. 413

Editorial Notebook

A very few events will live with you for the rest of your life. Over time you may forget the day of the week, the date, and even the year it happened, but you'll always remember where you were and when you heard the news.

Three of us were in a rented car, heading towards Pasadena, California, to Jet Propulsion Laboratories. We were doing an article on JPL as part of our series on NASA field centers. We had timed our visit to coincide with the day that Voyager 2 would be at its closest point to Uranus.

I was studying a few notes in the front seat, sipping my coffee and just half-listening to the radio as my colleague drove. It was January 28, 1986, 8:38 in the morning, and we were listening to the *Challenger* launch as we pulled off the freeway and headed to JPL.

That was just one short year ago. The change has been enormous in these subsequent twelve months. Morale throughout the agency suffered. It was as if the nation collectively discovered that the father they had always idolized was a mere mortal, a human being. NASA wasn't populated by a race of giants after all.

You don't have to be a giant to stand tall. The people I know at NASA have done just that. They're concentrating, stretching, and getting the job done.

Our visit to Marshall Space Flight Center in Huntsville, Alabama for the final installment of our series on the nine NASA field centers, brought this home all over again. We didn't know what we'd find.

What we found was a Phoenix. There was a spring in peoples' steps, and a sense of purpose that pervaded the atmosphere. I asked people about it. "We feel like it's a new beginning," said one, and, "It's almost like when von Braun was here," said another. Thompson, the new Center Director, talked with us about the present and the future. and his open door policy at all unclassified meetings.

We saw a hands-on manager who works well with people and encourages participation.

He didn't see us later at lunch in the cafeteria, but we saw him. He went up, grabbed a tray like everyone else, and shirtsleeves rolled up, went over and asked if he could join a group of people at one of the tables. Nobody was surprised, but he was certainly welcomed. It was obvious that this was no isolated incident.

We've tried to capture a sense of that renewal in this month's feature on Marshall. Not coincidentally, we like to feel, TU is a strong factor at MSFC. We hope you enjoy the feature. ☐

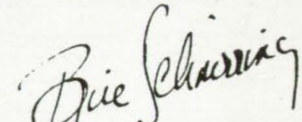

Thanks to all the people who reminded us that the peel-off labels did not peel-off. Unexpected problems prevented their use. Once the problems are resolved we will have peel-off labels in a matter of months.

Brave New World at Marshall

When Discovery *rises from its launch pad next year, it will be boosted in part by the rebirth and rededication of the people at Marshall Space Flight Center.*

J. R. Thompson, the new Center Director, has instituted a wide ranging open-door policy and plans to build on Marshall's traditional strengths in propulsion systems as they embark on Space Station and other payload projects that will carry into the 21st century.

Marshall has primary responsibility for preparing the Shuttle for launch in early 1988. Thompson not only calls the job "doable," but it is part and parcel of regenerating the Marshall spirit. He foresees a number of changes: "There are going to be changes in style, but there are also going to be changes in substance. Marshall does a lot of things right, and I want to retain [those things], and build on [them]." Thompson seeks to draw out discussions at all levels, especially encouraging the engineering and technical personnel, the heart of the Center, to voice any problems or differences of opinion.

Space Shuttle

The need to ensure high reliability is a constant in the Shuttle's multifaceted redesign program. An ambitious and aggressive ground test program will provide the needed confidence to launch, says Thompson. He adds, "These solid rocket boosters are so big and unforgiving, the reliability has got to be almost perfect. The only way to get that is to really understand the hardware (and the only way to do that is by intense and intensive ground testing).

"We're going to have to push the hardware to the limit to know where the margin is so we can fly safely. We can't have, in my opinion, a fault-free ground test program and a safe flight program. So we're going to put the risk on the ground."

Ambitious plans abound as Shuttle redesign continues. "The time is right," says Thompson, referring to industrial consortiums utilizing Shuttle-derived transportation technology for a mixed fleet system. An ideal way to accomplish this, and to build a strong, long term U.S. space program, he continues, is through two-way cooperative ventures with American industry, with the government providing a guaranteed market for the expendable launch vehicles.

Technology Utilization at Marshall

Marshall Technology Utilization Officer Ismail Akbay's staff has access to all Center employees, from the top down, to promote new technology reporting.

During their one-year probation period, new supervisors must complete ►

Marshall's activities link the earth to the stars. Top to bottom are the Power Factor Controller, the aurora borealis, the sun seen in a different light, and the Hubble Space Telescope.

The Pressure Extrapolation

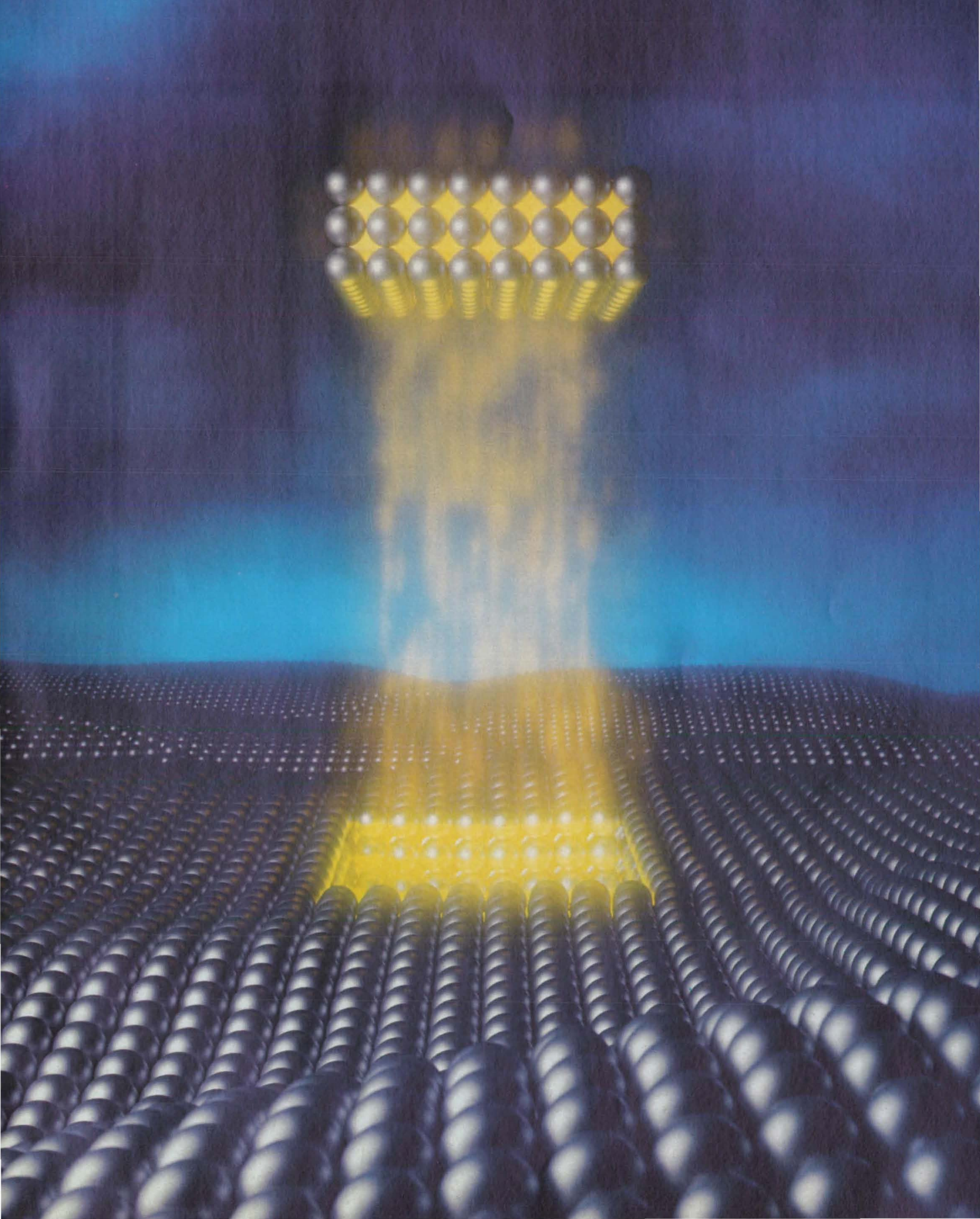

The Pressure Extrapolation

Modern automotive catalytic converters contain rhodium which promotes chemical reactions to remove pollutants from a car's exhaust. Scientists at the General Motors Research Laboratories have recently made discoveries about one such chemical reaction, the reaction between nitric oxide and carbon monoxide, pointing the way toward new or improved catalysts.

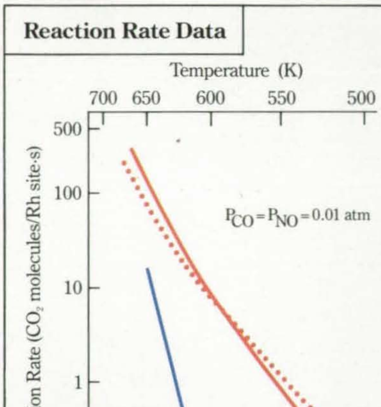

Figure 1: Rate comparisons for the NO-CO reaction. Measured data over single crystal Rh(111) (solid red line) and over supported Rh (blue line); model predictions (dotted red line).

Figure 2: Schematic representation of the elementary intermediate steps for the NO-CO reaction.

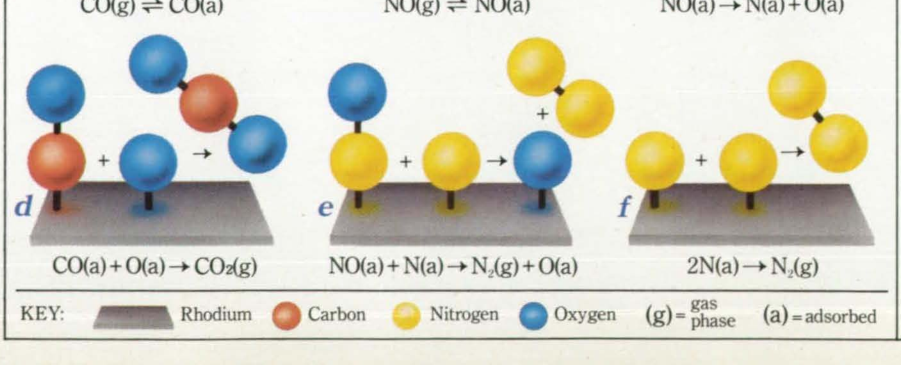

MOST FUNDAMENTAL catalytic studies using surface science techniques require an ultrahigh vacuum environment (10^{-13} atm). They are best suited for studying well characterized materials, such as metal single crystals. Catalytic reactions of practical interest, however, involve polycrystalline materials, in the form of small metal particles dispersed on supports. And they take place at atmospheric pressures rather than in an ultrahigh vacuum.

Now Dr. Galen B. Fisher and Dr. Se H. Oh have demonstrated how the wealth of chemical information obtained from ultrahigh vacuum (UHV) studies of ideal, single-crystal catalysts can be applied to the understanding of real-world systems that have different catalyst environments and that operate at much higher pressures.

These researchers concentrated their studies on the many chemical reactions that occur in modern automotive catalytic converters. One such reaction is the reduction of nitric oxide (NO) by carbon monoxide (CO) over a rhodium (Rh) catalyst to yield carbon dioxide (CO_2) and nitrogen (N_2) (Figure 2).

Dr. Fisher used various surface science spectroscopies in ultrahigh vacuum to study all of the elementary reactions over a rhodium single crystal [Rh(111)] that might be involved in this specific reaction. Over several years he measured the rates and determined the activation energies of each of these reactions. For most of these reactions, this was the first time these parameters had been measured. Based upon these results, Dr. Fisher hypothesized that the elementary reactions shown in Figure 2(a-f) were the significant steps involved in the NO-CO reaction and that nitrogen recombination and desorption (Figure 2f) was the rate-controlling step on Rh(111).

Dr. Fisher and Dr. Oh also initiated kinetic studies of this reaction at realistic reactant partial pressures and temperatures using two different catalysts—one was a rhodium single crystal [Rh(111)], and the other consisted of rhodium particles supported on alumina [Rh/Al_2O_3]. The rhodium concentrations on the support were similar to those used in an automotive catalytic converter. The studies with the single crystal at realistic, high pressures were done in collaboration with Dr. D. Wayne Goodman of Sandia National Laboratories.

At the same time, Dr. Oh devised a mathematical model for this reaction. The model consists

of steady-state conservation equations for the surface species, based on the reaction mechanism and the rate expressions for the individual reaction steps determined in Dr. Fisher's UHV studies. Overall reaction rates could then be computed from the surface concentrations satisfying the conservation equations. The reaction rates predicted by this model, which depend only on reactant partial pressures, are shown in Figure 1 (dotted red line).

The kinetics of the NO-CO reaction measured over a rhodium single crystal using realistic reactant partial pressures are shown in Figure 1 (solid red line). The agreement with the model predictions indicates that Drs. Fisher and Oh had correctly identified all of the intermediate reaction steps and confirms that, in this case, nitrogen recombination and desorption (Figure 2f) is the rate-controlling step on Rh(111). The fact that the agreement is so good also indicates that the rates of the elementary reactions measured under UHV conditions are still valid at realistic reactant partial pressures—a pressure extrapolation of more than ten orders of magnitude.

THE KINETICS of the NO-CO reaction measured over the supported rhodium catalyst (Figure 1, blue line), however, were much slower than predicted by the model. In addition, infrared studies have shown that NO is the predominant surface species on the catalyst, suggesting that in this case NO dissociation (Figure 2c) is the rate-controlling step. In fact, if the rate constant for NO dissociation measured under UHV conditions and used in the model is reduced by a factor of 2000, the kinetics of the NO-CO reaction measured over the supported rhodium catalyst are correctly predicted.

The difference between the kinetics of the NO-CO reaction measured over a rhodium single crystal and the kinetics measured over supported rhodium shows that this reaction depends on the environment of the rhodium in the catalyst. The reaction model strongly suggests that the NO dissociation reaction is the reaction step most sensitive to the rhodium environment.

"While our reaction model cannot tell us why NO dissociation is slower on supported rhodium," observes Dr. Oh, "it can help identify the kinds of studies necessary to clarify the origins of such sensitivity." Comparative kinetic studies can also provide useful insights for developing improved NO reduction catalysts. "Our studies have already told us," adds Dr. Fisher, "that one possible path to improving automobile catalysts is to make modifications that increase the NO dissociation rate."

General Motors

GM
MARK OF EXCELLENCE

THE MEN BEHIND THE WORK

Dr. Galen B. Fisher (left) and Dr. Se H. Oh are both Group Leaders in the Physical Chemistry Department at the General Motors Research Laboratories.

Dr. Fisher holds the title of Senior Staff Research Scientist, and heads the Surface Chemistry and Corrosion Science Group. He attended Pomona College as an undergraduate and received his graduate degrees from Stanford University in Applied Physics. Before coming to General Motors in 1978, he did post-doctoral studies at Brown University and worked at the National Bureau of Standards. Since then, his research has been involved with surface science studies of various catalytic reactions.

Dr. Oh is a Senior Staff Research Engineer, heading the Catalytic Kinetics Group. He received his undergraduate degree from Seoul National University and holds a doctorate in Chemical Engineering from the University of Illinois. Dr. Oh did post-doctoral work at the University of Toronto prior to joining GM in 1976. Since then, he has been involved in measuring and modeling the kinetics of catalytic reactions.

a number of training sessions, including one on technology transfer. The supervisors, in turn, encourage the engineers, scientists and researchers under them to report their technical innovations. Contract Monitors also participate in the technology transfer process by tracking the progress of new technologies developed by NASA contractors, and ensuring that they are fully documented for eventual dissemination.

Financial inducements help the technology transfer process. If *NASA Tech Briefs* publishes an innovation developed by a Marshall employee or contractor, the author receives a financial "Space Act Award." Should a private firm or entrepreneur commercially develop a NASA employee or contractor's innovation, the innovator can receive an additional sum. These awards are usually formally presented to the innovators in recognition of their achievements.

Marshall-developed spinoffs include a Power Factor Controller, which regulates the voltage supplied to alternating current motors in accordance with the power they require. To reduce the size and weight of wire in spacecraft, Marshall researchers developed Flat Conductor Cable (FCC). Thin as a credit card, FCC can reduce wiring costs as much as 40 percent in new buildings.

One Small Rocket To One Small Step

A Jupiter-C missile built at the Redstone Arsenal in Huntsville, Alabama launched America's first satellite into orbit on January 31, 1958. It simultaneously launched Huntsville into the space age.

The Huntsville Times front page story began, "The wail of sirens, blasting horns and the fiery trail of store-bought rockets ushered in the country's first step toward the conquest of space at Huntsville last night."

The Redstone Arsenal became the George C. Marshall Space Flight Center on July 1, 1960, and quickly established itself as NASA's leading center for propulsion systems and launch vehicles.

The Saturn Rocket Series, the world's first space station, the first materials processing experiments in space, and the propulsion system for the first Space Shuttle were all developed at Marshall.

In the mid-1940's, Dr. Werhner von Braun and 118 German rocket scientists emigrated to the United States, and found a home at the Redstone Arsenal in 1950. They were soon to become an integral part of the Army Ballistic Missile Agency.

The 1957 launching of Sputnik sounded the starting gun in the race for space. NASA was founded a year later to compete with the Russians. The fledging agency turned to Dr.von Braun's group to develop propulsion systems and launch vehicles. The scientists had tested dozens of Redstone and Jupiter rockets under the ABMA banner, resolving some of the difficulties in rocket design, propulsion, and performance. The ABMA's Development Operations Division was adopted into the NASA family in 1960 and given a new home in the Marshall Space Flight Center.

When President John F. Kennedy announced a year later his goal of a manned lunar landing within the decade, the responsibility to develop a larger rocket system fell squarely on the shoulders of the Marshall Scientists.They responded with the Saturn series: Saturn 1, Saturn 1B, and Saturn V.

Saturn challenged all the technological and managerial abilities at Marshall. The 70 foot Redstone had generated about 75,000 pounds of thrust for suborbital flight, but the Saturn V had one hundred times the thrust (7.5 million pounds) in the first stage alone, and another 1.2 million pounds in combined upper stage thrust.

The first Saturn rockets were powered by kerosene-liquid oxygen systems. Because such engines were used in the past to attain suborbital and orbital flights, Marshall's principle challenge was to cluster and enlarge them to achieve higher thrust. Innovations included directional gimbals for the eight engines, new ducting and venting techniques, and improved thrust chambers.

Liquid hydrogen propulsion systems, used in the Saturn Upper Stages, had never before been tried. The technology was unproven and the engineers faced numerous logistical problems in dealing with the new fuel. They developed two new engines, the RL-10 and J-2, which represented major technical breakthroughs in propulsion design. Innovations included lightweight, durable materials capable of withstanding extreme temperatures and stress, new heat treatments for alloys, and advancement in turbomachinery design.

The giant steps taken by these scientists and engineers were the basis for Neil Armstrong's "one small step" in 1969. Apollo 11 was a Saturn V result of Marshall's commitment to meeting the challenges of a new technological age. The roar of the Saturn rockets began with "wailing sirens, blasting horns and the fiery trail of store-bought rockets" on a January evening years earlier.

The Program Development Office—Turning Dreams into Reality

One of the most fascinating areas at the Center is the one with the mundane name—the Program Development Office. This is the office where ideas (sometimes seemingly science fiction) are turned into reality.

Organized after the Apollo program, the office was designed to centralize the future programs and futuristic ideas scattered around the Center. The office nurtures these ideas from the "time they are a glimmer in somebody's mind until they are approved as full fledged flight projects with permission to cut hardware," Deputy Director Bill Snoddy told *NASA Tech Briefs*. Programs "graduate" at that point, becoming their own Program Office, if large enough, or else merging with the Special Projects Office.

The Space Telescope and the Orbital Maneuvering Vehicle (OMV) are some of the ideas that originated in the Program Development Office. Recent graduates include "Gravity Probe B," orbiting X-ray telescope, and the Space Tether.

Trolling the Earth's Atmosphere with A Giant Rod and Reel

A maelstrom of activity occurs 50 to 90 miles high in the earth's upper atmosphere. Scientists have long wanted to study phenomena such as the aurora borealis that take place in this area, but heretofore it's been a never-never land—too high for balloons and airplanes, and too low for the Shuttle or satellites, where the drag would literally get them down.

The Program Development Office came up with the idea of using the Shuttle as a skyhook, lowering instruments from it on a 60 mile tether into the upper atmosphere. The instru- ►

NEW FROM ASTRO-MED

THE WORLD'S ONLY 8-CHANNEL RECORDER

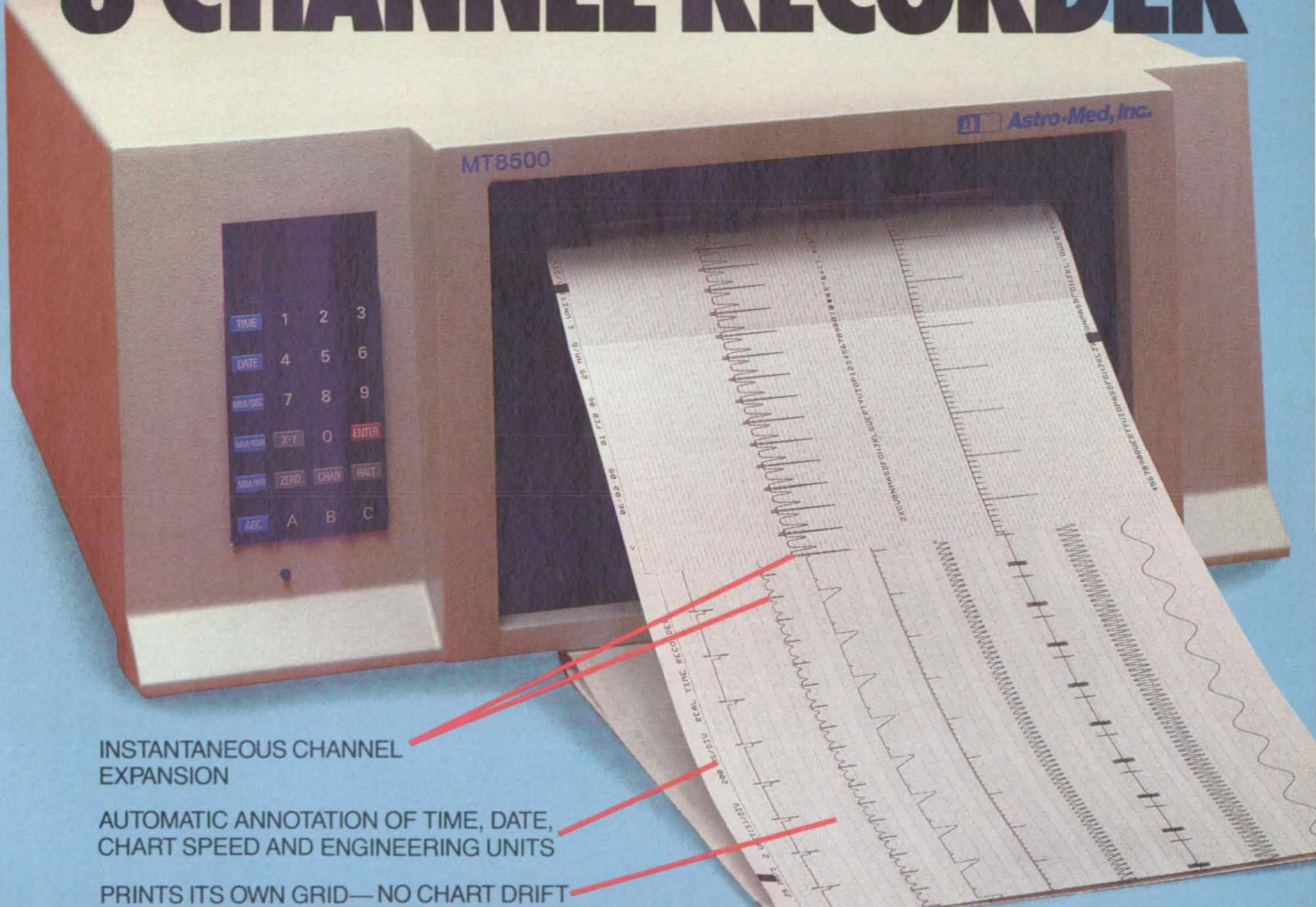

Introducing Astro-Med's new MT-8500.

Anything less does not meet today's standards for an eight-channel recorder. This new direct writing oscillograph overwhelms every other direct writer ever developed because its true performance begins where others leave off.

It will record waveforms up to 500 Hz full scale *real time,* absolutely flat. Or capture transients to 5 KHz. It allows you to e-x-p-a-n-d waveform channels for greater resolution, overlap channels, print alphanumerics with near-letter quality, transfer data to a host for display or archiving.

And it produces the most beautiful charts you've ever seen. On low-cost *permanent* thermal paper available everywhere. Without the mess or expense of inks, toners, or photo paper. Without moving parts, for long, problem-free service.

The Astro-Med MT-8500. You've got to see it to believe it. Call Toll Free today for a demonstration! **(800) 343-4039.**

Send for our comprehensive 16-page color brochure.

Name ____________________
Title ____________________
Company ____________________
Address ____________________
City ____________________
State ____________ Zip ________
Phone ____________________

☐ Phone me to arrange for a demonstration of the MT-8500. NASA 1/87

Astro-Med, Inc.

Astro-Med Industrial Park
West Warwick, Rhode Island 02893
(401) 828-4000 • Toll Free (800)-343-4039
Telex No. 710-382-6409

Circle Reader Action No. 424

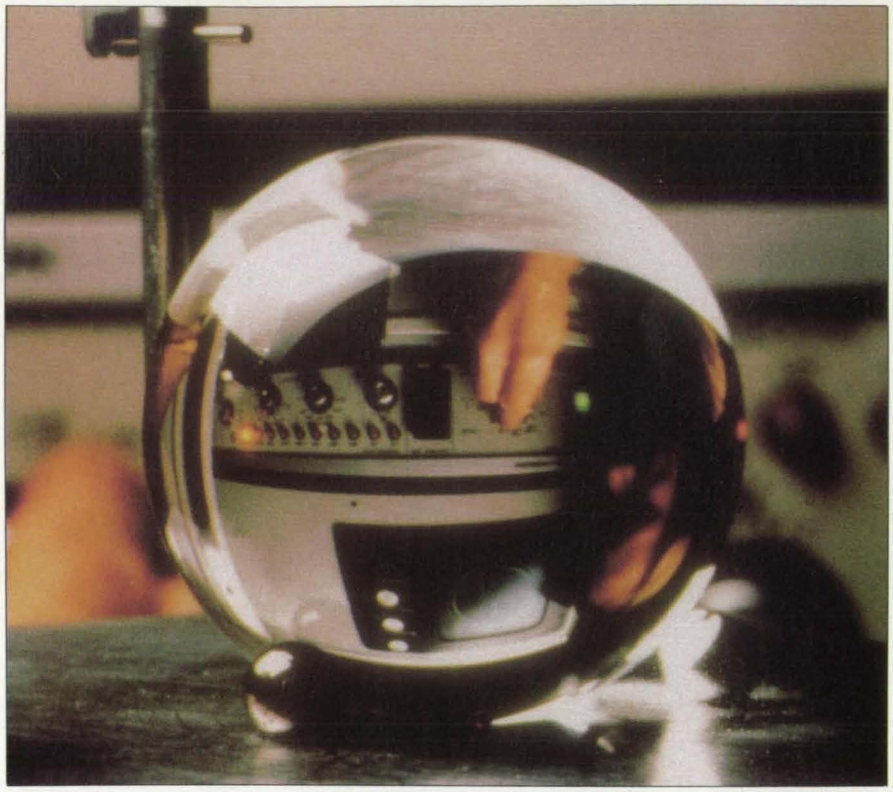

Marshall's engineers will levitate a crystal ball similar to this one as the heart of Gravity Probe B. The experiment will verify one of Einstein's theories.

ments would troll for days at a time, and would be reeled in after the experiment's completion. Variations include attaching tracer chemicals to the tether, and setting a series of instruments along its length for a cross sectional profile. An interesting side effect will be the electricity generated as the conductive cable moves through the earth's magnetic field.

Another Marshall project, Gravity Probe B (GPB), will use a crystal ball to see if space really warps as Einstein predicted. The ball is a solid quartz sphere about the size of a golf ball, which will function as the rotor of a gyroscope. Levitated in space through the interaction of a thin niobium coating and an electromagnetic field, this high stability gyroscope should tilt a predicted 42 milliarc seconds each year, in accordance with Einstein's theory of curved spacetime near a large mass. The project is scheduled to be tested on the Shuttle in approximately three years.

The Advanced X-ray Astrophysics Facility (AXAF) is another offspring of the Program Development Office. While protecting us from a variety of exotic radiation-induced cancers, the earth's atmosphere also inhibits the amount of data that can come out of ground-based X-ray observations. AXAF will be above all this, launched from the Shuttle in the 1990s and flying outside most of the atmosphere.

Quartz mirrors, coated with 500 angstroms of gold, will reflect incoming radiation onto nearby detectors, and images will be transmitted back to earth for computer analysis. The AXAF should detect X-ray sources 50 to 100 times weaker than earlier orbiting X-ray satellites, and will provide additional information on X-ray sources such as high energy quasars, spinning neutron stars and "black holes."

Two projects that have gone beyond program development are the Hubble Space Telescope and the Space Station. Both had significant development at Marshall. Though Space Station research and development continues at four different NASA Centers, the Hubble Space Telescope was managed totally by Marshall, which gained expertise on Skylab's Telescopes and the High Energy Astronomy Observatory satellites.

Recent Appointments At Marshall

J. R. Thompson, Director of the Marshall Space Flight Center, made four key appointments in the Science and Engineering Directorate. Dr. Judson A. Lovingood is named Associate Director for Propulsion Systems, responsible for assuring engineering adequacy of the Center's propulsion projects incorporating the Space Shuttle Main Engine, Solid Rocket Booster, External Tank, Orbital Maneuvering Vehicle and upper stages. Appointed Associate Director for Space Systems is E. Ray Tanner, responsible for assuring engineering adequacy of the Space Station, Hubble Space Telescope, Advanced X-Ray Astrophysics Facility, and Spacelab payload integration. John P. McCarty is named Director, Propulsion Laboratory, accountable for research and development, engineering and technical direction of propulsion systems design and analysis related to launch and space vehicles. Named Director, Structures and Dynamics Laboratory, is Dr. George F. McDonough. His responsibilities include research and development in structural design and analysis of launch and space vehicles, analysis of dynamics behavior, specification of dynamics-related design criteria and analysis of atmospheric and environmental processes. Changes became effective December 1, 1986.

Five new assignments in the Safety, Reliability and Quality Assurance Office were announced at the Marshall Space Flight Center. Charles R. Mauldin became Director of the Systems Safety and Reliability Office. Wiley C. Bunn was appointed Director of the Quality Assurance Office and is responsible for all of Marshall's quality programs. Donald L. Hartley is Director of the Institutional Safety Office. Arthur M. Carr is Director of the Project Assurance Office. Dewey Bowes Channell was named Chief of the Systems Safety Engineering Division within the Systems Safety and Reliability Office.

The new assignments, effective on December 18, are part of NASA's overall plan to expand its safety, reliability and quality assurance efforts throughout the agency. □

Fixed Focus From New York to Washington

Big as a railroad boxcar, the Edwin P. Hubble Space Telescope (HST), named after the astronomer whose theories led to the concept of an expanded universe, will peer 14 billion light years into space. Currently scheduled for a 1988 launch, HST will study ultraviolet, visible and near-infared radiation, increasing the observable universe 350 times over that seen by earth-based observatories. Such high magnification requires exceptional stability, and to meet the challenge, NASA developed a guidance system so precise that, were the HST emitting a narrow laser beam in Washington D.C., it would stay focused on a dime located in New York City.

Marshall Space Flight Center currently manages the Space Telescope, directing manufacture and component integration. Marshall gained experience for this role developing and operating the Apollo Telescope Mount ►

(ATM), a solar observatory used on Skylab in the seventies. ATM contained six solar telescopes and two cameras, instrumentation similar to HST's single radial and four axial instruments.

Marshall's management role will continue after launch, according to Fred S. Wojtalik, Deputy Manager of the HST Project Office. For the first 30 days after launch, Marshall will oversee orbital verification, "determining that the bird is doing what it's supposed to be doing," says Wojtalik. The Huntsville Operations Support Center, run by Marshall, will operate for six months after launch, supporting Goddard Space Flight Center as they conduct science verification tests.

No Tune Up in Space

With one foot poised on the stepping stone of Skylab, work continues on the Space Station. The Space Station will initially be used as a scientific observatory and service center for orbital craft and scientific payloads. It will eventually also become a transportation node for space vehicles and serve as a logistics base for large scale contruction projects in space or mining on the moon.

Marshall will define and design the Space Station's laboratory, living and logistics areas. Other work includes environmental control, life support and propulsion systems, along with Orbital Maneuvering and Transfer vehicles. Marshall is particularly well suited for these tasks, riding on the scientific and engineering expertise developed during the Skylab program and the Spacelab series. Skylab "showed us that man could productively operate in low gravity," says Luther Powell, Manager of the Space Station Projects Office at Marshall. Both laboratory programs gave Marshall experience in managing large manned systems for space science and applications. A number of challenges are posed by the Space Station's longevity. Previous manned programs lasted for predictable periods, adhering to strict timetables, but Space Station will last well into the 21st century. "We're going to drag technology with us," says Powell, when describing the innovations that will make this long-term effort possible. "The Space Station will be a centerpiece for automation and robotics for the nation," Powell adds. "We're going to make some major strides in technology, we're looking at spinoffs that will help U.S. industry."

The Hubble Space Telescope will peer 14 billion years into the past.

With the wide ranging leading edge activities underway in Huntsville, Center personnel exude a "can-do" attitude. The future looks bright with propulsion research paving the way for alternate ways to transport materials to and through space.

"We've got an awful lot of work ahead," says Center Director J.R. Thompson, "and people are really starting to hit it." □

Camping In The Great, Great Outdoors

Welcome to camp. There are no campfire songs, no weenie roasts, no hikes through the woods, no sailing, no tennis, no canoe races. This camp offers a simulated orbiter flight, tetrahedron assembly exercises, and a walk on the moon. Welcome to the U.S. Space Camp, at the Space and Rocket Center in Huntsville, AL.

The U.S. Space Camp is a 70,000 square foot reproduction of the Johnson Space Flight Center's astronaut training program. Built at a cost of 4.5 million dollars, the camp is cosponsored by the adjoining Marshall Space Flight Center.

"The idea behind Space Camp is to get young people interested in careers in math, science, and aerospace technology," explained Mr. Edward O. Buckbee, Director of the Space and Rocket Center's Space Museum. "We encourage them by showing just how exciting these fields can be."

Beginning in March and running through Labor Day, youths aged 11 to 16 travel to the Space and Rocket Center for a week of astronaut training and simulated Space Shuttle missions. The camp is divided into two levels—the basic Space Camp and the more advanced Space Academy.

Highlights of a week at Space Camp include Astronaut Training Day, Micro Gravity Day, and Space Shuttle Mission Day. Astronaut Training Day involves campers grades five through seven in basic training procedures, from packaged food and management systems to

life support systems. Micro Gravity Day prepares campers for space walks and coping with the zero gravity of space. They practice in a Moon Walk Trainer which simulates the sensation of walking on the lunar surface. On Space Shuttle Mission Day, each team of 12 youngsters is divided into crews and board the Space Shuttle, an orbiter mockup provided by the Marshall Center. Team members conduct a simulated mission, from checkout to return to earth.

The second training level is Space Academy, for grades eight through ten. Campers work in a full scale Spacelab module. The cockpit is authentic and includes four-directional capacity to manuever during launch and return. Campers are also involved in satellite deployment and operation of the large remote arm.

Adults can join in on the adventure. A three day intensive program is available in the fall. This camp highlights the Space Academy training and includes a tour of the Space Museum.

"The adults come away with a tremendously deepened knowledge of the Space Program— what our objectives are and where we're going," said Mr. Buckbee. "In the meantime they have a ball, a real blast."

Tuition ranges from $425 to $575, dependent on season and program. Included in the cost are meals, educational materials, and dormitory accomodations. Contrary to rumor, there is no waiting list.

Since opening in 1982, the U.S. Space Camp has attracted more than 12,500 youths from the world over. □

New Product Ideas

New Product Ideas are just a few of the many innovations described in this issue of *NASA Tech Briefs* and having promising commercial applications. Each is discussed further on the referenced page in the appropriate section in this issue. If you are interested in developing a product from these or other NASA innovations, you can receive further technical information by requesting the TSP referenced at the end of the full-length article or by writing the Technology Utilization Office of the sponsoring NASA center (see page 23). NASA's patent-licensing program to encourage commercial development is described on page 23.

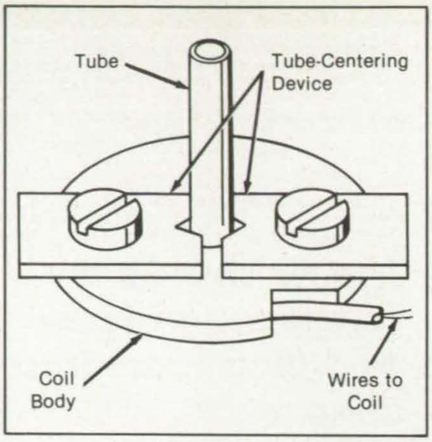

Eddy-Current Detection of Cracks in Tubes

An eddy-current probe detects incipient cracks inside small metal tubes. The probe consists of an eddy-current generating and detecting coil or pair of coils on which a pair of centering bars is mounted (see figure). The magnitudes and phases of the eddy currents induced in a tube as it passes between the bars indicate the depths of cracks; the current amplitudes and phases are displayed on an oscilloscope.
(See page 48).

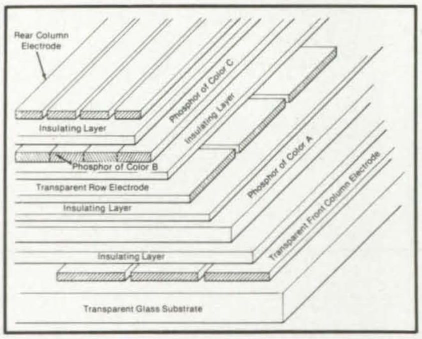

Two-Layer, Full-Color Electroluminescent Display

A full-color, matrix-addressed electroluminescent display uses three different color phosphors located in two separate, superimposed layers to provide higher brightness, better contrast ratio, and higher resolution than those of previous designs. In this new design, the area of one of the phosphor dots is twice the area of either of the other two. If the dimmest phosphor is used for the large dot, the display can be twice as bright as in designs where all dots are of equal area. Additionally, the new two-layer design increases the resolution by 50 percent over that of single-layer designs, requires roughly one-third fewer interfaces, and creates less undesirable capacitance than do present three-layer designs. This new design can be used for such transparent, flat-panel display media as thin-film electroluminescent phosphors, liquid crystals, or light-emitting diodes.
(See page 24).

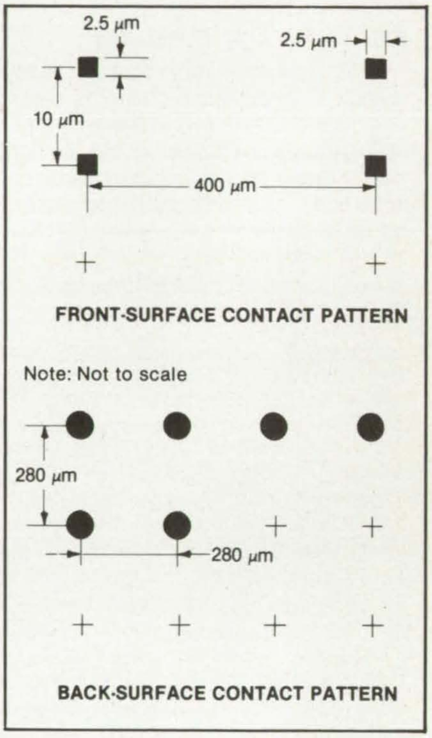

Solar Cells With Reduced Contact Areas

The efficiency of silicon solar cells is increased to about 20 percent by reducing the metal-contact area on silicon at the front and back of each cell. In the high-efficiency cell, the contact area on the front surface is reduced from 4-6 percent to 0.2 percent of the total; the back contact area is reduced from 100 percent to only 0.6 percent. As a result, the effective surface recombination velocity drops from about 10^4 cm/s to or below 10^3 cm/s. With reduced contact area on the back surface alone, the reverse saturation current density drops from 1.4×10^{-12} A/cm^2 to 0.91×10^{-12} A/cm^2, and the open-circuit voltage rises from 618 mV to 628 mV.
(See page 26).

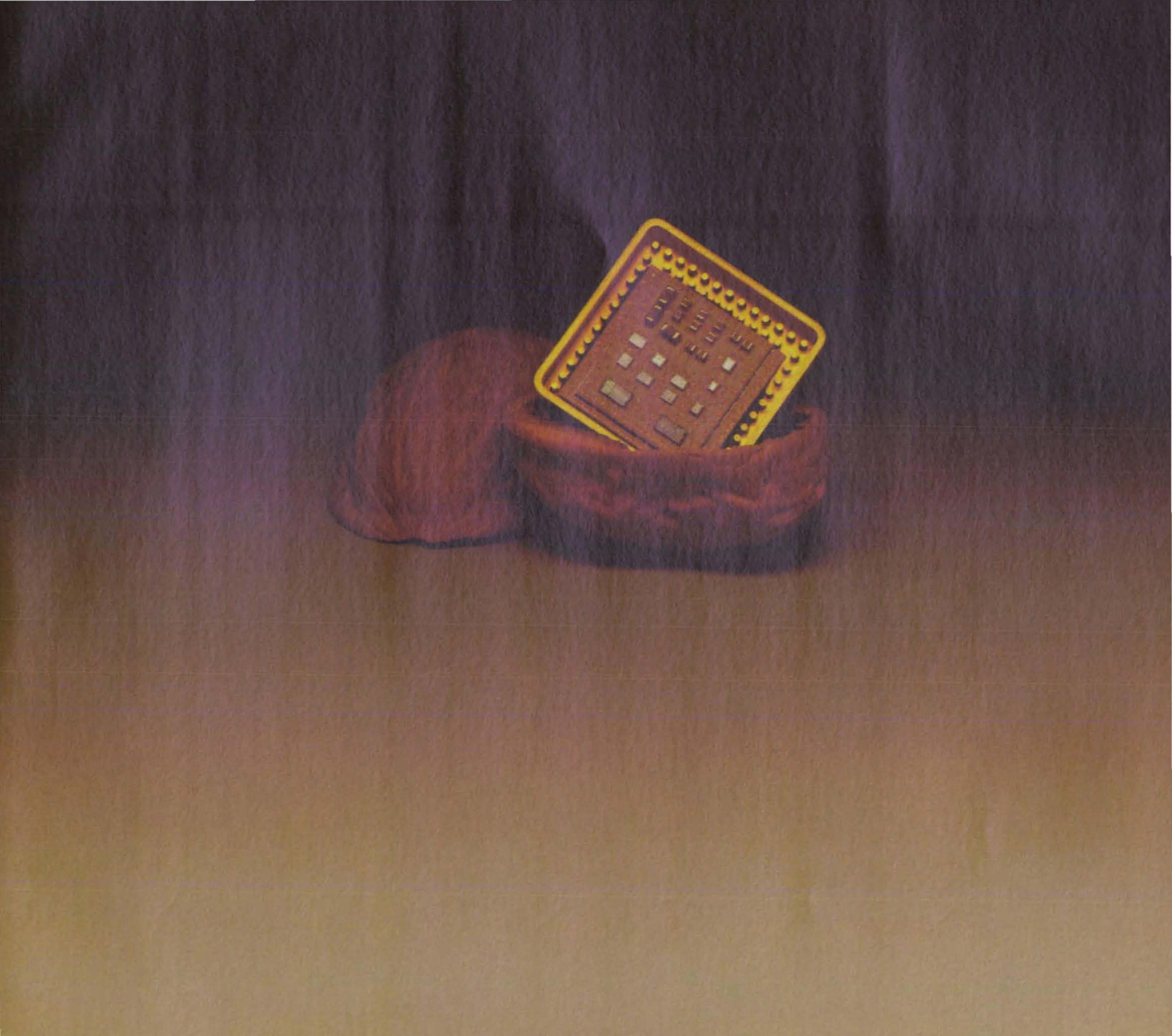

IN A NUTSHELL, BOEING CAN HELP WITH MILITARY/AEROSPACE ELECTRONICS.

Last year alone, Boeing Electronics Company supplied over a quarter billion dollars worth of high quality electronics. We can handle the toughest electronics assignments in the industry.

For instance, we've produced some of the most sophisticated microcircuits available. Including ceramic circuit boards, thick-film hybrids and thin-film circuits. We can provide everything from concept development to packaging and design. And Boeing delivers what it promises — on time.

If you have a special requirement for micro-circuits, power supplies, ceramic printed circuit boards, controllers or avionics, give us a call.

Contact Boeing Electronics Company, P.O. Box 24969, M/S 9N-41, Seattle, WA 98124-6269. Or call (206) 657-7474.

Boeing Electronics Company

Reliability By Design

Circle Reader Action No. 414

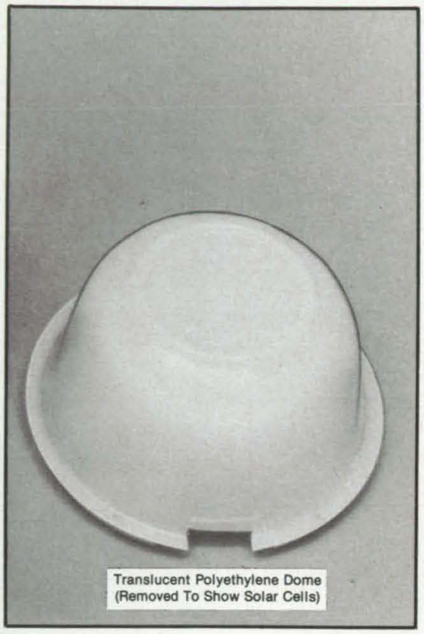

Translucent Polyethylene Dome (Removed To Show Solar Cells)

Inexpensive Meter for Total Solar Radiation

Developed as a simple, rugged, and inexpensive unit for agricultural use, a pyranometer containing solar cells measures the combined intensity of direct light from the Sun and diffuse light from the sky. The instrument includes a polyethylene dome that diffuses entering light so that the output of the light detectors does not vary significantly with the changing angle of the Sun during the day. Therefore, the instrument does not have to be calibrated for the response of each detector to the Sun angle, and the sensor outputs do not have to be corrected separately before they are summed and integrated. A leveling screw adjusts the tilt of the cell assembly to suit the local latitude. No further adjustments are needed to allow for seasonal changes in the solar declination.

(See page 38).

Remotely Adjustable Hydraulic Pump

The outlet pressure of a hydraulic pump can be adjusted remotely while the pump is operating. The pump can be used in aircraft and robots, for example, where hydraulic actuators are repeatedly turned on and off, changing the pump load frequently and over a wide range. The pump pressure can be reset as often as necessary to ensure adequate, but not excessive, pressure. The pump is a variable-displacement, pressure-compensated type; it contains a hydraulically operated pressure-regulation mechanism and an electrically operated pressure-adjustment mechanism.
(See page 65).

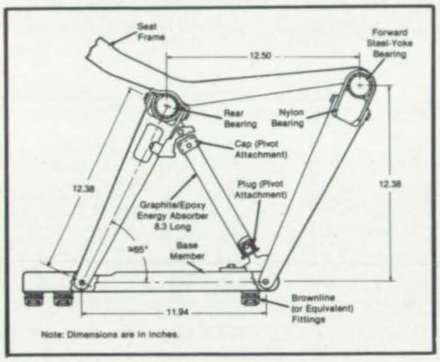

Energy-Absorbing Passenger Seat for Aircraft

An energy-absorbing passenger seat, designed to minimize injury in a commercial-aircraft crash, has been developed and impact tested. The design goal for the triple-passenger seat was to protect the passengers against a vertical impact velocity of 21 ft/s (6.4 m/s) and a longitudinal velocity of 21 ft/s (6.4 m/s). To limit acceleration, the seat was modified so that it would collapse or "stroke" under high load. To accomplish seat stroking, split-sleeve-type bearings were attached to the upper ends of the rear legs, and a combination nylon-bearing-block/steel-yoke unit was installed on the upper ends of the forward legs. Two graphite/epoxy energy-absorbing tubes, designed to crush as axial columns during the aircraft-impact shock pulse, were installed diagonally between the forward and rear seat legs.
(See page 57).

Depth Gauge for Liquids Under High Pressure

A continuous reading of the depth of a liquid in a vessel at pressures exceeding 5,000 psi (34 MN/m^2) is obtained from ultrasonic waves emitted from a transducer that is mounted in a modified high-pressure plug (see figure). In operation, the transducer excites the plug flange into vibration, sending an ultrasonic pulse through the liquid to the liquid/gas interface where the pulse is reflected. The returning pulse is intercepted by the transducer and transmitted to the supporting electronics that compute the liquid depth.
(See page 55).

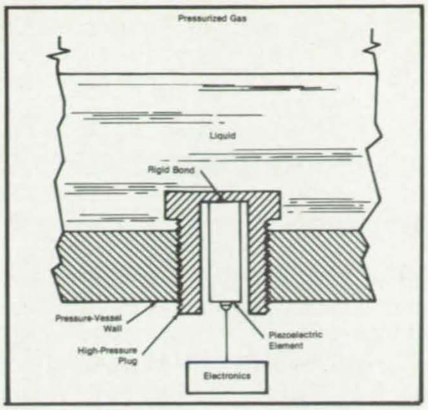

HOW YOU CAN BENEFIT FROM NASA's TECHNOLOGY UTILIZATION SERVICES

If you're a regular reader of TECH BRIEFS, then you're already making use of one of the low- and no-cost services provided by NASA's Technology Utilization (TU) Network. But a TECH BRIEFS subscription represents only a fraction of the technical information and applications/engineering services offered by the TU Network as a whole. In fact, when all of the components of NASA's Technology Utilization Network are considered, TECH BRIEFS represents the proverbial tip of the iceberg.

On the following pages, we've outlined NASA's TU Network—named the participants, described their services, and listed the individuals you can contact for more information relating to your specific needs. We encourage you to make use of the information, access, and applications services offered by NASA's Technology Utilization Network. You can save time and money by doing so.

HOW YOU CAN UTILIZE NASA'S

Industrial Applications Centers

A nationwide network offering a broad range of technical services, including computerized access to over 100 million documents worldwide.

You can contact NASA's network of Industrial Applications Centers (IACs) for assistance in solving a specific technical problem or meeting your information needs. The "user friendly" IACs are staffed by technology transfer experts who provide computerized information retrieval from one of the world's largest banks of technical data. Nearly 500 computerized data bases, ranging from NASA's own data base to Chemical Abstracts and INSPEC, are accessible through the nine IACs, which are located throughout the nation. The IACs also offer technical consultation services and/or linkage with other experts in the field.

You can obtain more information about these services by calling or writing the nearest IAC. User fees are charged for IAC information services.

Aerospace Research Applications Center (ARAC)
Indianapolis Center for Advanced Research
611 N. Capitol Avenue
Indianapolis, IN 46204
Dr. F. Timothy Janis, Director
(317) 262-5003

Kerr Industrial Applications Center (KIAC)
Southeastern Oklahoma State University
Station A, Box 2584
Durant, OK 74701
Tom J. McRorey, Director
(405) 924-6822

NASA Industrial Applications Center
823 William Pitt Union
University of Pittsburgh
Pittsburgh, PA 15260
Paul A. McWilliams, Executive Director
(412) 648-7000

NASA/Southern Technology Applications Center
State University System of Florida
307 Weil Hall
Gainesville, FL 32611
J. Ronald Thornton, Director
(904) 392-6760

NASA/UK Technology Applications Center
University of Kentucky
109 Kinkead Hall
Lexington, KY 40506-0057
William R. Strong, Director
(606) 257-6322

NERAC, Inc.
Mansfield Professional Park
Storrs, CT 06268
Daniel U. Wilde, President
(203) 429-3000

North Carolina Science and Technology Research Center (NC/STRC)
Post Office Box 12235
Research Triangle Park, NC 27709
J. Graves Vann, Jr., Acting Director
(919) 549-0671

Technology Application Center (TAC)
University of New Mexico
Albuquerque, NM 87131
Stanley A. Morain, Director
(505) 277-3622

NASA Industrial Applications Center (WESRAC)
University of Southern California
Research Annex
3716 South Hope Street
Room 200
Los Angeles, CA 90007
Radford G. King, Acting Director
(213) 743-6132
(800) 642-2872 (CA only)
(800) 872-7477 (toll-free US)

If you represent a public sector organization with a particular need, you can contact NASA's Application Team for technology matching and problem solving assistance. Staffed by professional engineers from a variety of disciplines, the Application Team works with public sector organizations to identify and solve critical problems with existing NASA technology.

Technology Application Team
Research Triangle Institute
P.O. Box 12194
Research Triangle Park, NC 27709
Doris Rouse, Director
(919) 541-6980

A SHORTCUT TO SOFTWARE:

COSMIC®

An economical source of computer programs developed by NASA & other gov't. agencies.

Software developed by the U.S. government may be applicable to your needs. To tap this valuable resource, contact COSMIC, NASA's Computer Software Management and Information Center. Approximately 1400 computer programs and related documentation comprise the current library. New and updated programs are announced regularly in NASA Tech Briefs' Computer Programs section, and COSMIC publishes an annual software catalog.

More information about COSMIC's services can be obtained by calling or writing:

COSMIC®
Computer Services Annex
University of Georgia
Athens, GA 30602
John A. Gibson, Director
(404) 542-3265

HOW YOU CAN ACCESS TECHNOLOGY TRANSFER SERVICES AT NASA FIELD CENTERS:

Technology Utilization Officers & Patent Counsels

Each NASA Field Center has designated a Technology Utilization Officer and a Patent Counsel to facilitate technology transfer between NASA and the private sector.

If you need further information about new technologies presented in NASA Tech Briefs, you should request the Technical Support Package (TSP) that accompanies the brief. In the event that a TSP is not available, you can contact the Technology Utilization Officer at the NASA Field Center that sponsored the research. He can arrange for expert assistance in applying the technology by putting you in touch with the people who developed it.

If you want additional information about the patent status of a particular technology or are interested in licensing a NASA invention, contact the Patent Counsel at the NASA Field Center that sponsored the research. Be sure to refer to the NASA reference number at the end of the tech brief.

Ames Research Center
Technology Utilization Officer:
Laurance A. Milov
Mail Code 204-10
Moffett Field, CA 94035
(415) 694-5761
Patent Counsel:
Darrell G. Brekke
Mail Code 200-11
Moffett Field, CA 94035
(415) 694-5104

Goddard Space Flight Center
Technology Utilization Officer:
Donald S. Friedman
Mail Code 702-1
Greenbelt, MD 20771
(301) 286-6242
Patent Counsel:
John O. Tresansky
Mail Code 204
Greenbelt, MD 20771
(301) 286-7351

Lyndon B. Johnson Space Center
Technology Utilization Officer:
Dean C. Glenn
Mail Code EA4
Houston, TX 77058
(713) 483-3809
Patent Counsel:
Edward K. Fein
Mail Code AL3
Houston, TX 77058
(713) 483-4871

John F. Kennedy Space Center
Technology Utilization Officer:
Thomas M. Hammond
Mail Stop PT-TPO-A
Kennedy Space Center, FL 32899
(305) 867-3017
Patent Counsel:
James O. Harrell
Mail Code PT-PAT
Kennedy Space Center, FL 32899
(305) 867-2544

Langley Research Center
Technology Utilization Officer:
John Samos
Mail Stop 139A
Hampton, VA 23665
(804) 865-3281
Patent Counsel:
Howard J. Osborn
Mail Code 279
Hampton, VA 23665
(804) 865-3725

Lewis Research Center
Technology Utilization Officer:
Daniel G. Soltis
Mail Stop 7-3
21000 Brookpark Road
Cleveland, OH 44135
(216) 433-5567
Patent Counsel:
Gene E. Shook
Mail Code 60-2
21000 Brookpark Road
Cleveland, OH 44135
(216) 433-5753

Jet Propulsion Laboratory
Technology Utilization Manager:
Norman L. Chalfin
Mail Stop 201-110
4800 Oak Grove Drive
Pasadena, CA 91109
(818) 354-2240

NASA Resident Office-JPL
Technology Utilization Officer:
Gordon S. Chapman
Mail Stop 180-801
4800 Oak Grove Drive
Pasadena, CA 91109
(818) 354-4849
Patent Counsel:
Paul F. McCaul
Mail Code 180-801
4800 Oak Grove Drive
Pasadena, CA 91109
(818) 354-2734

George C. Marshall Space Flight Center
Technology Utilization Officer:
Ismail Akbay
Code AT01
Marshall Space Flight Center, AL 35812
(205) 544-2223
Patent Counsel:
Leon D. Wofford, Jr.
Mail Code CC01
Marshall Space Flight Center, AL 35812
(205) 544-0014

National Space Technology Laboratories
Technology Utilization Officer:
Robert M. Barlow
Code GA-10
NSTL Station, MS 39529
(601) 688-1929

NASA Headquarters
Technology Utilization Officer:
Leonard A. Ault
Code IU
Washington, DC 20546
(202) 453-1920
Assistant General Counsel for Patent Matters: Robert F. Kempf
Code GP
Washington, DC 20546
(202) 453-2424

IF YOU HAVE A QUESTION...

NASA Scientific & Technical Information Facility

If you have a general or specific question about NASA's Technology Utilization Network or its services and documents, you can contact the STI facility for assistance. The STI staff can answer your questions, supply documents and provide referrals to meet your needs. You can use the feedback card in this issue to contact STI directly.

NASA Scientific and Technical Information Facility

Technology Utilization Office
P.O. Box 8757
BWI Airport, MD 21240
Walter M. Heiland, Manager
(301) 859-5300, Ext. 242, 243

Electronic Components & Circuits

Hardware, Techniques, and Processes

Books and Reports

Two-Layer, Full-Color Electroluminescent Display

A matrix-addressed, flat-panel display features increased resolution, brightness, and contrast.

Langley Research Center, Hampton, Virginia

A full-color, matrix-addressed electroluminescent display uses three different color phosphors located in two separate, superimposed layers to provide higher brightness, better contrast ratio, and higher resolution than those of previous designs. This design can be used for such transparent, flat-panel display media as thin-film electroluminescent phosphors, liquid crystals, or light-emitting diodes.

Matrix-addressed, flat-panel displays are rapidly gaining acceptance as computer terminal displays and as instrument displays in automobiles and in aircraft cockpits. To compete with cathode-ray tubes in more than limited applications, flat-panel displays must be offered in full color. Full-color displays require the use and control of the three primary colors: red, blue, and green. The best available red, blue, and green phosphors for thin-film electroluminescence differ from each other in maximum brightness, the green phosphor being ten times brighter than the red. In a typical color display, the brightness of the display is limited by the brightness of the weakest color phosphor.

In this new design, the area of one of the phosphor dots is twice the area of either of the other two. If the dimmest phosphor is used for the large dot, the display can be twice as bright as in designs where all dots are of equal area. Additionally, the new two-layer design increases the resolution by 50 percent over that of single-layer designs, requires roughly one-third fewer interfaces, and creates less undesirable capacitance than do present three-layer designs.

The device is constructed by consecutive deposition of materials onto a transparent glass substrate to form the following layers (see figure):

- A transparent front column of electrodes,
- An insulating layer,
- An electroluminescent phosphor of color A,
- An insulating layer,
- A transparent row of electrodes oriented perpendicularly to the column electrodes,
- A third insulating layer,
- Alternating side-by-side stripes of phosphors of color B and of color C oriented in parallel with the front column electrodes (the distance between centers of these stripes being one-half the distance between centers of the front

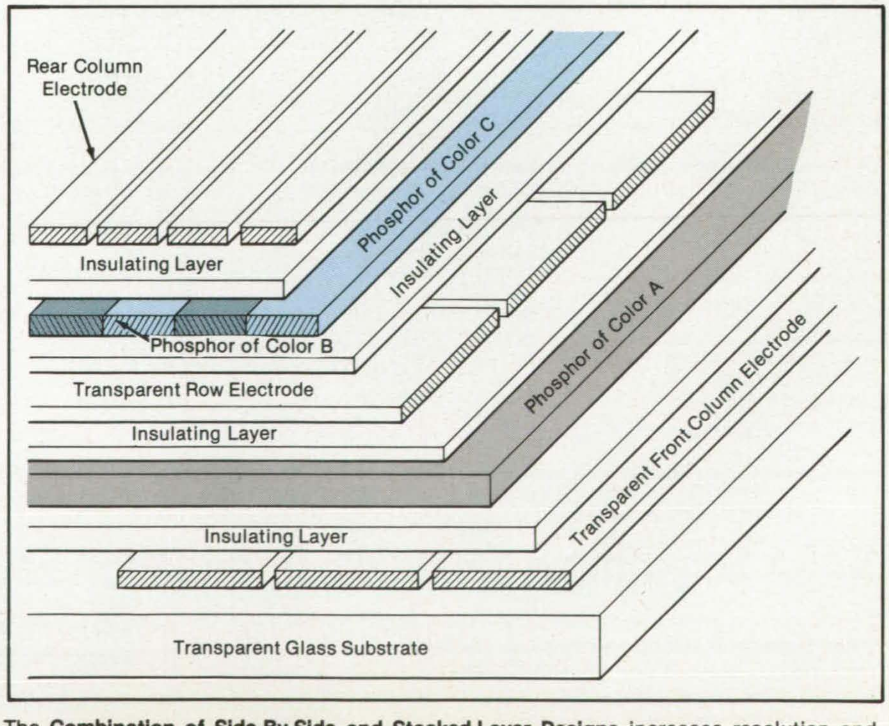

The **Combination of Side-By-Side and Stacked-Layer Designs** increases resolution and brightness in electroluminescent display panels.

The Precision Approach to Microwave Landing Simulation...When Accurate Calibration is Critical

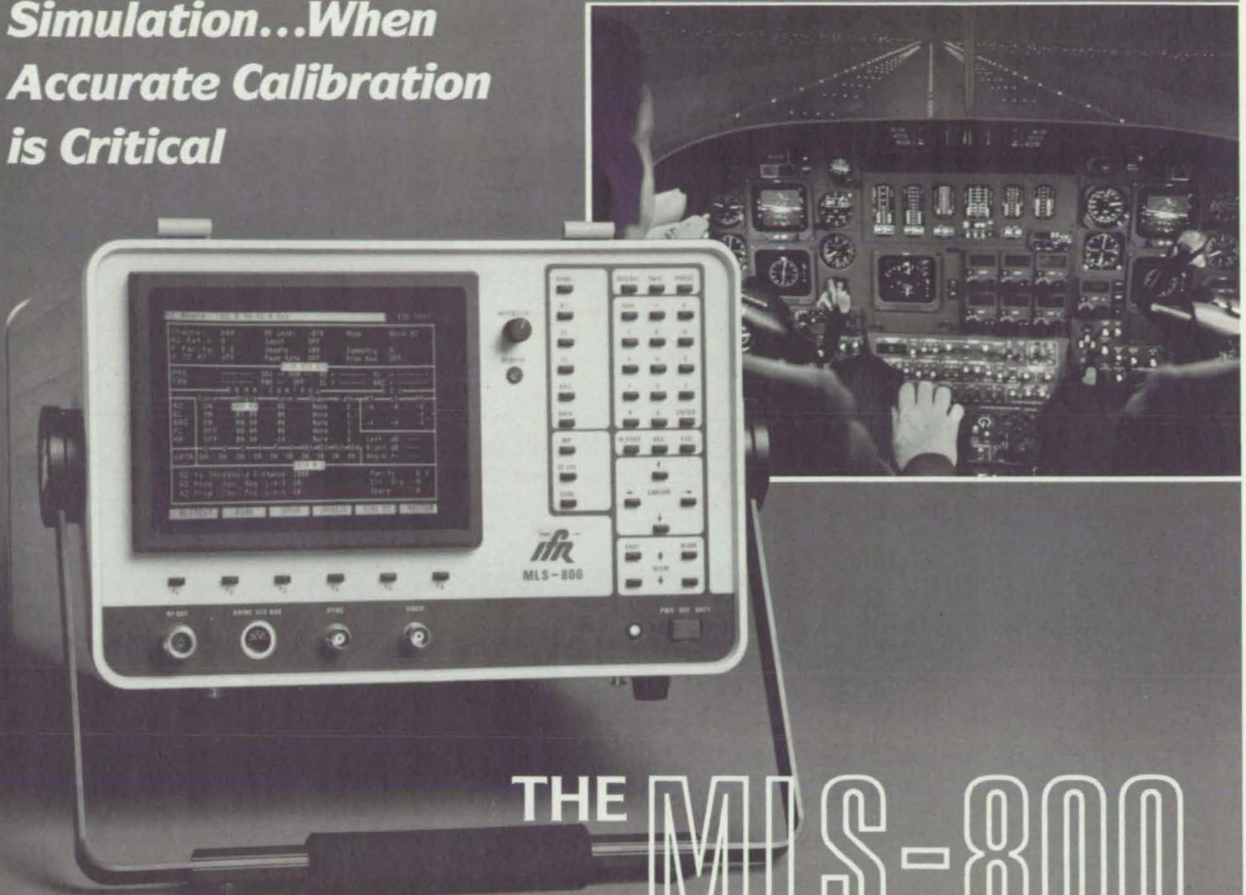

THE MLS-800

MICROWAVE LANDING SYSTEM TEST SET

High-precision test equipment for the industry's most precise landing system

A TYPICAL OPERATIONAL TEST MENU

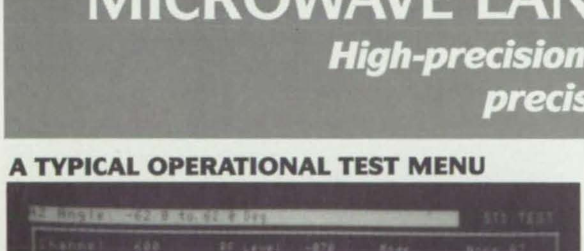

The parameters displayed on the MLS test menu are in accordance with the RTCA/DO-177 specifications, FAA STD 22b of October, 1983, ICAO SARPS of April, 1981 and the proposed ICAO SARPS of 1985.

The MLS-800: A microprocessor controlled simulator, designed to test airborne MLS angle receivers on the bench or verify system operation on the ramp.

Impressive Standard Features Include:

- Complete mainpath simulation
- Multipath simulation capability
- Control of all beam parameters
- Simulates all basic data words plus auxiliary data words with parity selection
- Full range of MLS channels
- ARINC 429 receiver data with PFE *(Path Following Error)* and CMN *(Control Motion Noise)* calculations

Precision Simulators from IFR

Remember IFR. The name you respect in test equipment. Write or call your IFR Distributor today and arrange for a demonstration. *The best is cost effective.*

IFR SYSTEMS, INC. 10200 West York Street / Wichita, Kansas 67215 U.S.A. / 316/522-4981 / TWX 910-741-6952

Circle Reader Action No. 317

column electrodes),
- A fourth insulating layer,
- A rear column of electrodes oriented in parallel with the phosphor stripes, with one electrode superimposed over each of these stripes, and

A passive layer or glass seal may be applied over the rear column of electrodes.

The design can be used with or without insulating layers between the electrodes and the display material. The layers of material deposited on the glass substrate may be deposited in reverse order, placing phosphors B and C in front of phosphor A as viewed from the glass substrate. The rear column electrodes may be reflective, transparent, or light absorbing. This combination of a partially side-by-side design with a partially stacked-layer design produces a flat-panel, full-color display that combines improved resolution, brightness, and contrast ratio with simplified fabrication.

This work was done by James B. Robertson of **Langley Research Center**. *No further documentation is available.*

This invention is owned by NASA, and a patent application has been filed. Inquiries concerning nonexclusive or exclusive license for its commercial development should be addressed to the Patent Counsel, Langley Research Center [see page 23]. Refer to LAR-13407.

Phase-Center Extension for a Microwave Feed Horn

A corrugated cylindrical tube relocates the phase center of a Cassegrain antenna feed.

NASA's Jet Propulsion Laboratory, Pasadena, California

As part of a proposed modification to increase the aperture of a Cassegrain antenna from 64 to 70 m, a relatively inexpensive extension will move the phase center of the feed (the point from which the horn appears to radiate) without incurring the cost of redesigning the horn and relocating low-noise equipment. Because of its large diameter and the corrugations on its interior, the extension tube (see figure) does not contribute significantly to the system noise temperature. The extension does not affect the polarization characteristics of the feed.

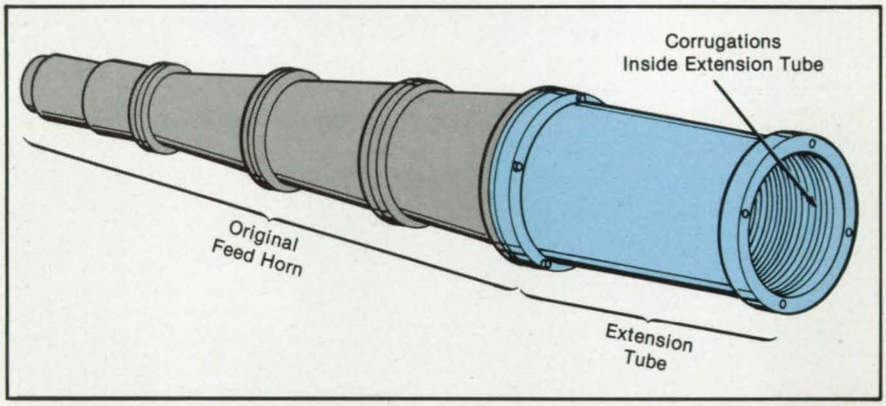

A **Cylindrical Extension Tube** could be used to shift the phase center of an existing conical feed horn to meet the requirements of a proposed antenna modification.

The extension was designed using a new corrugated-horn, scattering-matrix computer-aided-design program. The design is intermediate between dominant-mode waveguide and beam waveguide technologies. The length of the original horn did not have to be changed, but the program is designed to allow for this in other applications, when necessary.

Calculations and measurements show that the phase center can be placed anywhere from a few inches inside to a few inches outside the end of the extension, by appropriate choice of the length of the extension and, to a lesser extent, the depth of the corrugations. Since the phase center can be located outside the physical feed horn, the techniques used in the current design could be applicable in other problems; for example, to prevent a feed horn from interfering with other structures or airflow stream lines.

This work was done by Robert W. Hartop and Farzin Manshadi of Caltech for **NASA's Jet Propulsion Laboratory**. *For further information, Circle 32 on the TSP Request Card. NPO-16594*

Solar Cells With Reduced Contact Areas

Silicon cells are more efficient because less metal touches the semiconductor.

NASA's Jet Propulsion Laboratory, Pasadena, California

The efficiency of silicon solar cells is increased to about 20 percent by the use of a smaller metal-contact area on silicon at the front and the back of each cell. The reduction in contact area reduces the surface recombination velocity under the contact and thus reduces the reverse saturation current and increases the open-circuit voltage.

In a conventional solar cell, 4 to 6 percent of the front surface is covered by contact metal, and the back is completely metallized. Even after passivation of the front surface with an oxide layer, the overall surface recombination velocity is on the order of 10^4 cm/s, the reverse saturation current density is 1.4×10^{-12} A/cm^2, and the open-circuit voltage is 618 mV.

4 REASONS TO SPECIFY BELDEN FOR YOUR GOVERNMENT AND MILITARY APPLICATIONS

Selection. We offer a broad line of electronic wire and cable designed to meet military specifications such as MIL C 17, MIL C 49055, MIL W 16878, MIL W 22759 and others. Many are QPL listed.

From fiber optic cable to multi-conductor and high temperature cables, choose the cable best suited to your specific application. Or work with our Product Engineering Group to design specialty cable to your exact requirements.

Quality and Reliability. After working with governmental and military applications for over 30 years, we understand the interrelationship of quality components and critical requirements. We believe quality is the responsibility of leadership. That's why our Quality Assurance Department has full authority to maintain high quality standards for our products. And we use patented testing methods to guarantee our product reliability. Choosing Belden means choosing high quality, reliable products.

Belden Innovation. We're a leading innovator in shielding technology and patented testing methods. Our shielding is designed to meet the highest performance standards in the industry—including military TEMPEST requirements. To make your cable decision easier, we provide you with all the test data necessary to choose the proper and most cost-efficient shield for your application. We also offer a variety of insulations and jacketing materials designed to provide superior performance under hostile environmental conditions. Critical application requirements are not a problem when you work with Belden.

The Belden Government Department. Since we understand how the government and prime contractors work, we provide you with full support services—from sales and engineering support to contract administration. We're ready to help with your design decisions where and when you need us.

To make your design project easier, call us for technical assistance. Because when you specify Belden, There is no equal.

Contact the Belden Electronic Wire and Cable Government Department today. P.O. Box 1980, Richmond, IN 47375.

Phone: 1-800-BELDEN-4

There is no equal.™

COOPER INDUSTRIES **BELDEN**

Circle Reader Action No. 469

In a high-efficiency cell, the contact area on the front surface is reduced to only 0.2 percent of the total and the back contact area to only 0.6 percent. As a result, the effective surface recombination velocity drops to or below 10^3 cm/s. With reduced contact area on back surface alone, the reverse saturation current density drops to 0.91×10^{-12} A/cm^2, and the open-circuit voltage rises to 628 mV.

A p/n junction is formed in the silicon wafer in the usual way, then a thermal oxide layer 100 Å thick is grown on the front and the back. An array of square "windows" is etched through the front oxide, and an array of circular "windows" is etched on the back side (see figure). Layers of titanium, palladium, and silver are evaporated into the "windows" and sintered, forming arrays of metal contacts on both surfaces. Metal fingers are deposited on the front oxide so that they form conductive paths for electrical output through metal in "windows." The front surface is provided with an antireflection coating.

An aluminum layer is deposited on the back oxide where it forms an electrical connection to the back contact array and reflects light back into the silicon wafer. This is followed by metallization, using the titanium-palladium-silver for the back contact.

This work was done by Taher Daud, Gerald T. Crotty, Akaram H. Kachare, and Jeffrey T. Lewis of Caltech for **NASA's Jet Propulsion Laboratory**. *For further information, Circle 70 on the TSP Request Card.*

Inquiries concerning rights for the commercial use of this invention should be addressed to the Patent Counsel, NASA Resident Office-JPL [see page 23]. Refer to NPO-16762.

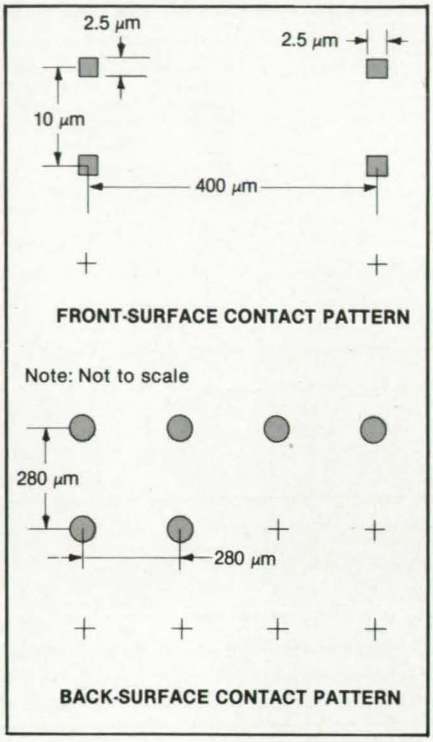

This **Detail of Electrical-Contact Arrays** shows how small a metal area touches the silicon wafer. The complete arrays are about 20 mm square.

CMOS Clock Synchronizer

A circuit synchronizes clock and gate signals within one-quarter of a clock cycle.

Ames Research Center, Moffett Field, California

A simple circuit develops a clock signal synchronized with an external gate signal, with a maximum skew of one-quarter of a clock cycle; yet it requires a synchronizing square wave of only twice the designated clock frequency. To effect the same maximum skew, previous circuits required synchronizing signals four times the clock frequency. The relatively low synchronizing frequency of the new circuit is particularly advantageous in radiation environments where the maximum clocking frequency of

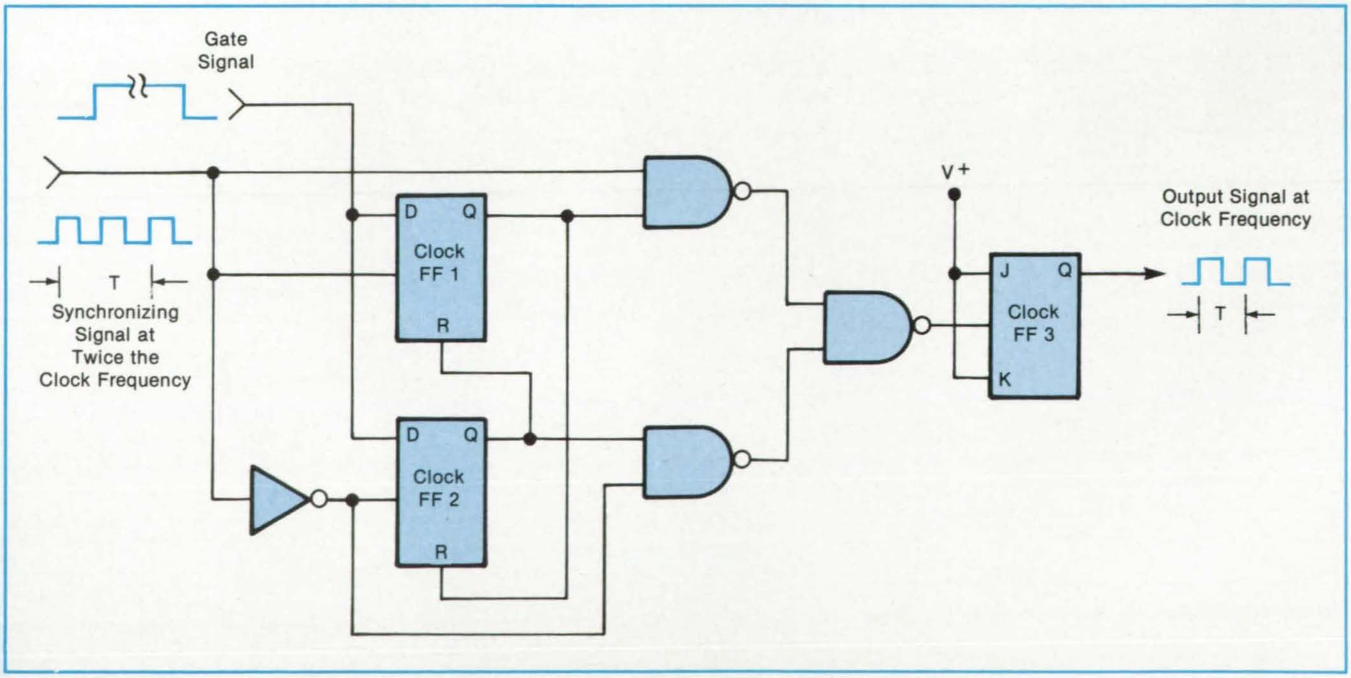

A **Clock Synchronizer** with one-quarter-cycle skew can be constructed from three flip-flops, three NAND gates, and an inverter. In addition to the gate signal to which the clock is to be synchronized, the circuit requires a square-wave input at twice the desired clock frequency.

complementary metal oxide/semiconductor (CMOS) circuits must be severely derated.

The circuit was originally developed for use in a dual-slope analog-to-digital converter. In such a converter, if the clock signal is simply gated without synchronization, the skew between the gate and clock signals can result in up to a 1-bit error in the converter output. With a one-quarter-cycle synchronization, the error from this source is reduced to one-quarter of a bit or less, provided that clock symmetry is good.

The new circuit (see figure) achieves its low skew by synchronizing an output clock with either the leading or the trailing edge of an input clock-signal pulse, whichever occurs first after the gate signal: the input clock signal is applied directly to flip flop FF_1 and, via an inverter, to FF_2. Thus either FF_1 is set by the next active edge of the input clock or FF_2 is set by the complement of the edge, whichever occurs first. The next active edge occurs within a one-half cycle of the synchronizing signal, which is one-quarter cycle of the designated clock signal.

The first FF to be set inhibits the other. Depending on the resulting settings of FF_1 and FF_2, the signal applied to the clock input of FF_3 is either the synchronizing signal or its complement. FF_3 acts as a divide-by-2 circuit to produce an output clock signal at one-half the synchronizing frequency.

This work was done by Robert B. Kepp of Martin Marietta Corp. for **Ames Research Center.** *For further information, Circle 25 on the TSP Request Card.*

Inquiries concerning rights for the commercial use of this invention should be addressed to the Patent Counsel, Ames Research Center [see page 23]. Refer to ARC-11692.

Books and Reports

These reports, studies, and handbooks are available from NASA as Technical Support Packages (TSP's) when a Request Card number is cited; otherwise they are available from the National Technical Information Service.

Designing High-Frequency Inductors

Procedures for both ferrite-core and Molypermalloy-core inductors are detailed.

A report presents design procedures for two types of high-frequency inductors: those with iron or ferrite cores and lumped airgaps and those with Molypermalloy powder cores and distributed airgaps. These components, which carry no direct current, are widely used in ferroresonant power regulators, pulse-width-modulation inverters, and other power-processing equipment. They are designed more easily than are dc inductors, using procedures like those for designing transformers. With no dc-generated flux in the core, the design calculations are straightforward. Essentially, the high-frequency ac inductor is designed to support the applied voltage without saturating the core, then the airgap for the proper inductance is calculated.

The report lays the groundwork for the procedures by discussing the two major effects of the inductor airgaps; namely, the increases in the inductance and the power loss due to the fringing flux. For design purposes, the airgap length should be minimized to minimize the fringing flux, thereby maximizing the efficiency. To keep the gap small, the number of turns of wire is kept to a minimum. The number of turns is also minimized to operate the core at the highest possible magnetic-flux density without saturating the core or generating excessive power loss in the core.

The airgap, power handling, and other considerations are represented in the equations for inductor design. The report gives the equations and an 11-step procedure for designing an inductor with a lumper airgap.

Distributed-airgap inductors reduce the losses caused by fringing fluxes. The report presents a design procedure for a toroidal inductor of this type. This procedure is even simpler than that for a lumped-airgap type.

The report concludes with a comparison of the losses among three inductors designed to operate at 20 kHz with a 90-V square wave and a 14-A peak-to-peak triangular wave. Two of the inductors had lumped-airgap cores, and one had a distributed-airgap Molypermalloy-powder core. The temperature rise in the distributed-gap core was less than that of the other two.

This work was done by Colonel W. T. McLyman and Albert P. Wagner of Caltech for **NASA's Jet Propulsion Laboratory.** *To obtain a copy of the report, "Designing High Frequency AC Inductors Using Ferrite and Molypermalloy Cores (MPP)," Circle 127 on the TSP Request Card. NPO-16553*

Electronic Systems

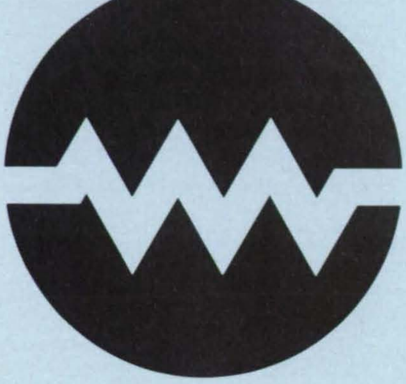

Hardware, Techniques, and Processes

Measuring Room Area or Volume Electronically

Results would be obtained rapidly with minimal effort.

NASA's Jet Propulsion Laboratory, Pasadena, California

A conceptual portable ranging instrument would measure the floor area or the volume of a room. The instrument would be advantageous where it is too difficult or time consuming to take linear measurements with tapes or rulers; for example, where a room is very large, where measurements have to be taken at dangerous locations, or where heavy objects have to be moved for access to the walls.

The instrument would include a pulsed, scanning radar, laser ranger (lidar), or sonar device capable of transmitting a beam sufficiently narrow for high angular resolution. For an area measurement, the instrument would be placed at a point in the room and set to take distance measurements to the walls in a horizontal plane, at all angular positions separated by small increments related to the angular resolution. If the angular increment is 360° ÷ M, then the area, A, is computed from the distance measurements by the formula

$$A = (\pi/M) \sum_{k=1}^{M} d_k^2$$

where d_k is the distance to the wall as measured at the *k*th angular position.

The volume would be measured in a similar manner, except that the instru-

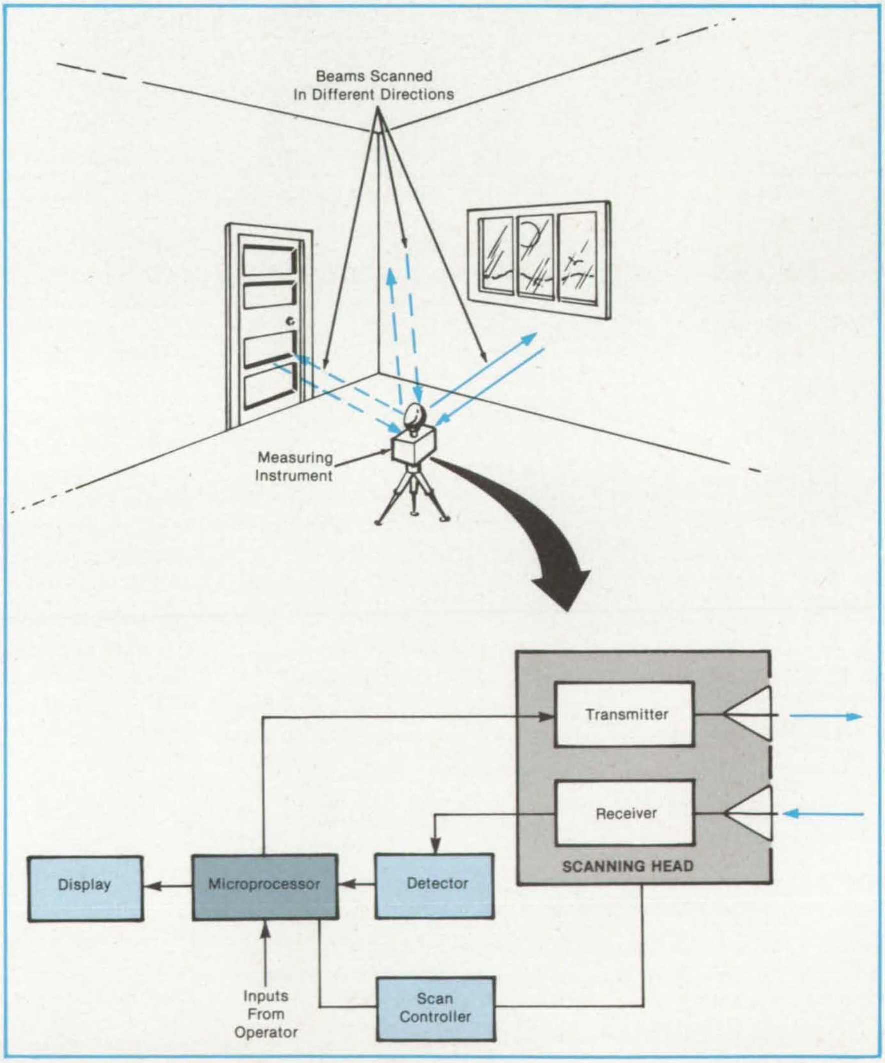

The **Area- and Volume-Measuring Instrument** could be hand-held or mounted on a tripod. The instrument would rapidly measure the distances to the walls, ceiling, or floor at many viewing angles and automatically compute the area or volume of the room.

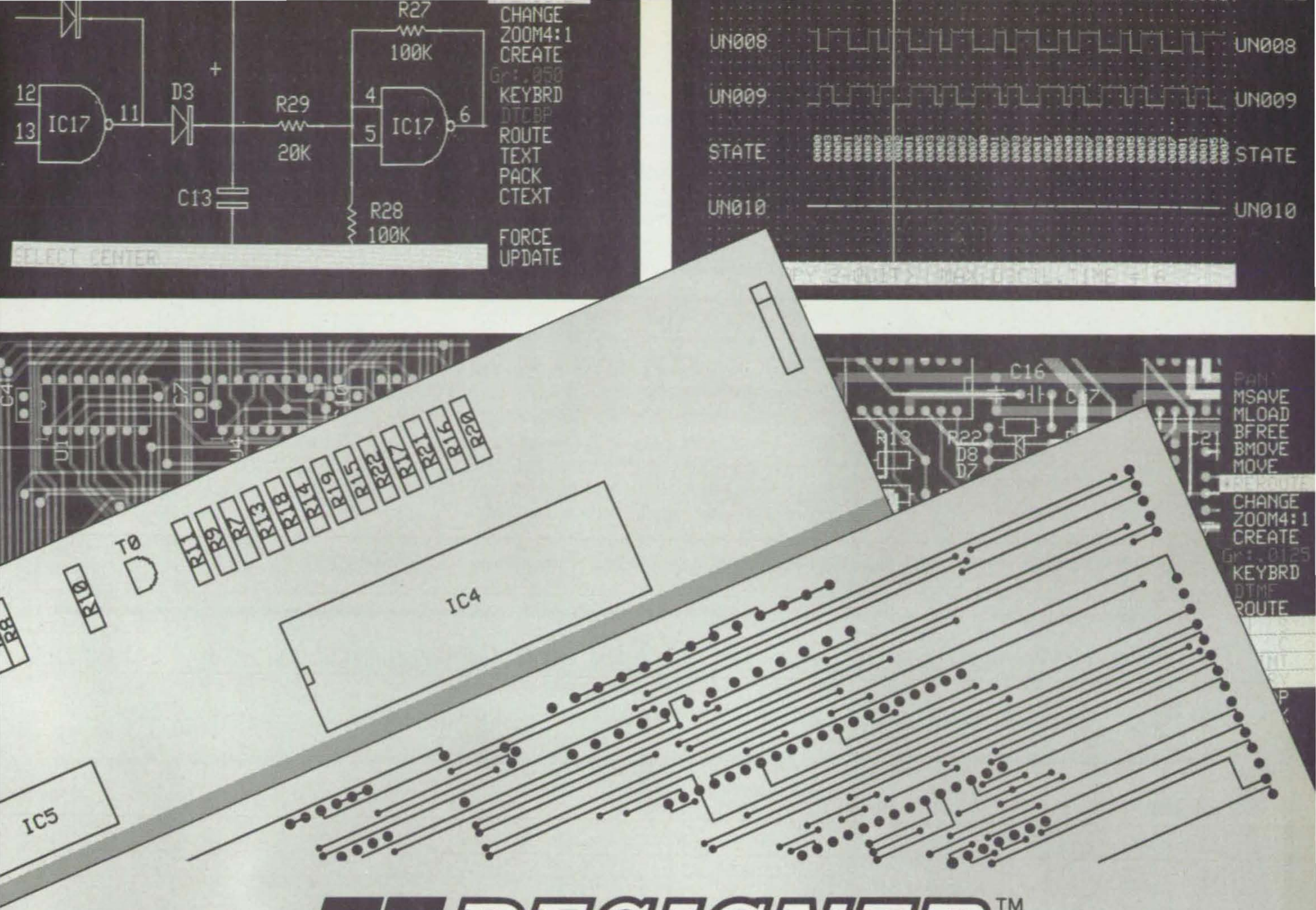

EE DESIGNER™

PROFESSIONAL CAE/CAD SOFTWARE STARTING AT $975.

A clear path through the CAE/CAD software maze. There are many CAE/CAD systems on the market today, but most are unproven in the work environment. With over 2,000 packages sold, the one system that has been getting the job done where it counts is EE Designer!

This is the IBM PC-based end-to-end CAE/CAD system that performs. Professionally. And affordably. That's why it's quickly become first choice of small and large companies alike. And the latter category includes companies like ***AT&T, Eastman Kodak, General Electric, IBM, Motorola, Sony, Texas Instruments, Westinghouse,*** and ***Xerox,*** to name just a few.

Join them and more than a thousand other companies in making the smart move—risk free. Order EE Designer or the advanced EE Designer II, try it for 30 days and be fully satisfied or your money back.

EE Designer. Schematic capture, digital logic simulation, manual interactive layout, limited multilayer capability. **$975.**

AutoRouter. Two layer AutoRouter for EE Designer. Uses vias and orthogonal routing style. **$975.**

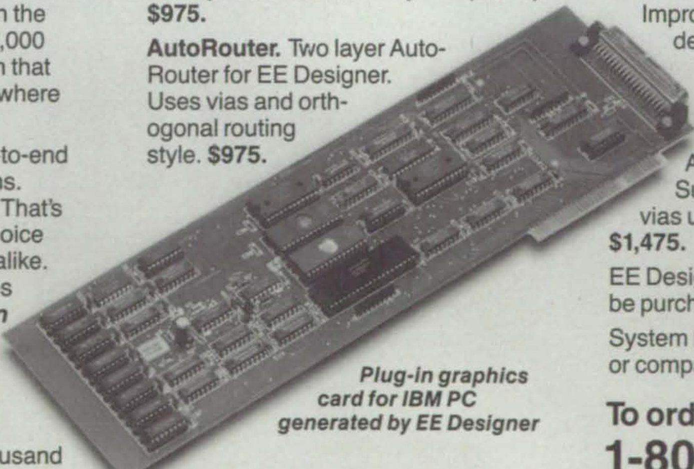

Plug-in graphics card for IBM PC generated by EE Designer

EE Designer II. Schematic capture, digital logic simulation, manual interactive layout, extended multilayer and surface mount (SMD) capability, enhanced graphics for symbol creation, dimensioning capabilities. Improved facilities for analog board design (improved ground planes, user definable trace widths.) **$1,875.**

AutoRouter II. Multilayer AutoRouter for EE Designer II. Supports routing with or without vias using orthogonal routing style. **$1,475.**

EE Designer II and AutoRouter II may be purchased together for **$2,975.**

System requirements: IBM PC/XT/AT or compatible with 640K memory.

To order, call toll-free 1-800-225-5669

VISA MasterCard

VISIONICS®
CORPORATION

1284 Geneva Drive •
Sunnyvale, CA 94089
(408) 745-1551

Circle Reader Action No. 473

ment would have to scan vertically as well as horizontally, with the beam aimed at the walls, floor, and ceiling. In a spherical coordinate system with a vertical polar axis, the azimuthal (changing-longitude) scan would consist of measurements at intervals of 360° ÷ M, while the polar-angle (change-latitude) interval would be 180° ÷ N. Then the volume, V, of the room would be given by

$$V = (4\pi/3MN)\sum_{k=1}^{M}\sum_{l=1}^{N} d_{kl}^3 \sin\theta_l$$

where d_{kl} is the distance to the wall, floor, or ceiling as measured at the kth longitude and the lth latitude and θ_l in the lth polar angle (colatitude).

The instrument is illustrated schematically in the figure. It should be possible to make the device small enough to be held by the operator. The unit would be powered by a battery. The rangefinder portion would be controlled by the microprocessor and very-large-scale-integrated control circuits. Operator inputs might include starting and stopping commands, scanning rate, angular resolution, and units of linear, area, or volume measurement. The program for the microprocessor might be contained in a plug-in read-only memory. A different memory could be plugged in to take a different kind of measurement.

To obtain an accurate area measurement, the scanning plane has to be level. The device could be placed on a tripod and leveled mechanically. The operator could also take several readings at different orientations, retaining the lowest reading. One of the computer programs could be set up to retain the lowest of several readings automatically.

For an accurate area reading, it is also necessary to place the instrument above any furniture or other large object in the room. Areas and volumes hidden from the beam by columns, pipes, or other obstructions will not be included in the measurements. The instrument might be programmed to recognize obstructions of small angular extent (for example, one angular interval) by ignoring distance measurements much shorter than those of adjacent angular positions and instead interpolating from the adjacent to the ignored values.

This work was done by Michael J. Kavaya of Caltech for **NASA's Jet Propulsion Laboratory**. *For further information, Circle 149 on the TSP Request Card. NPO-16629*

Double-Referenced, Pulsed, Phase-Locked Loop — DRP²L²

The phase shift between two tone-burst signals is measured precisely.

Langley Research Center, Hampton, Virginia

The DRP²L² system allows a precise measurement of the phase shift between two tone-burst signals initially derived from the same periodic source but delayed by different amounts through either path-length differences, propagation-velocity differences, or both. For example, the system can be used to measure accurately the phase shift encountered by an acoustic wave striking the front and back surfaces of a sample. With velocity known, the resulting measurement would be of sample thickness. With thickness known, the measurement would be of sound velocity. The technique applies to many sources of radiation and is not limited to acoustics.

The DRP²L² has one leg similar in design to the pulsed, phase-locked loop, P²L² (see figure). A voltage-controlled oscillator drives a gate/amplifier, which is turned on for several cycles by countdown-and-timing logic circuit 1. The gate/amplifier generates a tone burst exciting, for example, a first acoustic transducer. The sound wave propagates in the sample and is received at a second transducer, or as shown, at the first transducer.

The output of the second transducer is amplified/peak limited and split into two signals. One signal goes to phase detector 1, which receives its reference from the voltage-controlled oscillator through an electronically adjustable phase shifter. The signal from phase detector 1 goes through low-pass filter 1 to sample/hold

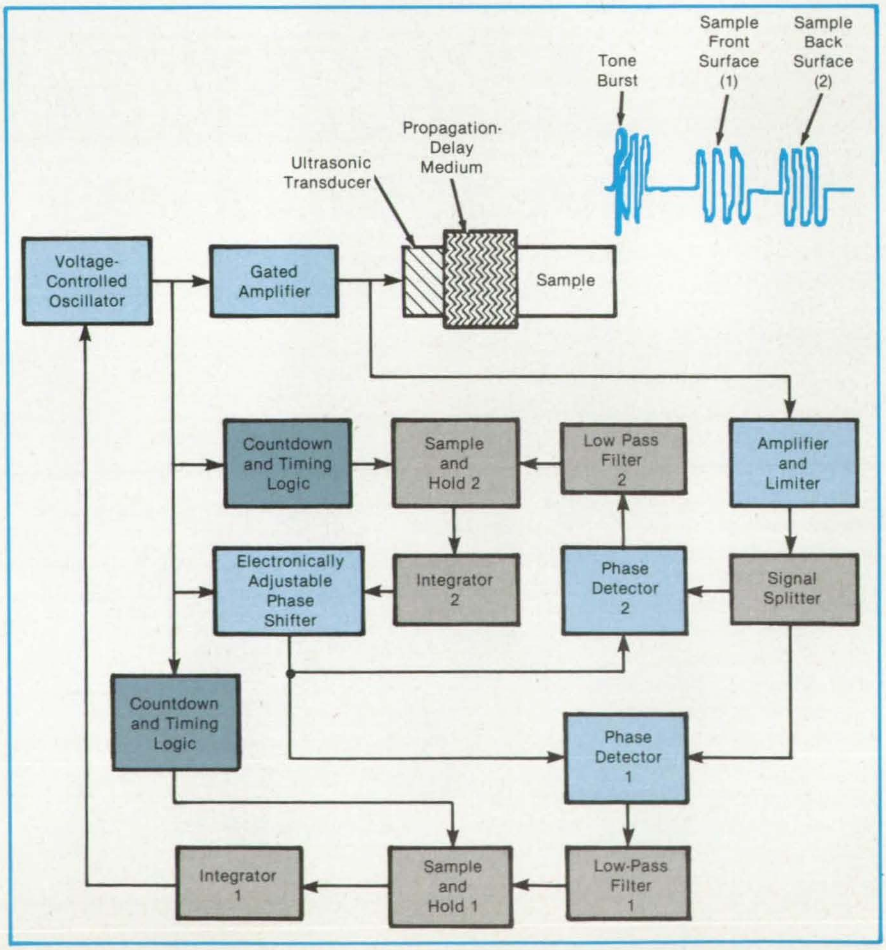

Loops 1 and 2 Share the Same Phase Shifter, thereby essentially eliminating the phase shift in the delay path.

module 1, which gets its logic signal from countdown-and-timing logic circuit 1. The output of sample/hold module 1 goes to integrator 1, the output of which is fed back to control the frequency of the oscillator.

If there is a propagation delay — for example, a water path between the sample and the second transducer — it will be included in the P^2L^2 phase measurement. That signal, called the sample front interface, is measured by phase-lock loop system 1. The signal from the sample back surface interface goes to phase detector 2, to low-pass filter 2, and to sample/hold module 2. This sample/hold module receives its logic pulse from countdown-and-timing logic circuit 2. The output of this sample/hold module is integrated and fed to the phase shifter.

Since both loops 1 and 2 are forced to quadrature and share the same phase shifter, a frequency representing a fixed number of waves or half-waves would exist in the sample. The effect of this would be to eliminate the phase shift in the water path. Countdown-and-timing logic circuits 1 and 2 ensure that each new tone burst occurs at a precise phase, that sufficient time has evolved to allow energy from the previous excitation to decay, and that the two sample/hold modules acquire their phase measurements at precise times.

The DRP^2L^2 system can use such other forms of radiation as electromagnetic waves (i.e., light or radio). The technique can be staged from one or both sides of a sample for accurate thickness or velocity measurements. Contour or shape measurements may be obtained by use of multiple transducer mountings. This system is insensitive to broad changes in signal amplitude (a phase-only signal), is ideal for the high resolution through the statistical averaging that is inherent in frequency measurements, and is independent of unwanted delays caused by the effects of coupling-path lengths or propagation.

This work was done by Joseph S. Heyman and Francis D. Stone of **Langley Research Center**. *For further information, Circle 119 on the TSP Request Card.*

This invention is owned by NASA, and a patent application has been filed. Inquiries concerning nonexclusive or exclusive license for its commercial development should be addressed to the Patent Counsel, Langley Research Center [see page 23]. Refer to LAR-13310.

Optical Interferometric Parallel Data Processor

Image data would be processed much faster than in present electronic systems.

NASA's Jet Propulsion Laboratory, Pasadena, California

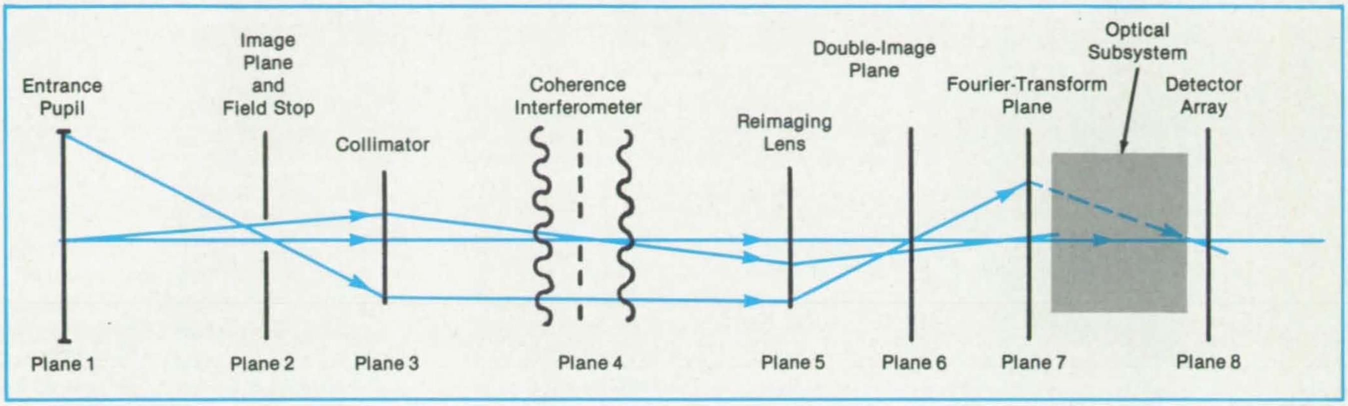

Figure 1. The **Optical Parallel-Processing System** would effectively calculate two-dimensional Fourier transforms in the time required by light to travel from plane 1 to plane 8.

A conceptual optical data-processing system would achieve throughputs as high as 4×10^{15} bits per second. This high computing speed is due to the inherently parallel nature of processing in an imaging system and to the short processing time, which equals the time required by light to travel through the system.

Figure 1 depicts the overall optical configuration. Plane 1 represents the entrance pupil of a foreoptic system (for example, a camera lens) that focuses light from the object into an image through a field stop at plane 2. A lens system at plane 3 collimates the light from the image at plane 2 and images the pupil of plane 1 into a coherence interferometer at plane 4.

The coherence interferometer is a specially-shaped beam-splitting prism similar to a type that has been used in optical, astronomical, and atmospheric research for more than 10 years. Essentially, this interferometer enables the system to perform the two-dimensional white-light spatial-frequency Fourier transform of the image. It splits the light energy into two parts corresponding to images that are inverted with respect to each other and located at opposite points with respect to the optical center line (see Figure 2).

The lens at plane 5 relays the interferometer output to plane 6, where the double images are actually formed and could be seen if a screen were to be placed there. However, there is no screen at 6; instead, the light is allowed to travel to plane 7.

Although the white light from different points on each of the double images is not coherent, the light from the two points corresponding to the same point of origin on the object is coherent. Thus, the electromagnetic fields radiating from the two images are correlated and form white-light interference fringes at plane 7. The spatial dependence of light intensity at this plane includes a uniform component plus a component proportional to the cosine Fourier transform of the white-light scene at plane 2.

A programmable spatial amplitude or phase filter or both would be placed at plane 7 to modulate spatially the Fourier transform with the transform of a function to be convolved with the image data. An optical subsystem would re-transform the filter output, forming a final two-dimensional correlation signal on plane 8. A detector array of charge-coupled devices would receive this signal and pass it to image- or data-processing circuitry.

This work was done by James B. Breckinridge of Caltech for **NASA's Jet Propulsion Laboratory.** *For further information, Circle 151 on the TSP Request Card.*
NPO-16382

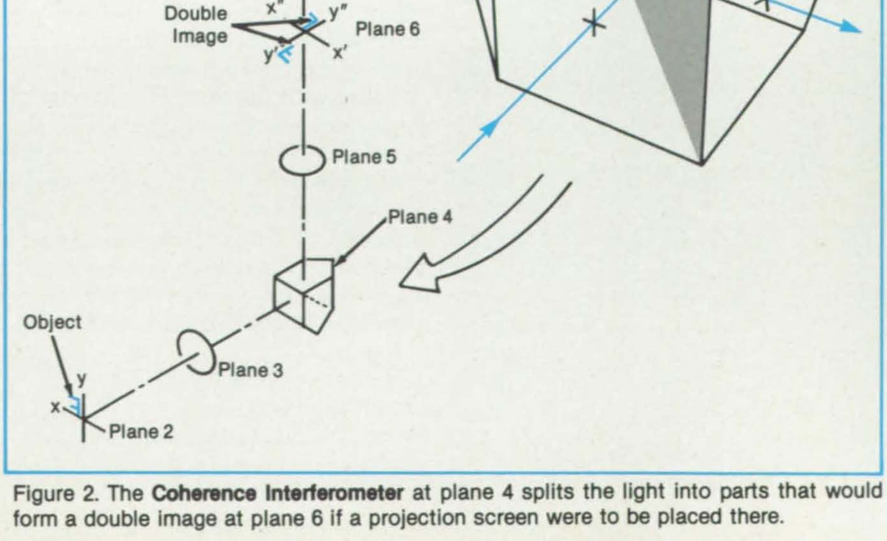

Figure 2. The **Coherence Interferometer** at plane 4 splits the light into parts that would form a double image at plane 6 if a projection screen were to be placed there.

Physical Sciences

Hardware, Techniques, and Processes

Books & Reports

Computer Programs

Liquid-Crystal Thermal-Control Panels

Radiative temperature regulators would have no moving parts.

Marshall Space Flight Center, Alabama

A conceptual temperature-regulating system proposed for spacecraft may be useful in the automatic or remotely controlled regulation of solar heating in buildings, provided that the cost can be reduced sufficiently. The system would consist of liquid-crystal panels that can be made to absorb or reflect sunlight.

A liquid-crystal panel is made absorbent or reflective by the application of a voltage. The voltage could be applied or removed according to the command from a thermostat, a photosensor, or a timer. To provide a controlled heating rate, the panel could be turned on and off according to a prescribed duty cycle.

Previously, panels with complicated mechanical linkages (reminiscent of venetian blinds) were used to alternate between absorption and reflection. Such panels are subject to breakage, wear, and jamming. Furthermore, they require considerable amounts of power. In contrast, the liquid-crystal panels have no moving parts and require very little power.

The liquid-crystal panels can be mounted on or near the surfaces to be heated or shielded from heating. They can be made with curved rear surfaces that conform to curved mounting surfaces. The panels can also be made in many small pieces in blankets that are unrolled like window shades over the areas to be heated or protected.

This work was done by Robert F. DeHaye, Teddy M. Edge, and William R. Feltner of **Marshall Space Flight Center**. *No further documentation is available.*

Inquiries concerning rights for the commercial use of this invention should be addressed to the Patent Counsel, Marshall Space Flight Center [see page 23]. Refer to MFS-28036.

Inexpensive Meter for Total Solar Radiation

This instrument aids in deciding on the proper time to harvest crops.

NASA's Jet Propulsion Laboratory, Pasadena, California

A pyranometer containing solar cells measures the combined intensity of direct light from the Sun and diffuse light from the sky. The instrument includes a polyethylene dome that diffuses entering light so that the output of the light detectors does not vary significantly with the changing angle of the Sun during the day. The instrument therefore does not have to be calibrated for the response of each detector to the Sun angle, and the sensor outputs do not have to be corrected separately before they are summed and integrated.

The pyranometer was developed as a simple, rugged, and inexpensive unit for agricultural use. In particular, it can help in deciding when to harvest such crops as sugarcane and grapes, the ripenesses of which are closely tied to total solar exposure.

Five silicon solar cells are placed with one on each of the sides and one on the top of a truncated pyramid (see figure). The cells are connected in parallel, and their outputs feed to a current meter or recorder. The current could also be fed to an integrator that indicates the cumulative solar radiation in terms of the solar-cell energy output, perhaps in convenient units of milliwatt-hours. A leveling screw adjusts the tilt of the cell assembly to suit the local latitude. No further adjustments are needed to allow for seasonal changes in the solar declination.

This work was done by Eric G. Laue of Caltech for **NASA's Jet Propulsion Laboratory.** *For further information, Circle 18 on the TSP Request Card.*
NPO-16741

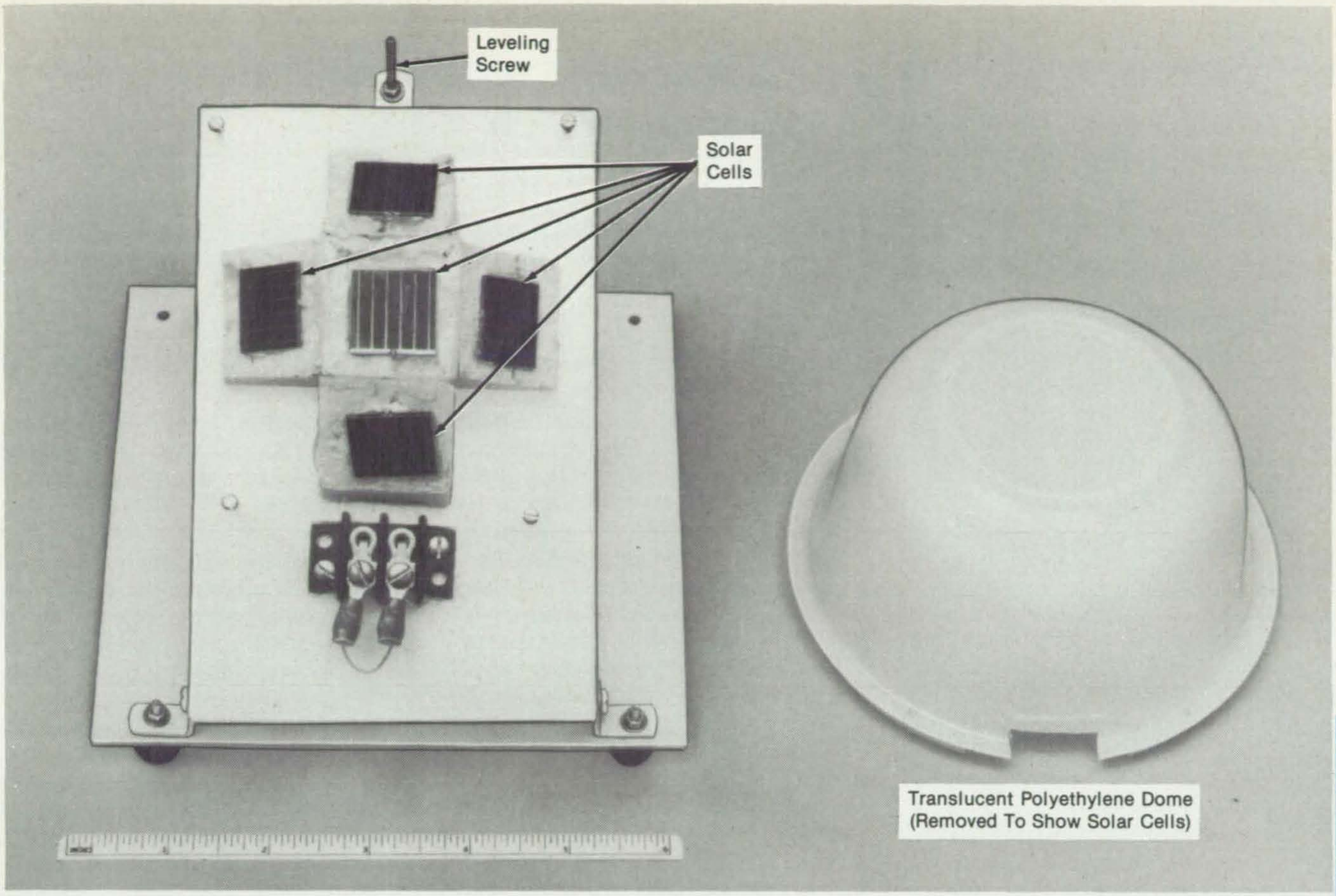

A **Translucent Dome** is placed over an array of silicon solar cells. By suppressing the effect of the Sun angle, the dome makes extra circuitry for angular corrections unnecessary.

Books and Reports

These reports, studies, and handbooks are available from NASA as Technical Support Packages (TSP's) when a Request Card number is cited; otherwise they are available from the National Technical Information Service.

Microwave Properties of Quiet Seas

Measurements from a satellite provide information for comparisons and analyses.

The microwave fluxes from three quiet seas have been documented for five microwave frequencies. The measurements were taken by a satellite in Earth orbit with a mechanically scanned antenna. A 10-channel receiver was used to record simultaneously the signal intensities in both horizontal and vertical polarizations at each frequency.

A quiet sea is one in which the products of air/sea interaction — foam, bubbles, and spray — are minimal. The quiet sea serves as a reference-level sea that can be used for comparisons with other sea states as observed from Earth orbit.

The three quiet seas are an area on the Equator in the Pacific near South America, one at a middle latitude in the Sargasso Sea, and one at a high latitude in the Indian Ocean between Madagascar and Antarctica. Comparisons of the flux measurements of the three quiet seas are drawn, and the results are discussed and analyzed.

Microwave measurements can be used to deduce the thermal properties of the sea surface. They are not seriously degraded by tenuous and moderately dense clouds. However, raining clouds and clouds that contain water droplets do attenuate microwaves significantly.

A further advantage of microwave sensing is that the polarities of sea reflections may be discerned. Differences and ratios of polarized signals may be formed to provide information on important sea properties. For example, the difference between horizontally and vertically polarized fluxes can be used to infer sea roughness and the presence of such pollutants as oil films.

The plots taken from the measurements show the following:

- The effects of the relative, on-axis gain of the collecting aperture for each frequency (6.6, 10.69, 18, 21, and 37 GHz);
- The effects of polarization rotation in the outputs of the receiver when the collecting aperture mechanically rotates about a fixed feed;
- The difference between the flux magnitudes for the horizontal and vertical channels, at each of the five frequencies, and for each pointing position, over a 44° scan angle; and
- The root-mean-square value of the clutter, as reckoned over the interval of a full swath and derived from the standard error of estimate of the plotted swath response for each channel.

The expected value of the background temperature is computed for each of the three quiet seas that were observed. The background temperature includes contributions from the cosmic background, the downwelling path, the sea surface, and the upwelling path.

This work was done by Joseph M. Stacey of Caltech for **NASA's Jet Propulsion Laboratory**. *Further information may be found in NASA CR-176199 [N85-35322/NSP], "Microwave Properties of a Quiet Sea."*

Copies may be purchased [prepayment required] from the National Technical Information Service, Springfield, Virginia 22161, Telephone No. (703) 487-4650. Rush orders may be placed for an extra fee by calling (800) 336-4700.
NPO-16691

Materials

Hardware, Techniques, and Processes

Books and Reports

Rapid Synthesis of Nonstoichiometric Lanthanum Sulfide

A new process is relatively fast and simple.

NASA's Jet Propulsion Laboratory, Pasadena, California

An improved method of synthesizing nonstoichiometric lanthanum sulfide is faster and simpler than the former method. The product may be purer because some of the prior sources of contamination are eliminated.

In the former method, a lanthanum ingot was cut or ground into small chips. Along with the required amount of sulfur, the chips were sealed under vacuum in a quartz ampoule. The ampoule was placed in a resistance-heated furnace at a temperature of 500 to 800 °C, which was below the melting point of lanthanum. The reaction took several days because the sulfur had to diffuse through and into the lanthanum chips.

In the new method, the lanthanum ingot is placed directly in a flat-bottomed graphite boat and enclosed in a heat- and chemical-resistant glass ampoule. The sulfur is placed in a sulfur reservoir that communicates with the ampoule, and the ampoule/reservoir system is sealed under vacuum.

The lanthanum ingot is melted by radio-frequency heating of the graphite boat. The liquid lanthanum spreads over a large area in the boat. The sulfur is heated to 300 to 450 °C, causing it to vaporize. This vapor reacts quickly with the lanthanum; the reaction is complete in about 2 hours.

The reaction is faster in the new process because the lanthanum is molten. The elimination of grinding or cutting not only simplifies the process but also eliminates contamination from the grinding or cutting machinery. In the new method, the oxidation of the lanthanum by oxygen in the glass is suppressed in two ways: (1) The lanthanum does not touch the glass, and (2) the glass remains below 400 °C during the radio-frequency heating, thereby reducing the rates at which oxygen diffuses from within and permeates through the glass.

This work was done by Seigo Matsuda, Edik Shapiro, Lee Danielson, and Harold Hardister of Thermo Electron Corp. for **NASA's Jet Propulsion Laboratory.** *For further information, Circle 82 on the TSP Request Card.*
NPO-16631

Books and Reports

These reports, studies, and handbooks are available from NASA as Technical Support Packages (TSP's) when a Request Card number is cited; otherwise they are available from the National Technical Information Service.

Fire-Retardant, Decorative Inks

The effectiveness of fire-retardant additives is evaluated.

The fire retardance of decorative acrylic printing inks for aircraft interiors may be enhanced by certain commercial and experimental fire-retardant additives, according to a study. In the study, standard brominated fire retardants and new polymeric brominated retardants were incorporated into a commercial acrylic ink. The resulting formulations were evaluated for solubility in methyl ethyl ketone (the acrylic-ink solvent), thermal stability, compatibility with acrylic-ink processing, flammability, and smoke emission.

The following retardants were evaluated:

- 2,3-dibromopropyl acrylate, a commercial vinyl-terminated product;
- Bis(β-chloroethyl)vinyl phosphonate, another vinyl-terminated product;
- Brominated polymeric additive (BPA) F2001P, a commercial brominated fire retardant containing 50 percent bromine largely as aromatic bromine, which is highly thermostable;
- F2001P with tribromophenol (TBP) — the TBP increases the bromine content to 58 percent;
- F2001P with rubberized TBP — carboxy-terminated butadiene acrylonitrile rubber gives this additive greater resistance to impact;
- F2001P with pentabromophenol (PBP) — the PBP increases the bromine content to 63 percent, even higher than TBP; and
- F2001P with rubberized PBP.

The limiting oxygen index (LOI) was used as one of the measures of flammability. The

inks with the commercial vinyl-terminated additives proved to be slightly more effective than the neat acrylic ink in retarding fire. The derivatives of F2001P produced LOI's higher than those of the commercial additives. The higher the rubber content, the higher the LOI.

Thermogravimetric analysis and differential scanning calorimetry were used to evaluate thermostability. The rank order turned out to be somewhat different from that for flammability. The simple F2001P additive produced the most stable ink and was followed by the rubberized formulations. The inks with commercial additives and the plain acrylic ink were lowest on the scale of stability.

This work was done by D. A. Kourtides of **Ames Research Center,** *Z. Nir of the National Research Council, and J. A. Mikroyannidis of the University of Patras. To obtain a copy of the report, "Fire-Retardant Decorative Inks for Aircraft Interiors," Circle 61 on the TSP Request Card.*

Inquiries concerning rights for the commercial use of this invention should be addressed to the Patent Counsel, Ames Research Center [see page 23]. Refer to ARC-11499.

Radiation Effects on Polymer Properties

Tables present lowest doses for which effects are noticeable.

A report compiles data on the effects of radiation on the physical properties of synthetic organic materials. Emphasis is on materials of interest to nuclear-equipment and nuclear-reactor designers. The data cover five categories of polymeric materials: Insulators, elastomeric seals and gaskets, lubricants, adhesives, and coatings. More than 250 materials are represented. The document reflects a continuation of the work reported in the preceding article.

A table gives available data on physical, electrical, and optical properties for each material in terms of the lowest reported threshold dose (LTD), which indicates the radiation level at which radiation effects become apparent and the dose for a 25 percent change in the specified property. The literature source for the data is indicated.

Both the LTD and the 25-percent-change dose vary widely within each of the five categories of polymer. Most of the polymeric materials have thresholds above 10^5 rads. Five materials have thresholds below 10^5 but above 10^4 rads; namely, fluorocarbons, nylons, epoxy resins, polyethylene oxides, and polyalphamethyl chloroacrylates.

The LTD data are useful for setting a lower limit at which changes can be expected. They may also be used as a guide for deciding when the expected radiation is low enough to be disregarded for a given polymer. The 25-percent-change dose is a valuable radiation statistic because changes are real at this dose level and are neither artifacts of the experiments nor results of sample variations.

This work was done by Frank L. Bouquet and John W. Winslow of Caltech for **NASA's Jet Propulsion Laboratory.** *To obtain a microfiche of the report, "Radiation Data Definitions and Compilation for Equipment Qualification Data Bank," Circle 1 on the TSP Request Card.*
NPO-16426

Effects of Radiation on Capacitor Dielectrics

Data have been gathered on key design parameters.

A report discusses a study of the electrical and mechanical properties of irradiated polymer dielectric materials. These data were compiled for use by designers of high-energy-density capacitors that operate in the presence of ionizing radiation.

The study focused on polycarbonates, polyetheretherketones, polymethylpentenes, polyimides (including polyetherimide), polyolefins, polysulfones (including polyethersulfone and polyphenylsulfone), and polyvinylidene fluorides. The properties considered were the dielectric loss factor or loss tangent, tensile strength, dissipation factor, volume resistivity, surface resistivity, dielectric constant, gas evolution (during irradiation), and mechanical-strength parameters. Recent test data, previously unpublished, were obtained from both foreign and domestic industry sources. Measurements of properties before, during, and after irradiation were sought. Radiation doses from zero to as much as 10^{10} rad were considered.

The data are presented in tables, graphs, and in text. The report also includes references to the published literature, diagrams of the molecular structures of the polymers studied, definitions of abbreviations, and a glossary.

On the basis of the compiled data, the study reached the following conclusions:

- The polyetheretherketones, polymethylpentenes, polyimides, and polysulfones retain their mechanical strengths at the highest radiation levels.
- The lowest dissipation factors were exhibited by polyetheretherketones, polymethylpentenes, and polyimides.
- Polyethylene and polypropylene should probably not be used, because they emit undesirable amounts of gases when irradiated.
- Of the materials studied, the polyimides and polyetheretherketones are the best materials for use in high energy-density capacitors.

This work was done by Frank L. Bouquet, Robert B. Somoano, and Peter O. Frickland of Caltech for **NASA's Jet Propulsion Laboratory**. *To obtain a copy of the report, "Dielectric Materials for High Energy Density Capacitors," Circle 40 on the TSP Request Card.*
NPO-16761

Screening Mechanically-Defective Solar Cells

A flexure test eliminates failure-prone wafers before further processing.

The probability of cracking of silicon solar cells can be substantially reduced by mechanical proof testing of silicon wafers before further processing, according to a report. The report is based on a study that demonstrated that weak wafers can be eliminated by subjecting all the wafers in a manufacturing batch to a biaxial-flexure test.

The test is performed after the wafers have been chemically polished but before junctions are formed in them. Wafers that are likely to crack in service or during processing break as soon as they are flexed in a test jig. Those wafers having no internal flaws that would eventually cause mechanical failure withstand the flexure test.

The study showed that the biaxial-flexure test does not induce additional damage in otherwise good wafers; that is, if a wafer is sound, the testing does not create flaws that would later weaken the specimen.

The experimental results were analyzed statistically. The biaxial-strength distribution of silicon wafers that failed from surface flaws was found to correspond to a Weibull equation. The critical flaw sizes were found to be 4.6, 3.1, and 2.1 μm for proof-testing stress levels of 215, 260, and 310 MPa, respectively.

This work was done by Chern P. Chen and Martin H. Leipold of Caltech for **NASA's Jet Propulsion Laboratory.** *To obtain a copy of the report, "Stress Rate and Proof Testing of Silicon Wafers," Circle 5 on the TSP Request Card.*
NPO-16573

Thermoelectric Properties of Lanthanum Sulfide

At 300 to 1,400 K, γ-phase $La_{3-x}S_4$ is an extrinsic semiconductor.

A report describes the measurement of the Seebeck coefficient, electrical resistivity, thermal conductivity, and Hall effect in γ-phase lanthanum sulfide with composition of $La_{3-x}S_4$ ($0.04 \leqslant x \leqslant 0.3$). Results of this study, part of the search for high-temperature thermoelectric energy-conversion materials, indicate that this sulfide behaves like an extrinsic semiconductor over the temperature range of 300 to 1,400 K, with a degenerate carrier concentration controlled by the stoichiometric ratio of La to S.

Lanthanum sulfide was prepared by the reaction of lanthanum ribbon with sulfur in quartz ampoules, the melting of the product in tungsten crucibles, and then the grinding of the powder. The specimens for thermoelectric study were then prepared by hot pressing in vacuum at a temperature of approximately 1,800 K and at a mechanical pressure of 10^4 psi (69 MN/m^2) for about 1 h. X-ray diffraction showed the hot-pressed pellets to be γ-phase. The composition of the pellets was determined by the amount of hydrogen evolved when they were dissolved in acid.

A four-probe method was used to measure the electrical conductivities. The Seebeck coefficients were determined by use of small temperature gradients. These measurements were confirmed by measurements at large temperature gradients; that is, by the Seebeck voltages measured as functions of temperature and then differentiated to obtain the Seebeck coefficients. The dc van der Pauw technique was applied to obtain the Hall-effect measurements. These were made as a function of temperature on 1-mm-thick slices cut perpendicularly to the axes of cylindrical samples.

Thermal conductivities were calculated from the thermal diffusivities, the densities (determined by Archimedes' principle), and the specific heat (measured between 300 and 900 K by a differential scanning calorimeter). The mass loss rate of the sulfide was determined in situ as a function of temperature by a mass-spectrometer thermal gravimetric apparatus in a vacuum of 10^{-8} torr (1.3×10^{-6} N/m^2).

Results showed that all Seebeck coefficients are n-type, and both the resistivities and Seebeck coefficients increase approximately linearly with increasing temperature. In these respects, the materials resemble metals. There is no indication from the data that the materials in this composition and temperature range become intrinsic semiconductors. The Hall constants and thus the carrier concentrations are almost invariant with temperature. The Hall mobilities are low and are approximately proportional to the reciprocal of temperature, as expected for metallike behavior.

The data are consistent with lanthanum sulfide in the specified composition range being an extrinsic semiconductor; i.e., the conduction process is by the itinerant motion of large (nearly degenerate) concentrations of quasi-free electrons undergoing acoustic-mode scattering. A theoretical analysis of the data yielded fairly high values for the electron effective mass (in the range of 2 to 3) and low values for electron mobilities (in the range of 1 to 6 $cm^2V^{-1}s^{-1}$), which suggest that the energy bands are fairly narrow.

Experimental results and theoretical analysis showed that the optimum figure of merit (Z) should occur for compositions in the range $x = 0.30$ to 0.32. The highest experimental value for Z was approximately 5×10^{-4} at 1,000 °C. Although it may be possible to exceed this value slightly by a slight adjustment in composition, large improvements are not anticipated because of the low electron mobilities. These results suggest that to realize higher Z, a search should be made for rare-earth chalcogenides of comparable electron effective masses but having higher charge-carrier mobilities.

This work was done by Charles Wood, R. Addis Lockwood, James B. Parker, Andrew Zoltan, Leslie D. Zoltan, Lee Danielson, and Valvo Raag of Caltech for **NASA's Jet Propulsion Laboratory**. *To obtain a copy of the report, "Thermoelectric Properties of Lanthanum Sulfide," Circle 56 on the TSP Request Card.*
NPO-16662

Evaluation of GaAs Fracture Mechanics

These data can aid the design of solar cells.

A report provides data on the fracture properties of single-crystal GaAs. These data are required for the design of reliable GaAs solar cells and modules.

Measured by ultrasonic-velocity techniques, the elastic moduli of GaAs single crystals were found to be highly anisotropic. The Young's moduli in the <100>, <110>, and <111> crystal orientations are 8.93×10^{11}, 12.50×10^{11}, and 14.40×10^{11} dyn/cm^2, respectively. The effect of temperature on the elastic modulus was not appreciable in the range of -130 to 450 °C, and no effect of dopant (Si vs. Te) was observed.

The measured coefficients of thermal expansion in the range of -130 to 450 °C were 5.6×10^{-6} $(°C)^{-1}$ for Si-doped GaAs and 5.3×10^{-6} $(°C)^{-1}$ for Te-doped GaAs: The small difference between these values was not statistically significant. These values were also not significantly affected by the temperature or the crystal orientation.

The fracture toughness was measured under four-point bending, with a controlled flaw produced by a pyramid-shaped diamond indentation. GaAs was found to be extremely fragile, with fracture toughnesses of 0.43, 0.31, and 0.45 $MN/m^{3/2}$, respectively, in the {100}, {110}, and {111} cleavage planes. In comparison, single-crystal silicon has corresponding fracture toughnesses of 0.95, 0.90, and 0.82 $MN/m^{3/2}$. The fracture toughness of GaAs was not affected by Te vs. Si doping or by temperatures in the range of -8 to 121 °C.

The delayed emergence of cracks after the removal of the indentor suggests that crystalline GaAs is susceptible to subcritical crack growth. This is important because subcritical cracks introduced during manufacture could cause the fracture of GaAs solar cells long after installation.

Similar fracture tests were also performed on GaAs wafers after successive processing stages in the manufacture of solar cells. Wafers were tested as cut and polished, coated by chemical-vapor deposition, metallized, and soldered. The fracture-stress data were then analyzed using Weibull statistics. Chemical-vapor deposition appeared to produce some damage on the wafer surface, possibly as a result of the thermal shock during deposition. However, the wafer edges were not damaged. Antireflection coating and soldering materials increased the apparent strengths of cells. Mechanical polishing of cut wafers did not produce significant increases in their strengths. The strengths of GaAs wafers were not affected by temperatures within the range of -87 to 121°C. Preliminary results indicate that the strength of GaAs tends to increase with increasing etch-pit density within the range of 5,000 to 20,000 etch pits per cm^2.

A long tail at the low-stress portion of the strength-distribution curve was found for several types of samples. The wafers or cells in the low-strength distribution are

likely to be fractured during subsequent cell processing and handling. A proof test would be useful to eliminate these weak samples.

This work was done by Chern P. Chen of Caltech for **NASA's Jet Propulsion Laboratory.** *For further information, Circle 13 on the TSP Request Card.*
NPO-16604

Microstructure and Aging of Powder-Metallurgy Al Alloys

Peak hardness is achieved at lower aging temperatures than with standard ingot-metallurgy alloys.

A report describes an experimental study of the thermal responses and aging behaviors of three new aluminum alloys. The alloys are produced from rapidly solidified powders and contain 3.20 to 5.15 percent copper, 0.24 to 1.73 percent magnesium, 0.08 to 0.92 percent iron, and smaller amounts of manganese, nickel, titanium, silicon, and zinc. These alloys are of interest for automobile, aircraft, and aerospace applications.

In this study, Rockwell B hardness measurements; optical, scanning-electron, and transmission-electron microscopy; and energy-dispersive x-ray analysis were used to correlate the microstructures with the measured mechanical properties (yield strength, ultimate tensile strength, elongation to failure, and notched tensile strength). These tests were performed on the alloy specimens both as received and after various heat treatments. The fracture surface of each tensile specimen was examined by scanning-electron microscopy.

This study led to the following conclusions:

- Increased temperatures of solution heat treatment were effective in re-dissolving coarse primary constituents in the alloy containing 5.15 percent copper, but had little effect on the microconstituents in the alloys containing less copper.
- Studies of aging at room temperature, 120, 150, and 180 °C for times ranging up to 60 days indicated that classic aging-response curves, as determined by hardness measurements, occurred at aging temperatures lower than those previously studied or generally used for ingot-metallurgy alloys of similar compositions. The principal microstructural feature associated with peak hardness is an extremely fine and homogeneously distributed S′ or θ' phase.
- High tensile strengths of notched specimens were typically associated with fine, homogeneous distributions of strengthening S′ or θ' phases and decreases in the sizes and volumes of dispersoids or large soluble precipitates, as compared to those of the specimens of lower strength. The fracture surfaces of notched specimens of low strength exhibited homogeneous distributions of equiaxial dimples resulting from microvoid coalescence initiated at second-phase particles. The fracture surfaces of the stronger notched specimens were more irregular, exhibiting numerous smooth regions attributed to matrix shear.
- Variations in heat-treatment procedures, including changes in the temperatures and times of the solution heat treatments and of aging, produced mechanical properties comparable to those achieved previously by cold working and natural aging.

This work was done by Linda B. Blackburn of **Langley Research Center.** *To obtain a copy of the report, "Microstructure-Mechanical Property Relationships for Various Thermal Treatments of Al-Cu-Mg-X PM Aluminum Alloys," Circle 36 on the TSP Request Card.*
LAR-13298

Computer Programs

COSMIC: Transferring NASA Software

COSMIC, NASA's Computer Software Management and Information Center, is the one central office established to distribute software that is developed with NASA funding. COSMIC's role as part of NASA's Technology Utilization Network is to ensure that NASA's advanced software technology is made available to industry, other government agencies, and academic institutions.

Because NASA's software development efforts are dynamic and ongoing, new programs and updates to programs are added to COSMIC's inventory on a regular basis. *Tech Briefs* will continue to report information on new programs. In addition, the 1986 edition of the *COSMIC Software Catalog* is available with descriptions and ordering information for available software. Several new programs for control systems/robotics, expert systems, thermal analysis, turbomachinery design, structural analysis, and computer graphics are offered.

For additional information on any programs described in this issue of *Tech Briefs*, circle the appropriate number on the TSP card at the back of the publication. If you don't find a program in this issue that meets your needs, you can call COSMIC directly at (404) 542-3265 and request a review of programs in your area of interest. There is no charge for this information review.

COSMIC®
Computer Services Annex, University of Georgia, Athens, GA 30602; Phone (404) 542-3265
John A. Gibson, Director

Computer Programs

These programs may be obtained at a very reasonable cost from COSMIC, a facility sponsored by NASA to provide tested and reliable software to the public. For information on program price, size and availability, circle the reference number on the TSP and COSMIC Request Card in this issue.

Physical Sciences

Planning Orbiter Flights

Maps and ephemeris data are generated.

The Shuttle Mission Design and Operations Software (SMDOS) assists in the design and operation of missions involving spacecraft in low orbits around the Earth by providing orbital and graphics information. SMDOS can plot radar-impingement swaths, nadir tracks (projections of spacecraft orbital paths on Earth), and maps with or without specific site locations. SMDOS was successfully used in the 1984 Space Shuttle Imaging Radar project (SIR-B). This mission involved the recording of radar pulses aimed at designated areas of the Earth for new agricultural, oceanographic, and geological information.

SMDOS can perform the following five functions: (1) display two world and two polar maps or any user-defined window 5° high in latitude by 5° wide in longitude in one of eight standard projections, (2) designate Earth sites by points or polygon shapes, (3) plot the spacecraft ground track with 1-min demarcation lines, (4) display, by means of different colors, the availability of the Tracking and Data Relay Satellite to the Shuttle, and (5) calculate the available times and orbits to view a particular site, and the corresponding look angles.

SMDOS is menu-driven and displays prompts for the required input. The user creates an ephemeris with SMDOS, generating the latitude, longitude, and altitude of the spacecraft. This file can be manually created using orbital elements, or automatically generated by using such formal state vectors as those supplied by the Johnson Space Center.

SMDOS is written in Laboratory Microsystems FORTH (1979 standard) for interactive execution and has been implemented on an IBM XT computer operating under DOS with a central-memory requirement of approximately 512 Kbytes. IBM AT graphics are not compatible. SMDOS requires the following hardware: 8087 math coprocessor, monochrome display, color graphics board and RGB monitor, and a hard disk. A dot-matrix printer and an IBM EY-750 Plotter are optional to exercise all capabilities. SMDOS was developed in 1984.

This program was written by Henry M. Harris, Mark J. Bergam, Su L. Kim, and Elizabeth A. Smith of Caltech for **NASA's Jet Propulsion Laboratory**. *For further information, Circle 133 on the TSP Request Card.*
NPO-16933

Program for Thermospheric Calculations

Atmospheric properties at high altitudes are predicted.

MSIS83 is a computer program for an empirical model of the thermosphere based on mass-spectrometer and incoherent-scattering data. It provides a description of the atmospheric temperature, density, and composition at altitudes higher than 85 kilometers. There are coefficients in MSIS83 to account for yearly and daily variations, geodetic latitude and longitude, and solar activity. Variations due to magnetic storms are represented by 3-hour magnetic a_p indices. The MSIS83 model enables a more timely prediction of aeronomic densities for such specific events as rocket flights.

The data base for this model is a comprehensive summary of rocket flight, satellite, incoherent-scattering radar, grenade, and falling-sphere measurements. Subsets of data were formed by random selection after sorting on altitude, latitude, time of day, etc. Curve fitting was done with 4- to 5-thousand data points at a time. The resulting coefficients are presented in subroutines that calculate the thermospheric composition and temperature for a position and time supplied by the user.

MSIS83 is written in FORTRAN 77 for use with batch or interactive programs and has been implemented on a DEC VAX-series computer operating under VMS with a central-memory requirement of approximately 18K of 8-bit bytes. MSIS83 is based on a 1977 implementation of a thermospheric model and was last updated in 1983.

This program was written by A. E. Hedin of **Goddard Space Flight Center**. *For further information, Circle 75 on the TSP Request Card.* GSC-12989

Machinery

Evaluating Performances of Solar-Energy Systems

Efficiencies can be calculated and maximized.

The CONC11 computer program calculates the performances of dish-type solar thermal collectors and power systems. The solar thermal power system consists of one or more collectors, power-conversion subsystems, and power-processing subsystems. CONC11 is intended to aid the system designer in comparing the performance of various design alternatives.

The solar collectors may be flat or paraboloidal. Each is composed of a concentrator and a receiver to concentrate reflected or refracted sunlight and convert the energy to heat in a working fluid. The power-conversion subsystem converts this heat into mechanical or electrical energy. If the desired output is heat, this subsystem is omitted. The power-processing subsystem transfers the mechanical or electrical energy to the system output device.

Given the characteristics of the various subsystems, CONC11 calculates collector efficiency and overall power-system efficiency as functions of receiver temperature for a specified steady insolation. CONC11 has options to optimize the receiver aperture, receiver temperature, and intercept factor for providing the highest efficiency at a given insolation.

CONC11 is written in Athena FORTRAN and Assembler for interactive execution and has been implemented on a UNIVAC 1100-series computer with a central-memory requirement of approximately 16K of 16-bit (minimum) words. CONC11 was developed in 1984.

This program was written by Leonard D. Jaffe of Caltech for **NASA's Jet Propulsion Laboratory**. *For further information, Circle 104 on the TSP Request Card.* NPO-16717

Mechanics

Hardware, Techniques, and Processes

Books & Reports

Eddy-Current Detection of Weak Bolt Heads

An electronic test identifies flawed units that pass hardness tests.

Marshall Space Flight Center, Alabama

An eddy-current test detects weakness in the head-to-shank junctions of ¼-28 cup-washer lock bolts. The test was developed for alloy A286 steel bolts in the Space Shuttle main engine fuel turbopump. Some of the bolts were failing in tension tests, even though they had passed hardness tests designed to measure strength.

A complex process is required to increase the tensile strength of the steel to 2×10^5 lb/in.^{2} (1.4 GPa), compared with the normal fully heat-treated value of 1.4×10^5 lb/in.^{2} (0.97 GPa). This process sometimes leaves relatively weak regions in the bolt head, even though a Rockwell C hardness test on the shank end yields the minimum allowable value of 39 or more. The shape of the head prevents hardness tests from being made there. The eddy-current test examines the full volume of the head, including the head-to-shank transition and thus can nondestructively screen out potentially defective units.

Since alloy A286 is a precipitation-heat-treatable austenitic nickel/chromium steel, it is readily inspectable by eddy currents. This inspection is possible because as the strength of the alloy is increased by heat treatment or cold working, its electrical conductivity decreases. A region of higher conductivity in the head, as indicated on the eddy-current meter, is therefore a weaker region.

Calibration standards, special induction coils, and a procedure have been prepared for the eddy-current test. The test can be performed by unskilled people with a minimum of training. The test sorts bolts at a rate of 20 per minute. It rejects a small percent of marginally strong bolts but does not accept any weak bolts. The test can be adapted to any other alloys, the mechanical properties of which are improved by solution heat treatment and aging or by cold working or by both.

This work was done by Carmen P. Messina of Rockwell International Corp. for **Marshall Space Flight Center**. *No further documentation is available.*
MFS-29092

Eddy-Current Detection of Cracks in Tubes

A nondestructive device tests narrow, sharply-bent metal tubes.

Marshall Space Flight Center, Alabama

An eddy-current probe detects incipient cracks inside small metal tubes. The probe was developed for coolant tubes in the Space Shuttle main engine nozzle. The tubes are bent sharply just before they are assembled in the engine. Previously, the tubes were inspected for post-bend cracks by destructive metallographic examinations of samples in a batch. If only a few samples were found defective, the entire batch had to be scrapped. Since the value of the tubes is significant at this stage of fabrication — more than $250 each — a substantial investment is lost when a batch is discarded. If half of the tubes are good and can be used instead of being scrapped, an estimated saving of $125,000 would be realized on an engine. The new probe makes it possible to distinguish the

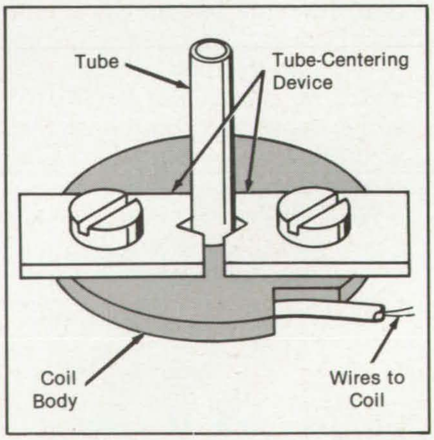

A **Tube-Centering Device** consisting of a pair of opposed bars ensures that a tube is centered on the eddy-current coil. The probe can be moved along the length of a bent tube to inspect repeatably for cracks.

Multiple Pages Intentionally Left Blank

good bent tubes from the cracked ones.

The probe consists of an eddy-current generating and detecting coil or pair of coils on which a pair of centering bars is mounted (see figure). The magnitudes and phases of the eddy currents induced in a tube as it passes between the bars indicates the depths of cracks; the current amplitudes and phases are displayed on an oscilloscope.

The probe is thin and can therefore accommodate small-radius bends in tubes. The diameter of the coil and the distance between the centering bars can be changed to suit a variety of tube diameters. Instead of a single coil, a pair of coils can be used for differential current measurements. The coil-excitation frequency can be adjusted to give adequate penetration for a particular tube alloy and wall thickness. The probe is compatible with tubes of many different cross sections — oval, flattened, square, rectangular, or irregular.

Besides its Space Shuttle application, the probe could be adapted for inspecting formed tubes in petrochemical, automotive, nuclear, and medical equipment. Its tube-centering feature makes it useful in testing straight tubes as well.

This work was done by R. G. Parent and D. D. Kettering of Rockwell International Corp. of **Marshall Space Flight Center**. *No further documentation is available.*
MFS-29081

Depth Gauge for Liquids Under High Pressure

An ultrasonic transducer is protected from high pressure and is easy to connect.

Langley Research Center, Hampton, Virginia

A continuous reading of the depth of a liquid in a vessel at pressures exceeding 5,000 psi (34 MN/m^2) is obtained from ultrasonic waves emitted from a transducer that is mounted in a modified high-pressure plug. A flat-bottom hole is drilled into the plug, leaving enough wall to meet the pressure-vessel code. An ultrasonic transducer is rigidly bonded to the inner end of the hole. The plug is inserted into the pressure-vessel wall in a way that leaves the transducer exposed to the atmosphere (see figure). This protects the transducer from high pressure and makes it easier to connect supporting electronic devices.

In operation, the transducer excites the plug flange into vibration, sending an ultrasonic pulse through the liquid to the liquid/gas interface where the pulse is reflected. The returning pulse is intercepted by the transducer and transmitted to the supporting electronics that compute the liquid depth.

The prototype device was used in a high-temperature-structures tunnel that has cooling water pressurized to 6,000 psi (41 MN/m^2). A 7/16-in. (11-mm) hole was drilled into a 3/4-in. (19-mm) high-pressure plug, leaving at least a 1/8-in. (3-mm) wall at the inner end of the hole. A piezoelectric element having a fundamental vibration frequency of 10 MHz was bonded to the inner end of the hole. The combined piezoelectric element and plug vibrate at 258 kHz.

This new configuration transmits the ultrasonic vibration directly into the liquid, enhancing signal strength, accuracy, and range, yet the piezoelectric element is protected from the high-pressure liquid.

This work was done by Allan J. Zuckerwar of **Langley Research Center** *and David S. Mazel of Old Dominion University. No further documentation is available.*

This invention is owned by NASA, and a patent application has been filed. Inquiries concerning nonexclusive or exclusive license for its commercial development should be addressed to the Patent Counsel, Langley Research Center [see page 23]. Refer to LAR-13300.

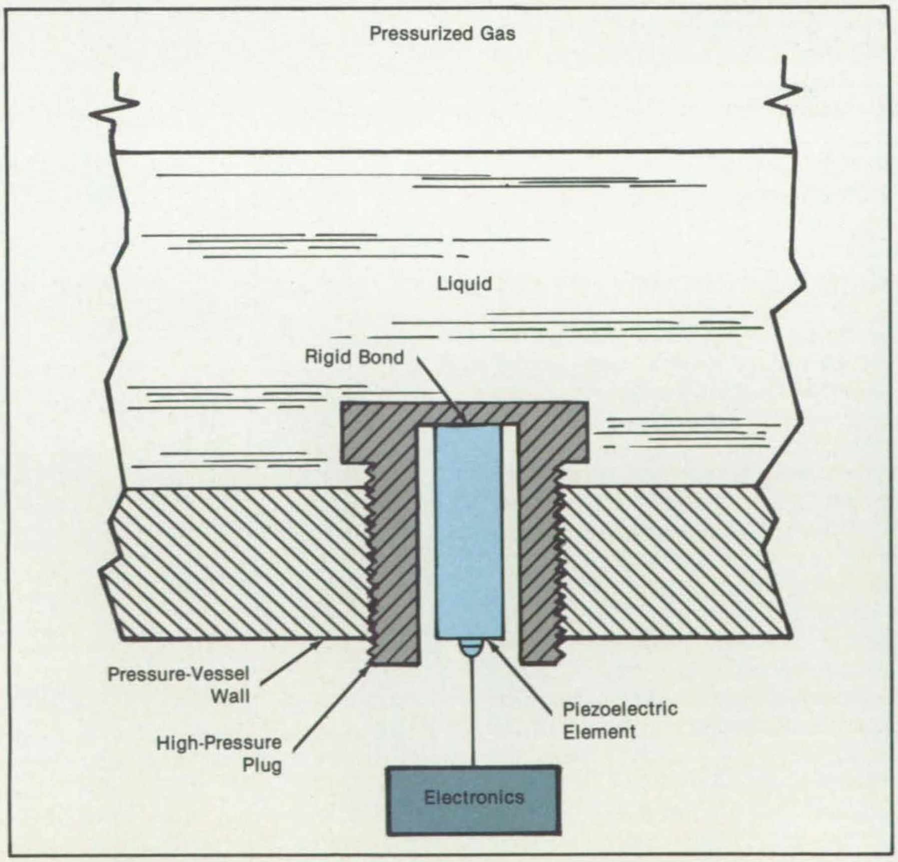

The **Piezoelectric Element** is mounted in a hole drilled in a high-pressure plug. The transducer is used to measure the depth of the liquid when the pressure in the vessel is high.

Measuring Fluid Velocities With Glowing Particles

Particle trajectories are recorded photographically.

NASA's Jet Propulsion Laboratory, Pasadena, California

The directions and magnitudes of velocities in an unsteady liquid flow are measured with the aid of a fluorescent- and phosphorescent-tracing technique. The method is accurate and proceeds automatically, requiring minimal labor.

Small, uniformly sized particles of mass density close to that of the fluid are introduced into the flow. The particles have previously been coated with a fluorescent/phosphorescent material. A brief pulse of light is flashed on the flow. The particles fluoresce for about 10^{-5} s as the dye re-emits the absorbed light through electronic transitions. After the fluorescence has subsided, the dye continues to give off a less-intense phosphorescent glow for about 0.4 s. The light is flashed once more so that the particles fluoresce brightly again, then glow phosphorescently again.

The flow, meanwhile, is photographed in a continuous exposure. A particle path appears as a bright spot followed by a narrow streak and another bright spot and streak. This represents the initial fluorescence, the afterglow, and the initial fluorescence from the second flash followed by a second afterglow. The direction of a particle can be inferred from the intensity gradient on the tail.

The speed of the particle can be calculated from the length of its path between bright spots, because the elapsed time between light flashes is known accurately. The velocity of a particle is essentially the same as that of the flowing liquid immediately surrounding it, and the photograph of the many particle paths thus gives a picture of the velocity distribution in the liquid.

The photographic image is examined by a computer that generates an analysis of the flow. Previous attempts at computerized image analysis were unsuccessful, because the particles were photographed by reflected light. The particle paths on film had uniform brightnesses from beginning to end, and the computer had no way of determining the directions of particle movement. An operator had to decide the direction of each trace individually. The double dot/tail structure eliminates the directional ambiguity so that the direction can readily be determined automatically by the image-analyzing computer.

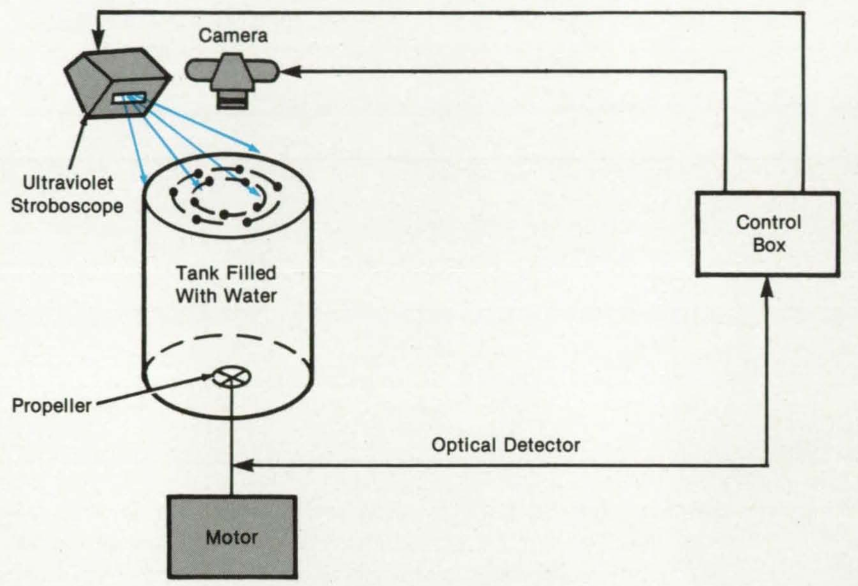

EXPERIMENTAL APPARATUS

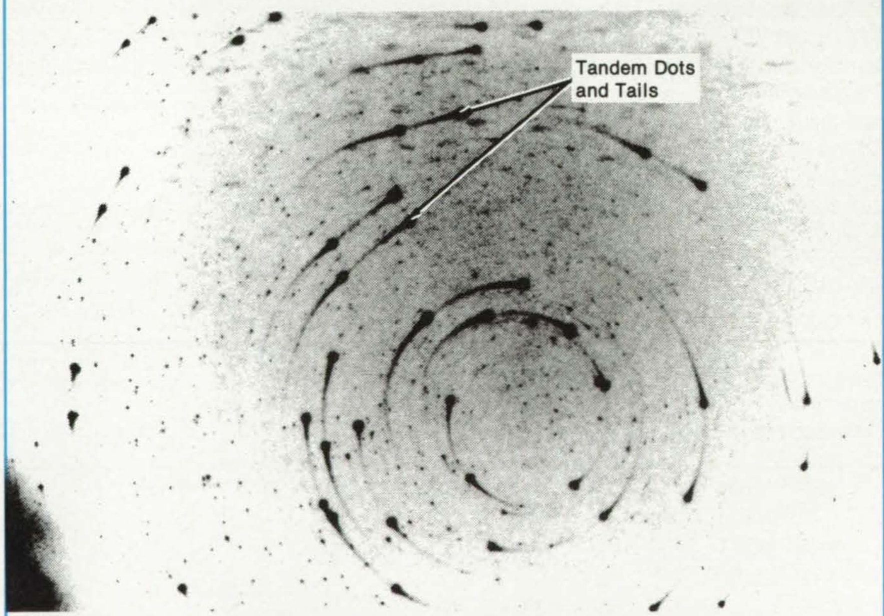

PHOTOGRAPHIC NEGATIVE AFTER DOUBLE PULSE

A **Camera Views Glowing Particles** in a water vortex. The photograph shows tandem dot-and-tail pairs created on film by each pair of illumination pulses.

This work was done by Morteza Gharib, Miguel A. Hernan, Andre H. Yavrouian, and Virendra Sarohia of Caltech for **NASA's Jet Propulsion Laboratory**. *For further information, Circle 68 on the TSP Request Card.*

Inquiries concerning rights for the commercial use of this invention should be addressed to the Patent Counsel, NASA Resident Office-JPL [see page 23] Refer to NPO-16653.

Taking Impressions of Hidden Cavity Walls

A device for field checks makes casts of internal contours.

Marshall Space Flight Center, Alabama

A lightweight, portable internal-molding device makes it possible to measure the radii of, or otherwise examine the contours of, passageways in hidden or complicated cavities. With the device, measurements can be made in the field, without returning assemblies to a shop or laboratory for inspection.

An acrylic molding head is wrapped with a polytetrafluoroethylene tube encapsulated by a surgical tube. The head is inserted in the cavity. When air at 40 lb/in.^{2} (280 kPa) pressure is applied to the head, the surgical tube expands and forms an airtight seal around the periphery of the cavity. The polytetrafluorethylene tube is held in place by a retaining ring that also controls the expansion of the surgical tube. As the surgical tube expands, it raises the head, forcing a molding compound (Citrocon or equivalent) into the cavity. The head is then rotated 180° and the procedure repeated to make a mold of the bottom part of the cavity.

After the head is removed from the cavity, the dimensions of the molded impression can be measured. A nylon string is extruded into the cavity along with the molding compound so that the casting can be easily retrieved if it breaks away from the head during its extraction from the cavity.

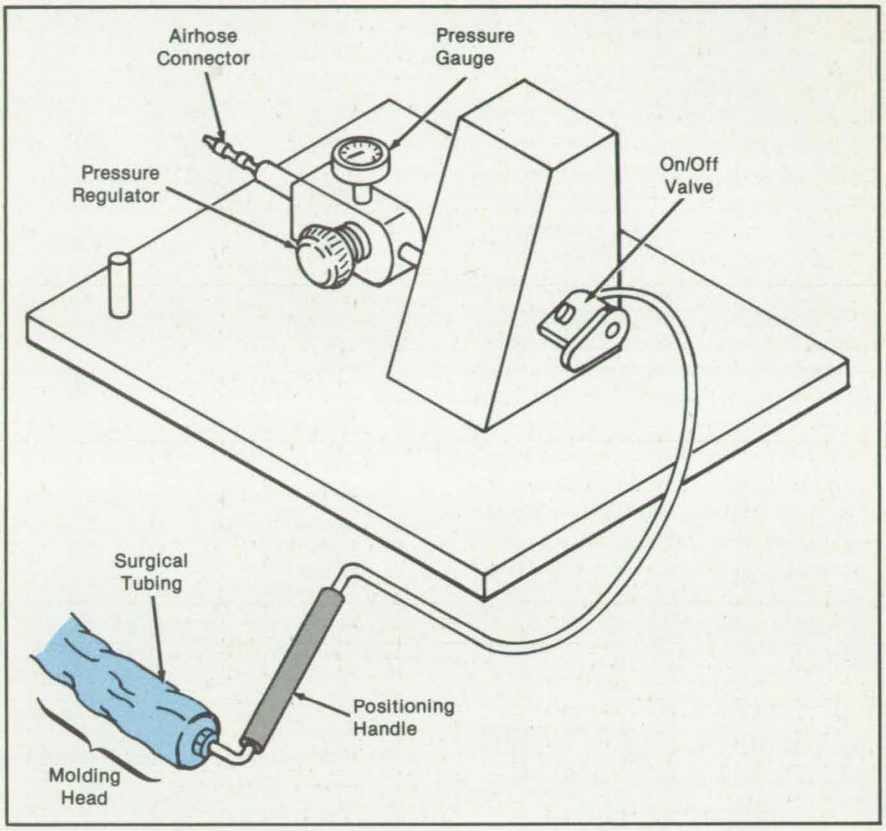

The **Molding Head Expands** when compressed air is applied. Inflatable tubes around the head perform a dual sealing and aligning function.

This work was done by Dick Burley and Walter Mayer of Rockwell International Corp. for ***Marshall Space Flight Center****. No further documentation is available.*

Inquiries concerning rights for the commercial use of this invention should be addressed to the Patent Counsel, Marshall Space Flight Center [see page 23]. Refer to MFS-29135.

Energy-Absorbing Passenger Seat for Aircraft

Tests show probability of passenger survival to be high.

Langley Research Center, Hampton, Virginia

The development of an energy-absorbing passenger seat, designed to minimize injury in a commercial-aircraft crash, was part of a joint FAA/NASA controlled-impact flight test of a transport-category commercial aircraft. After developmental tests were successfully completed at NASA's Langley Research Center, the seat assembly was flight-tested on a Boeing 720B aircraft at NASA's Dryden Flight Research Facility.

A commercially available triple-passenger seat was selected for conversion to an energy-absorbing seat assembly. The design goal was to protect the passengers, simulated by three 165-lb (75-kg) anthropomorphic dummies, against a vertical impact velocity of 21 ft/s (6.4 m/s) and a longitudinal velocity of 21 ft/s (6.4 m/s). To limit acceleration, the seat was modified so that it would collapse or "stroke" under high load. To accomplish seat stroking, split-sleeve-type bearings were attached to the upper ends of the rear legs, and a combination nylon-bearing-block/steel-yoke unit was installed on the upper ends of the forward legs. All bearings encircled the seat-frame tubes to allow rotation.

Conventional aircraft bolts were used as hinge pins to permit the rotation of both the forward and rear legs at the lower seat/rail-attachment ends. Two graphite/epoxy energy-absorbing tubes that crush as the seat moves down and forward were used. The tube assemblies, designed to crush as axial columns during the aircraft-impact shock pulse, were installed diagonally between the forward

and rear seat legs.

The figure depicts a cross section of the modified seat. To overcome a local bending problem encountered at the ends of the graphite/epoxy tubes, an axially-aligning pivot attachment was added to each end of the tubes. As the seat stroked forward and downward, the pivot-attachment mechanism caused the tubes to crush uniformly in an axial compressive mode, turning them literally into granular dust.

The seat assembly was installed in the Langley Research Center Dynamic Impact Facility, and a series of dynamic drop tests were successfully conducted to simulate the vertical and forward shock-pulse characteristics. In the subsequent flight test at Dryden Flight Research Facility, a highly instrumented B-720, remotely controlled from the ground by pilots in a simulated cockpit, was crashed on a specially prepared, gravel-covered impact site to provide various crash data in addition to the information desired on the seats. The aircraft was crashed in an air-to-ground, gear-up mode at 150 kn (77 m/s) and a 4° glide slope. The results of the simulation tests indicate the probability of passenger survival to be high. This proposed seat mechanism could very well mitigate passenger injuries by reducing impact forces in a crash.

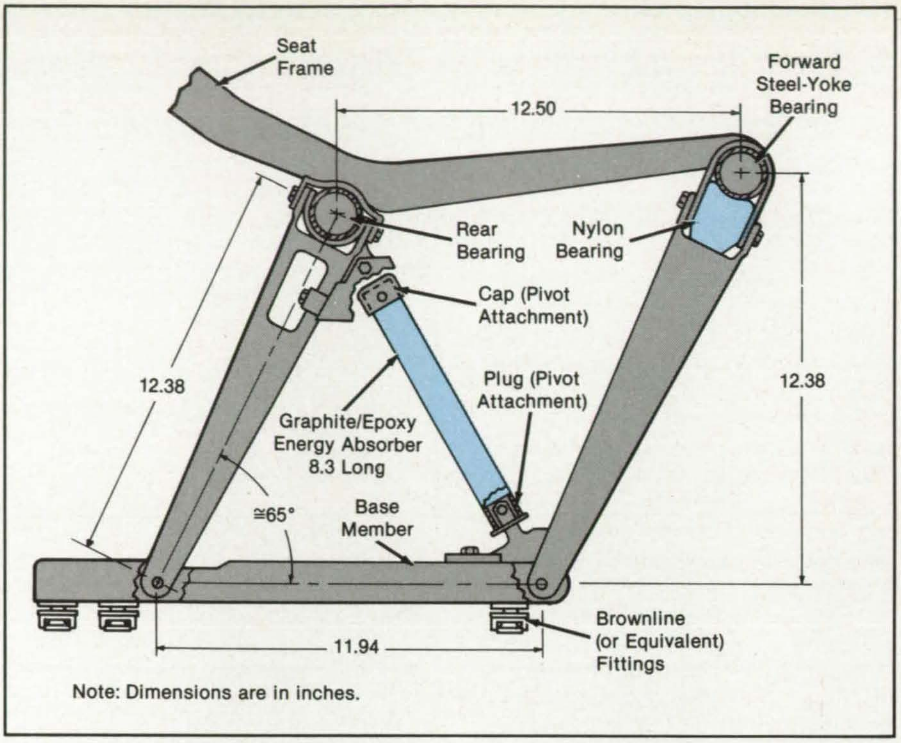

The **Modified Seat Mechanism** collapses under a heavy load to absorb impact energy and thereby protect the passenger.

This work was done by Charles P. Eichelberger and Emilio Alfaro-Bou of **Langley Research Center** *and Edwin L. Fasanella of Kentron International, Inc. For further information, Circle 30 on the TSP Request Card.* *LAR-13385*

Improved Heat-Transfer Calculations for Hypersonic Flow

The Lewis number is corrected for extremely high airspeeds.

Lyndon B. Johnson Space Center, Houston, Texas

An algorithm calculates an improved, variable value of the Lewis number, a factor in the equation for the heat-transfer coefficient at the stagnation point of a body in hypersonic flow (mach numbers of approximately 25). In the past, a constant value of 1 had been used for the Lewis number. The new algorithm improves the accuracy of calculations of the heat generated by hot air acting on a moving body.

Input data for the algorithm are the stagnation-point density, temperature, and pressure; the stagnation-point wall temperature; the viscosity at the wall; the Prandtl number at the wall; and the total enthalpy. The steps in the algorithm are as follows:

- Calculate the stagnation-point compressibility from the stagnation-point density, temperature, and pressure;
- Find the weight percentages of the various air components;
- Using the weight percentages, find the dissociation enthalpy;
- Calculate the collision cross sections at the wall and average them;
- Calculate the improved Lewis number from a formula that relates this quantity with the previously calculated quantities; and
- Insert the improved Lewis number in the equation for the stagnation-point heat-transfer coefficient.

This work was done by Samuel N. Greenschlag of Rockwell International Corp. for **Johnson Space Center**. *For further information, Circle 2 on the TSP Request Card.* *MSC-20756*

Books and Reports

These reports, studies, and handbooks are available from NASA as Technical Support Packages (TSP's) when a Request Card number is cited; otherwise they are available from the National Technical Information Service.

Environmental Testing of Glass-Fiber/Epoxy Pressure Vessels

Strength diminishes during long exposure to the environment.

A pair of reports discusses long-term environmental tests of glass-fiber/epoxy composite pressure vessels. Some of the hardest data to obtain on materials and structures are the long-term effects of environmental exposure. Since such data were necessary for accurate design of long-life structures such as pressure vessels, NASA Lewis Research Center built an outdoor test stand in 1973. This test stand maintains a system under constant pressure loading without the frequent intervention of personnel.

Accumulators were used to maintain a constant pressure (within 10 percent). The accumulator pressure and outside temperature were recorded twice daily. Automated data recording and pressure-limit warning systems were incorporated to minimize the number of man-hours required to monitor the system.

With this test equipment in place, a test program was started in January of 1984 to determine the environmental effects on glass-fiber/epoxy composite pressure vessels incorporating aluminum liners. The first pressure vessels put into test were designed by Martin Marietta/Denver Division (MM) and by Structural Composites Industries (SCI) as a part of a NASA L. B. Johnson Space Center program to develop a lightweight emergency breathing system such as those used by firemen. Both designs were filament wound with 20 end S-2 glass filaments. The SCI pressure vessels used a Dow Chemical epoxy (DER-332) while MM used a Shell epoxy (50:50 blend of Epon 828 and Epon 1031). Both the SCI and MM resins used an anhydride curing agent, which required an elevated-temperature cure.

The test environment was continuous outdoor exposure in Cleveland, Ohio. Some vessels were held under a constant pressure of 4,500 psi (31 MPa), some were pressure cycled 1,000 times from 200 to 4,500 psi (1.4 to 31 MPa) every year (in addition to constant pressure during the balance of the year), and, for control, some were not pressurized. The 4,500-psi (31-MPa) pressure was approximately 50 percent of the ultimate vessel capability and resulted in a composite stress of 31 percent of the ultimate composite capability.

Vessels of each type were removed from the test rack at scheduled intervals and subjected to a single-cycle-to-failure pressurization (burst test). All of the original group of pressure vessels (36 in all) were unpainted, and those that were exposed for more than 24 months showed significant visual effects of the exposure in addition to a reduction in the residual burst strength. This was true regardless of test conditions although the vessels that were subjected to pressure cycling tended to be most significantly affected.

There was considerable data scatter with a worst-case extrapolation indicating a 65-percent reduction in burst strength over a 10-year period for the unpainted pressure vessels. These data are not significantly different from those

developed by other investigators in a benign laboratory environment, where it was found that one glass-fiber/epoxy sample in 100 would fail in a 10-year period due to a sustained load of 33 percent of the original ultimate.

However, to demonstrate the effectiveness of coatings in protecting the fiberglass structures and in reducing environmental degradation, a second series of glass-fiber/epoxy pressure vessels was placed on the test rack in 1980. To date, these vessels have not shown any degradation in residual burst strength. The test program on these bottles is expected to run into the 21st century.

Conclusions that can be drawn at this time are that the exposure of unpainted glass-fiber/epoxy composites to the varying environment of Cleveland, Ohio will result in a degradation of the ultimate strength of the material. The environmental effects are variable, and structural effects do not correlate with visual surface effects. The worst case degradation is on the order of what would be expected in a benign laboratory environment, but paints or ultraviolet-protective coatings can be expected to minimize any loss of strength.

This work was done by James R. Faddoul of **Lewis Research Center**. *Further information may found in:*

NASA TM-87058 [N85-30034/NSP], "Ten Year-Environmental Test of Glass Fiber/Epoxy Pressure Vessels" and NASA CR-165320 [N81-25492/NSP], "Survey of Long-Term Durability of Fiberglass-Reinforced Plastic Structures."

Copies may be purchased [prepayment required] from the National Technical Information Service, Springfield, Virgina 22161, Telephone No. (703) 487-4650. Rush orders may be placed for an extra fee by calling (800) 336-4700.
LEW-14371

A Modal-Parameter Extraction Procedure

The procedure accommodates multiple input excitations.

An improved modal-parameter extraction procedure applicable to linear, time-invariant systems is derived in a 92-page report. The algorithm allows multiple noncoherent input excitations to be applied to a structure and generates a consistent set of modal parameters.

The procedure is an extension of simultaneous frequency-domain (SFD) techniques that was achieved through an investigation of two automatic methods for reducing the effective problem size while minimizing the amount of user interaction. (Problem-size reduction is an important consideration because practical modal analyses often require numerous measurement locations.) In several sample runs, the independent-coordinate reduction method is shown to be the more accurate method for small sample size. The principle-component method can be used to estimate the number of modes active in a given frequency range.

No restrictive assumptions are made concerning the damping matrix. In contrast to the prior SFD techniques, the derivation provides for skew-symmetric and nonproportional damping matrices. Accurate damped frequencies, decay rates, and complex modes are calculated for such a system despite relatively high noise levels.

The procedure uses solution methods more stable than those of the prior SFD techniques. Of two solution methods noted for accuracy and stability, Householder's method is preferable to the singular-value decomposition techniques because of its faster execution and easier use.

The procedure accurately resolves closely spaced modes. An experimental comparison showed that the parameters obtained by the new method are comparable to those obtained with the Polyreference and the complex-exponential algorithms.

The report also notes topics worthy of further investigation; for example, it recommends numerical study of the methods suggested in the report for calculating standard and residual attachment modes from experimental data. As another potential application of the procedure, it recommends the investigation of the use of the experimental reduced systems matrices directly in a substructure-coupling procedure. Possible avenues for modifying and improving the procedure are also given.

This work was done by Andrew H. Kurdila and Roy R. Craig, Jr., of the University of Texas at Austin for **Marshall Space Flight Center**. *Further information may be found in NASA CR-178509 [N85-33747/NSP], "A Modal Extraction Procedure Applicable to Linear Time Invariant Dynamic Systems."*

Copies may be purchased [prepayment required] from the National Technical Information Service, Springfield, Virginia 22161, Telephone No. (703) 487-4650. Rush orders may be placed for an extra fee by calling (800) 336-4700. The report is also available on microfiche at no charge. To obtain a microfiche copy, Circle 84 on the TSP Request Card.
MFS-27139

Multiple-Scale Turbulence Model

The turbulence in complex, recirculating flows is not in spectral equilibrium.

A report discusses a mathematical fluid-flow model that includes multiple turbulence scales. The model was developed for the numerical prediction of confined, recirculating flows. Based on multiple-time-scale concepts introduced in a previous study, the model takes into account that the turbulence in recirculating flow is not in spectral equilibrium and that the different energy-transfer rates for eddies of different spatial scales should be treated separately.

First, the fluctuating parts of the velocity are decomposed into components defined in terms of the turbulent-kinetic-energy densities of large- and small-scale eddies. The principal feature of the multiple-scale model is that the kinetic-energy spectrum of turbulence is divided roughly into three regions: large-scale energy production, intermediate energy transfer, and small-scale dissipation eddies.

The partition of the energy spectrum allows the energy transfer of large-scale eddies to be related directly to the mean strain. For sufficiently small eddies, the model includes an assumption regarding the isotropy of fluctuations. This justifies the use of a triple-velocity correlation function (of large- and small-scale fluctuation components) that was indicated, in another previous study, to act as an energy-transfer rate from one fluctuating field to another.

Invoking the same justification, an energy-dissipation term representing the eddies of smallest scale is derived from a double-velocity correlation function that includes the small-scale-eddy velocity components alone. Thus, the energy-transfer rates of the small eddies are treated as though they were due to the actions of the small eddies alone and are mathematically decoupled from the mean flow field.

The model equations include gradient-type transport equations in which the spectral-energy and energy-transfer densities are the transported quantities, the effective fluid velocity is the mean (nonfluctuating component of the total) fluid velocity, and the energy-generation source terms include an effective eddy viscosity and other coefficients.

The partition between the energy-production and transfer regions of the spectrum is characterized by the coefficients, which have yet to be determined. Some preliminary coefficient values have been assigned by calibration against a simple homogeneous-flow experiment, by inference from limiting single-turbulence-scale model results and by requiring that the spectral-energy and energy-transfer densities remain positive throughout time in the simulations.

This work was done by C. P. Chen of **Marshall Space Flight Center**. *Further information may be found in NASA CR-178536 [N86-12551/NSP], "Multiple-Scale Turbulence Closure Modeling of Confined Recirculating Flows."*

Copies may be purchased [prepayment required] from the National Technical Information Service, Springfield, Virginia 22161, Telephone No. (703) 487-4650. Rush orders may be placed for an extra fee by calling (800) 336-4700. The report is also available on microfiche at no charge. To obtain a microfiche copy, Circle 6 on the TSP Request Card.
MFS-27141

Identifying Vibration Parameters in Large Structures

An analytical method separately examines low-frequency and high-frequency behavior.

A report discusses techniques for identifying rigid-body parameters, flexible-body parameters, and quasi-static disturbances in large structures. The techniques are being developed to aid in planning the space station. Although this effort has been directed towards the space station dynamic model and environment, the proposed methodology for systems identification is generic enough to allow application to arbitrarily large space structures and spacecraft configurations.

The space station will consist of five pressurized modules and supporting framework. A transverse truss on a vertical keel supports four solar panels, rotatable so that they can follow the Sun. Farther down on the keel is a pair of radiator panels that are also rotatable. At the base of the keel is a docking facility for the Space Shuttle. The structure configuration and attitude will be controlled by control-moment gyroscopes, magnetic torquers, and reaction-control thrusters.

The parameter-identification problem can be separated into low-frequency (0 to 0.01 Hz) and high-frequency (above 0.01 Hz) parts. The low-frequency disturbances come from attitude-control-system, aerodynamic, and gravity-gradient torques. These disturbances provide adequate excitation for the identification of such rigid-body parameters as the location of the center of mass and the inertia tensor and for such quasi-static parameters as the average atmospheric density, diurnal bulge, peak density, phase lag, and center of pressure. The high-frequency disturbances come from crew movements, thruster firing, and Space Shuttle docking. These disturbances can be used to identify the parameters associated with flexible-body dynamics.

The rigid-body parameters and the quasi-static parameters can be identified from accelerometer readings. The algorithm that processes the readings is based on a formulation of the rotation and vibration problems that is linear in the parameters sought. Using dynamic excitations, one can identify the flexible-body parameters by a maximum-likelihood estimation. This requires the solution of a nonlinear parameter-optimization problem. At present, this type of solution is restricted to non-real-time processing.

The techniques have been used to identify modal frequencies in a 15 degree-of-freedom space station model. This case study revealed problems arising from modes that are not excited, modes that are excited but not enough to ensure good identification, and modes that are not resolvable with the chosen sensor configuration. The solution can be made easier by resorting to a large number of sensors and to intentional excitation at prescribed locations around the structure. Whether the advantages of these provisions outweigh their cost remains to be determined.

This work was done by David S. Bayard, (Fred) Y. Hadaegh, and Che-Hang Charles Ih of Caltech for **NASA's Jet Propulsion Laboratory**. *To obtain a copy of the report, "On-orbit Parameter and Disturbance Identification for Space Station," Circle 57 on the TSP Request Card.*
NPO-16770

Machinery

Hardware, Techniques, and Processes

Books & Reports

Computer Programs

Air-Powered Projectile Launcher

A small, high-pressure reservoir conserves compressed air.

NASA's Jet Propulsion Laboratory, Pasadena California

An air-powered launcher fires plastic projectiles without using explosive propellants. It therefore does not generate high temperatures. The launcher was developed for combat training for the U.S. Army. It also has potential applications in seismic measurements, avalanche control, and testing impact resistance of windshields on vehicles.

In comparison with prior air launchers, the new launcher is lightweight and reliable. It is intended to consume a minimum amount of compressed air for each high-velocity launch and, therefore, was designed with a small-volume, high-pressure air reservoir. The reservoir surrounds the breech of the launcher so that the airflow path is short and flow losses small.

The valve that releases high-pressure air to the breech was built as a sleeve to

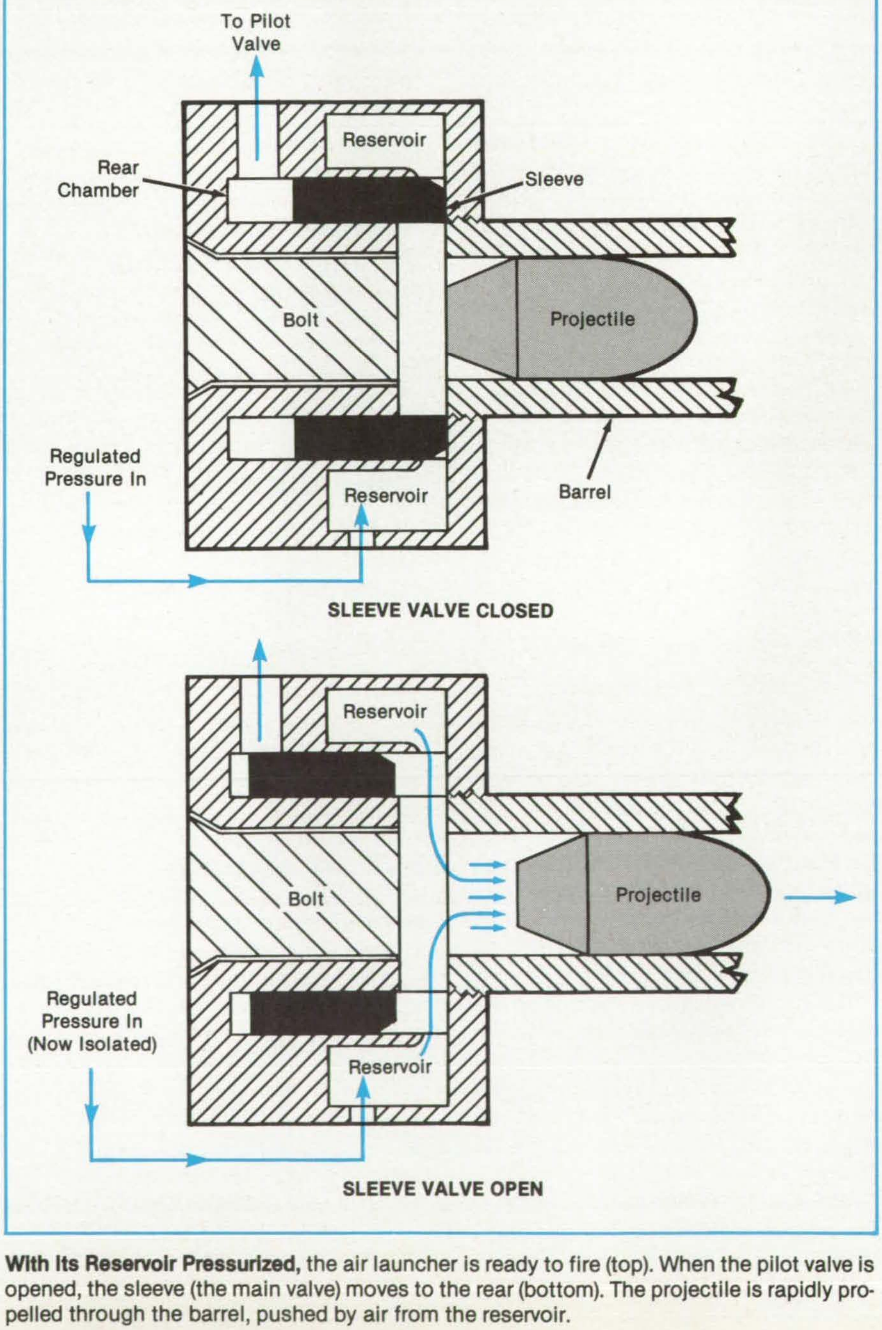

With Its Reservoir Pressurized, the air launcher is ready to fire (top). When the pilot valve is opened, the sleeve (the main valve) moves to the rear (bottom). The projectile is rapidly propelled through the barrel, pushed by air from the reservoir.

keep the stroke short and enable the valve to open rapidly. The sleeve configuration also allows projectiles to be loaded in the conventional way, either manually or automatically.

When the reservoir is pressurized before a launch, the rear valve chamber is also pressurized. The valve is thus held in its closed (forward) position by differential pressure (see figure). Just before a launch, the pressure inlet is sealed. At the launch time, a pilot valve is energized and vents the rear valve chamber. The pressure in the reservoir then forces the sleeve to its open (rearward) position. As the sleeve opens, the high-pressure air in the reservoir discharges into the barrel and propels the projectile outward.

After the discharge, the valve is quickly closed again by differential air pressure, and the reservoir is recharged with compressed air. At the same time, the breech bolt is opened and a new projectile inserted into the barrel.

This work was done by Thomas Andrews, Roy A. Bjorklund, David G. Elliott, and Larry K. Jones of Caltech for **NASA's Jet Propulsion Laboratory**. *For further information, Circle 135 on the TSP Request Card.* *NPO-16763*

Easy-to-Install Link for Track Treads

Proposed link would save assembly and maintenance time.

NASA's Jet Propulsion Laboratory, Pasadena, California

A link with integral tapered pins is proposed as a means of joining treads on tracked vehicles. Unlike the links now in common use, the new links would not require a tensioning tool for installation and would not be subject to loosening from shock and vibration during use.

In a conventional tread connection, pins project from the treads. A conventional link is pushed onto a pair of pins after the adjacent treads have been pulled close to each other by a tensioning tool. The link is locked to the pins by tightening an internal bolt. It is common practice for vehicle operators to stop fre-

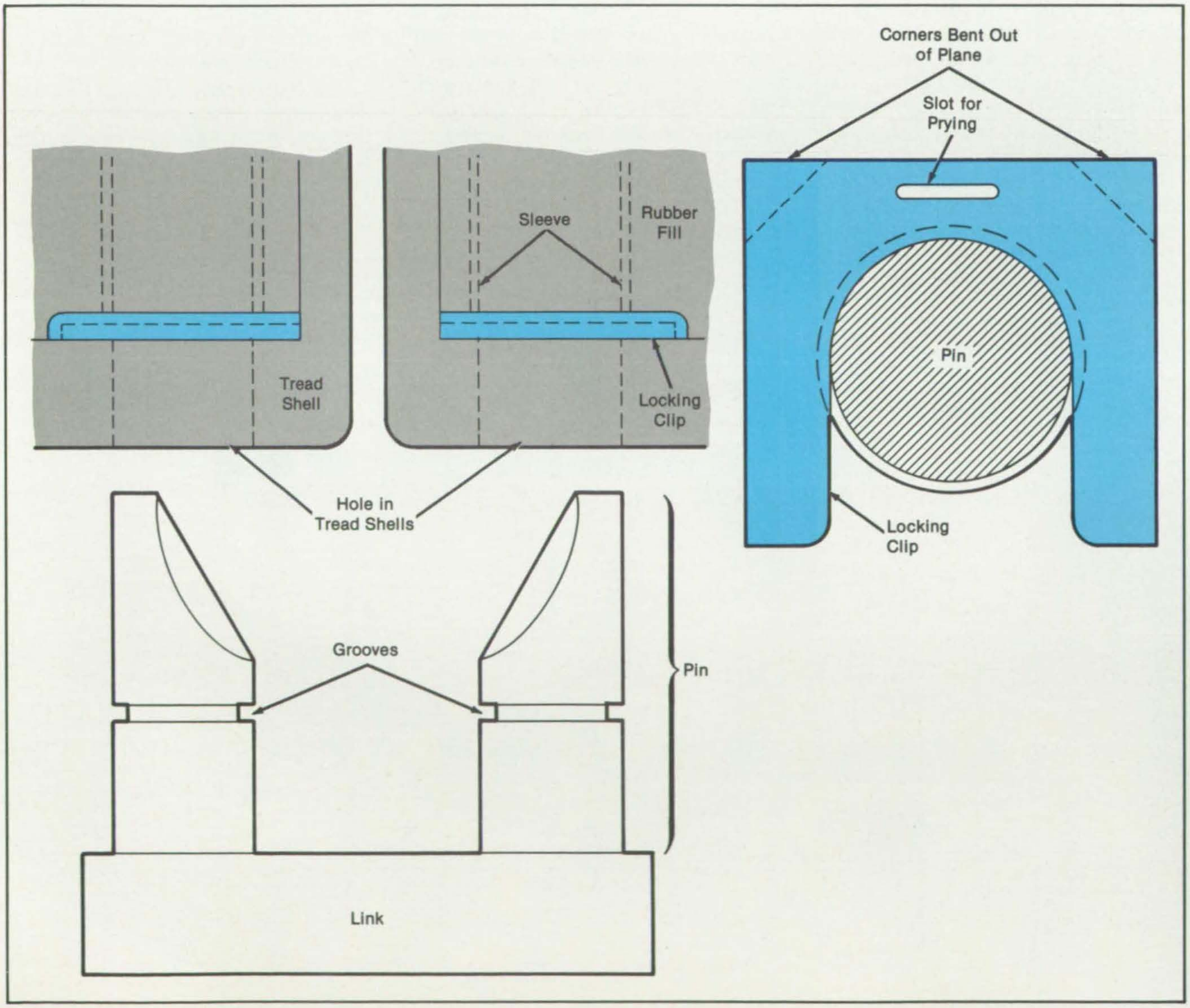

Dual Pins on a Link fit into a pair of holes on adjacent tread shells. The pins are secured by a locking clip pressed into the grooves on the pins.

quently to retighten the bolts on every link of the tread track.

In the new link, the pins would be part of the link itself, forged with it or joined to it by welding (see figure). When the pins are driven into the sleeves in the tread shells, their tapered ends act as cams to draw the track tight — without a tensioning tool. When the pins are seated, locking clips are pushed down into the tread shell and hammered into place in grooves or notches in the pins. The clips are deformed in the process and hold the pins tightly. One end of a clip abuts the tread-shell wall and is therefore prevented from rotating and wearing away its deformed edges and the groove or notch wall.

Slots at the top of the shells allow access to the clips. Clips can be pried loose through the slots to disassemble the track. The disassembly procedure is no faster than that for conventional links. However, assembly is much faster — a few blows of a hammer are needed instead of many turns of a wrench. Moreover, the work time and vehicle idle time of frequent bolt tightening are avoided.

This work was done by Earl R. Collins, Jr., of Caltech for **NASA's Jet Propulsion Laboratory**. *For further information Circle 3 on the TSP Request Card.*

Inquiries concerning rights for the commercial use of this invention should be addressed to the Patent Counsel, NASA Resident Office-JPL [see page 23]. Refer to NPO-16332.

More Durable Tracks for Heavy Vehicles

Tie bars instead of threaded fasteners make track throwing less likely.

NASA's Jet Propulsion Laboratory, Pasadena, California

A proposed undercarriage for a tank or bulldozer would have flanged edges to prevent rocks and other road debris from getting caught in the track drive and damaging it or casting off the track. The improved track would have no threaded fasteners to be loosened by road shock and vibration.

Like conventional tracks, the proposed track includes a jointed, vertically flexible, horizontally stiff, continuous chain of sliding guide bars. Unlike conventional tracks, however, the new track includes tie bars forged integrally with webs of the guides — no bolts are used. In addition, the tie bars are forged with square cross sections so that they resist rotation when the track bends. The tie bars are cast into the rubber fillings on the treads to ensure a strong bond to the rubber.

Each pair of adjacent tie rods is held together by a staple, a massive, strong forging that is hammered into place on the webs. A pin holds each staple — again, no bolts are used.

The floating guide bar runs between web pairs in a track segment. Together the guide bars form a continuous guiding surface. The guide bars are inserted in open mortises in the web and retained by pins. The guide bars float in grooves in the top surface of the rubber fill and form

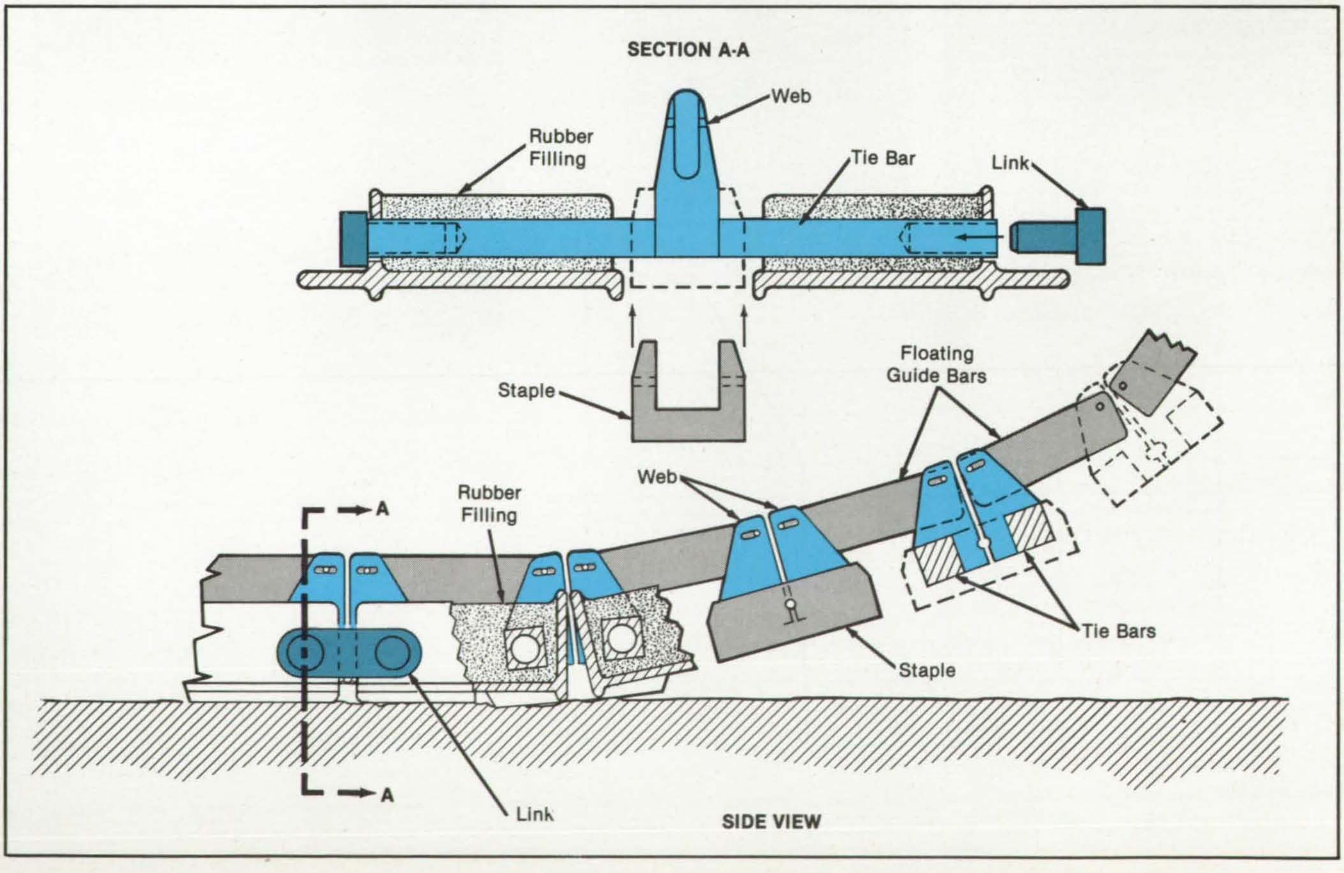

A **Continuous Chain of Floating Guide Bars** would be articulated at web junctions. Pins would replace bolted connections. The guide bars and the flanges on the vehicle (not shown) would keep out stones.

a wall to keep out foreign objects. The upper edges of the bars and webs run within continuous flanges on the vehicle undercarriage so that foreign objects are excluded there. The retaining pins float in slots in the sides of the webs to accommodate the changes in the alignments of mating parts as the track bends around the end wheels and rides over bumps.

This work was done by Earl R. Collins, Jr., of Caltech for **NASA's Jet Propulsion Laboratory**. *For further information, Circle 4 on the TSP Request Card. NPO-16478*

Remotely Adjustable Hydraulic Pump

Outlet pressure can be adjusted to match varying loads.

Lyndon B. Johnson Space Center, Houston, Texas

The outlet pressure of a hydraulic pump can be adjusted remotely while the pump is operating. The pump can be used in aircraft and robots, for example, where hydraulic actuators are repeatedly turned on and off, changing the pump load frequently and over a wide range. The pump pressure can be reset as often as necessary to ensure adequate — but not excessive — pressure.

The pump pressure does not have to be preset for the worst case — all actuators operating simultaneously, a condition that may prevail only briefly. It therefore does not demand as much energy from its motor drive. Moreover, it is not necessary to reduce the high worst-case pressure for its regulation mechanism, and its internal leakage is less. The remotely controllable pump is therefore more efficient than are conventional pumps.

The pump is a variable-displacement, pressure-compensated type. It contains a hydraulically-operated pressure-regulation mechanism and an electrically-operated pressure-adjustment mechanism.

Pistons in a motor-driven barrel slide on an inclined plate as the barrel rotates (see figure). Following the plate surface, the pistons reciprocate in bores in the barrel with each revolution. As they reciprocate, the pistons draw in hydraulic fluid at low pressure from an inlet port and expel it at high pressure from an outlet port.

Hydraulic feedback maintains the outlet pressure at a nearly constant value by altering the angle of the inclined plate as necessary. A small passage connects the pump-outlet port with a spool bore inside the regulator. There the pressure acts on the right side of a control land on the sliding spool, opposing the compensator-spring pressure acting on the left side of the spool.

If the pressure at the pump outlet drops, the compensator spring forces the spool to the right. The rightward movement of the control land uncovers a control port and reduces the pressure on the control piston. The control piston moves upward. The inclined plate is forced by a tilting spring to follow the piston, so that the angle of the inclined plate increases. The displacement of the pump is thereby increased, and its outlet pressure rises.

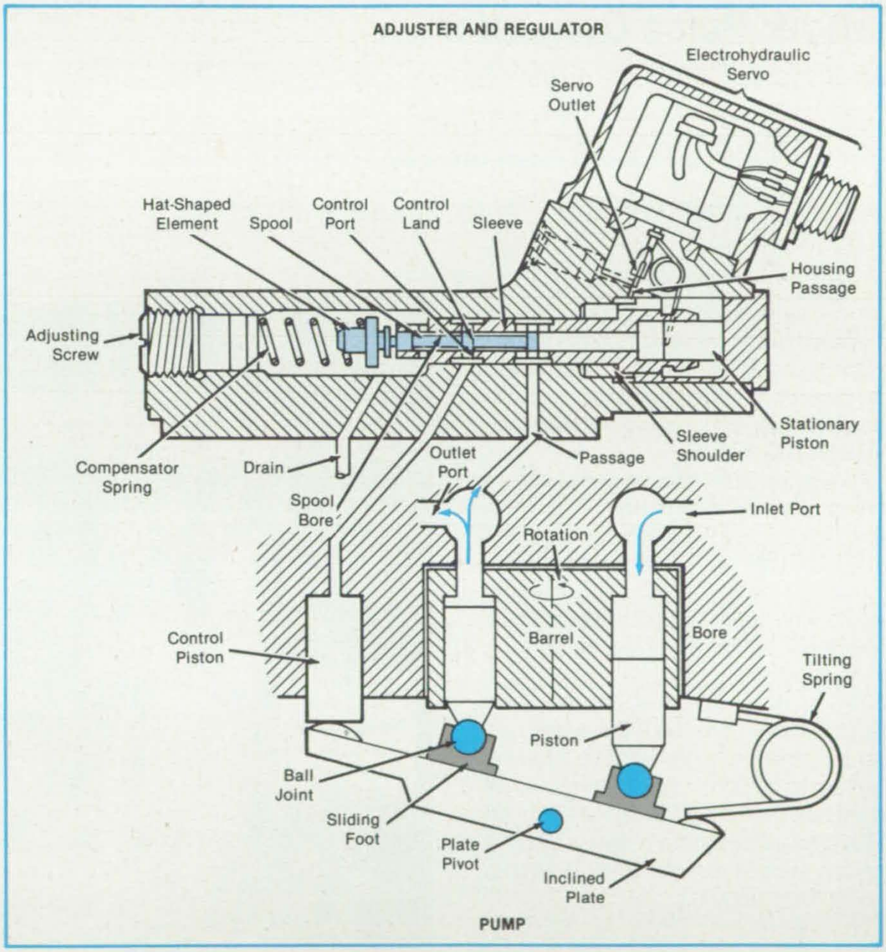

The **Electrohydraulic Servo Has Positioned the Sleeve** in its leftmost position, thereby adjusting the outlet pressure to the maximum value. The sleeve is in an equilibrium position, with the control land covering the control port. For the lowest pressure setting, the sleeve would be shifted toward the right by increased pressure on the sleeve shoulder from the servovalve.

As the pressure in the spool bore simultaneously rises, it returns the control land to its original position, closing the port once more and returning the system to equilibrium. For overpressure at the pump outlet, the regulator works in reverse, decreasing the tilt angle and reducing the outlet pressure.

Meanwhile, the pressure-adjusting

mechanism is an electrohydraulic servovalve. It continuously supplies hydraulic fluid at the pump-outlet pressure through a passage in the housing to a shoulder on the sleeve that forms the spool bore. To change the outlet pressure, an operator or an automatic controller changes the electric current to the servomotor. This changes the output pressure of the servo and the pressure on the sleeve shoulder, thereby shifting the sleeve with respect to the compensating spring.

To increase the outlet-pressure setting, the operator decreases the servocurrent. The servo decreases the pressure on the shoulder and thereby allows the outlet pressure between the stationary piston and the sleeve to push the sleeve to the left. This moves the control port to the left. The outlet pressure on the spool must then compress the compensator spring farther to move the control land past the control port. Thus, the control piston will not push the inclined plate down to decrease the pump displacement until a higher outlet pressure is reached. In a similar but opposite manner, the outlet-pressure setting is reduced when the servocurrent is increased.

This work was done by Herbert H. Kouns and Loren D. Gardner of Abex Corp. for **Johnson Space Center**. *For further information, Circle 112 on the TSP Request Card.*

Title to this invention has been waived under the provisions of the National Aeronautics and Space Act [42 U.S.C 2457 (f)], to the Abex Corp. Inquiries concerning licenses for its commercial development should be addressed to:

Abex Corp.
P.O. Box 10268
Stamford, CT 06904-2268

Refer to MSC-21007, volume and number of this NASA Tech Briefs issue, and the page number.

Hot-Air-Pulse Generator

Mixer blades interrupt airflow for rapid testing of insulating materials.

Lyndon B. Johnson Space Center, Houston, Texas

A device for producing periodic blasts of heated air can be used for rapid testing of flexible insulating materials. The device can be used to compare materials and to select candidates for more detailed testing in wind tunnels.

An electric paint mixer is positioned so that its propeller is at the outlet of a hot-air-jet nozzle (see Figure 1). The propeller blades are flattened and oriented perpendicularly to the jet; they thus interrupt the jet when they pass the orifice. Between interruptions, the hot air strikes the surface of the specimen.

The propeller speed is adjusted with the aid of a stroboscope. The pulse rate can be varied up to 85 Hz. The strobe is then set to a slightly different frequency so that the effects of the pulsating jet on the tested article can be observed. Figure 2 shows some nozzle parameters used in typical test setups.

This work was done by Mark C. Ammerman of Rockwell International Corp. for **Johnson Space Center**. *No further documentation is available.*
MSC-20768

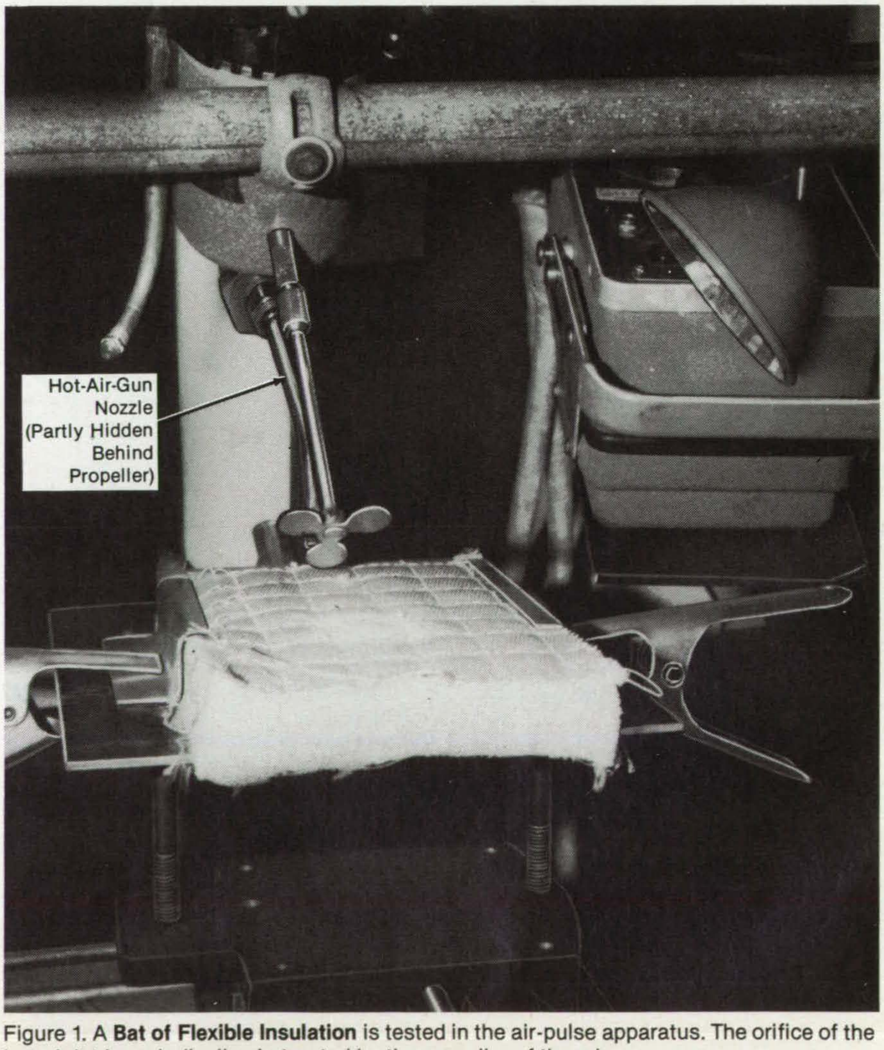

Figure 1. A **Bat of Flexible Insulation** is tested in the air-pulse apparatus. The orifice of the hot-air jet is periodically obstructed by the propeller of the mixer.

Note: Dimensions are in inches (millimeters)

	W	H
1/4 (6.4) O.D. Nozzle	0.30 (7.6)	0.06 (1.5)
3/16 (4.6) O.D. Nozzle	0.22 (5.6)	0.06 (1.5)
1/2 (12.7) O.D. Nozzle	0.70 (17.8)	0.05 (1.3)

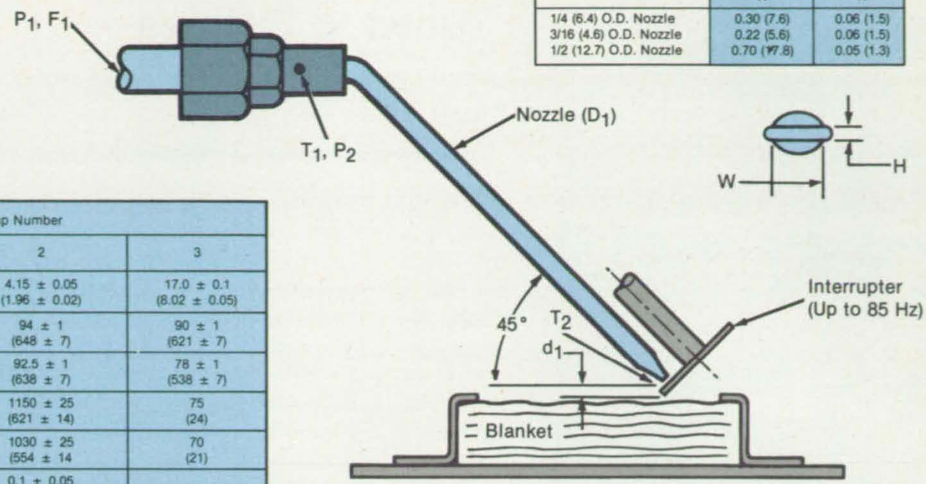

Parameter	Setup Number		
	1	2	3
F_1	4.5 ± 0.1 (2.1 ± 0.05)	4.15 ± 0.05 (1.96 ± 0.02)	17.0 ± 0.1 (8.02 ± 0.05)
P_1	45 ± 2 (310 ± 14)	94 ± 1 (648 ± 7)	90 ± 1 (621 ± 7)
P_2	42 ± 2 (290 ± 14)	92.5 ± 1 (638 ± 7)	78 ± 1 (538 ± 7)
T_1	1150 ± 50 (621 ± 28)	1150 ± 25 (621 ± 14)	75 (24)
T_2	1050 ± 50 (566 ± 28)	1030 ± 25 (554 ± 14	70 (21)
d_1	1/16 (1.5) (FIXED) 0.05 (1.3) TO 0.2 (5.1) 1.Hz Oscillation	0.1 ± 0.05 (FIXED) 0.05 (1.3 TO 0.2 (5.1) 1-Hz Oscillation	0.46 (11.7)
D_1	1/4 (6.4)	3/16 (4.8)	1/2 (12.7)
W	0.30 (7.6)	0.22 (5.6)	0.7 (17.8)
H	0.06 (1.5)	0.06 (1.5)	0.05 (1.3)
V	1,150 (514)	1,150 (648)	800 (358)
ν	0.079 (0.54)	0.129 (0.89)	?

Definitions

F_1 = Gas Flow Rate, scfm (l/s)
P_1 = Line Pressure, psi (kPa)
P_2 = Nozzle Inlet Pressure, psi (kPa)
T_1 = Nozzle Inlet Temperature °F(°C)
T_2 = Nozzle Exit Temperature °F(°C)
d_1 = Nozzle Distance From Blanket
D_1 = Nozzle O.D.
V = Nozzle Exit Velocity, mi/h (m/s)
ν = Theoretical Surface Shear, psi (kPa)

Figure 2. Some **Nozzle Parameters** were determined for typical test setups.

Books and Reports

These reports, studies, and handbooks are available from NASA as Technical Support Packages (TSP's) when a Request Card number is cited; otherwise they are available from the National Technical Information Service.

Blade-Tip-Clearance Forces in Turbines

A study reviews the field and proposes experiments.

A report summarizes the present knowledge and discusses plans for experiments on blade-tip-clearance excitation forces in turbines. Of particular interest are the Alford forces, named after a pioneering worker in this field. These are the cross forces due to uneven clearances, which are in turn caused by and also cause rotor vibrations. Because blade-tip clearances affect turbine efficiency and excitation forces affect rotor stability, the report should prove useful to researchers and designers of advanced turbomachinery.

The study was carried out in three phases documented in the report. The first phase was a literature search and evaluation. In addition to showing the state of the art, this phase exposed the need for theoretical and experimental efforts to provide design data and a rational basis for extrapolation to new configurations and operating conditions.

The authors found that a very small data base exists for excitation blade-tip forces in unshrouded turbines. A more extensive data base exists for shrouded blading under static effects. In both cases, however, a detailed fluid-mechanical understanding of the effect is lacking. Consequently, extrapolations to untested conditions remain dubious. Furthermore, there are no reliable data on forces proportional to the rate of change of the clearance.

In the second phase of the study, several of the assumptions contained in the usual theoretical analyses of the Alford force were removed. The problem was then posed in terms of a rigorous linearized flow analysis of the behavior of an eccentric rotor approximated by an actuator disk with two-dimensional flow. This theoretical study revealed an important contribution to the Alford force from the redistribution of flow around the turbine annulus. It also showed an important contribution from the annulus pressure, even in unshrouded turbines.

The third phase was a preliminary design study of a turbine-testing facility. The objective of this phase was to extend the data base by development of the capability to measure excitation forces and the associated (and causative) flow patterns over a realistic range of turbine-stage loadings, flow angles, flow speeds, and Reynolds numbers, among other parameters. This demands a variety of turbine configurations, especially in the blade-tip region, thereby necessitating frequent total or partial assembly and disassembly. Consequently, the facility was designed with modular parts.

The design also includes the instrumentation and numerous instrumentation ports in the turbine. Plans call for the measurement of mass-flow rates, temperatures, pressures, gas compositions, rotor speeds, braking torques, casing vibrations, rotor positions, bearing forces, and local flow velocities. The facility thus presents a problem in data reduction. There are 132 data channels, of which about 26 are likely to be used during a typical experiment. This will require some software development for correct data acquisition.

This work was by M. Martinez-Sanchez and Edward M. Greitzer of the Massachusetts Institute of Technology for **Marshall Space Flight Center**. *Further information may be found in NASA CR-171534 [N85-29963/NSP], "Turbine Blade-Tip Clearance Excitation Forces."*

Copies may be purchased [prepayment required] from the National Technical Information Service, Springfield, Virginia 22161, Telephone No. (703) 487-4650. Rush orders may be placed for an extra fee by calling (800) 336-4700. The report is also available on microfiche at no charge. To obtain a microfiche copy, Circle 115 on the TSP Request Card.
MFS-27122

Fabrication Technology

Hardware, Techniques, and Processes

Simplified Explosive Joining of Tubes to Fittings

A ribbon explosive and mild detonating fuse allow the use of a smaller charge.

Langley Research Center, Hampton, Virginia

This technique simplifies tube-to-fitting joining, as compared to fusion welding, and provides an improvement on the standard procedures used to join tubes explosively to tube fittings. A special tool is inserted into the tube to be joined. This tool allows a strip of ribbon explosive to be placed right at the joint.

The state-of-the-art explosive joining of tubing has relied on the loading of a granulated explosive into the tube by means of a short plug. The use of the special tool with a ribbon explosive and a mild detonating fuse (MDF) and tube initiator requires much less explosive to achieve a metallurgical bond, thereby reducing collateral damage to the tube itself. The bond can be enhanced by machining a V-shaped notch into the fitting prior to joining. The joint thus created exhibits parent-material properties and is hermetically sealed.

The tool and process can be used when tube diameters are 0.20 inch (5.1 millimeters) and higher. The 0.20-inch lower limit is based on the physical restrictions imposed by the diameter of the initiator and the minimum diameter to which the ribbon explosive can be wrapped without causing the breakup of the explosive load. The initiator uses an open-ended steel cylinder (booster sleeve) loaded with explosive, allowing the insertion of an MDF in each end. To enhance safety, this process uses only secondary explosives; i.e., those explosives that require an explosive input, not a flame, for initiation. Therefore, complete assembly of the tool with maximum safety is possible before a blasting cap is introduced to effect initiation.

Larger diameter tubes can accommodate an electrical blasting cap to simplify the initiation system, where safety procedures can be enhanced.

The tool and process can be modified to join a tube within a cylindrical interface for repair or strengthening. Also, the tool with two ribbon explosives and two initiators could be inserted into an internal tube configured to provide the necessary explosive-joining interface. In this way, any number of joints can be made with any

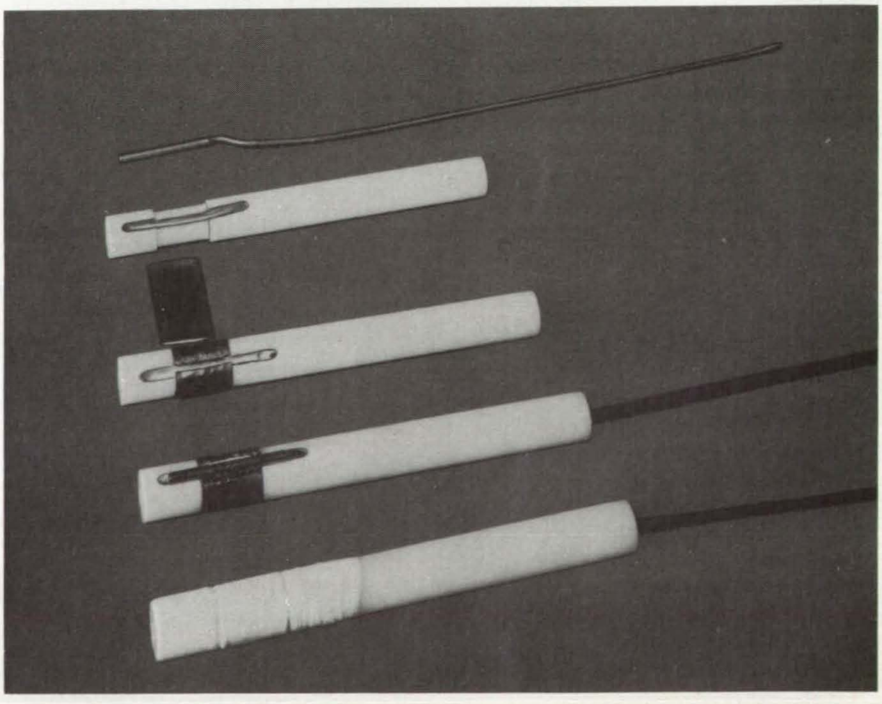

The **Components of the Joining Tool** and process are, from the top: the tube and MDF initiator, tool, ribbon explosive, ribbon explosive on tool, and assembled tool wrapped with polytetrafluoroethylene tape or heat-shrink tubing (used to size the tube exactly).

number of tubes.

The assembled tool is storable, and the process is amenable to automation. The assembly of the components, insertion of the tool into the weld site, and the joining operation could be mechanized without human contact. This technique is being considered for assembly of tubes into a heat exchanger in the Space Shuttle main engine. It could also be used to assemble components in nuclear reactors or in other environments hostile to humans.

This work was done by Laurence J. Bement of **Langley Research Center** *and James W. Bailey, Ronnie Perry, and Marvin S. Finch of Kentron International, Inc. For further information, Circle 73 on the TSP Request Card.*

This invention is owned by NASA, and a patent application has been filed. Inquiries concerning nonexclusive or exclusive license for its commercial development should be addressed to the Patent Counsel, Langley Research Center [see page 23]. Refer to LAR-13309.

Cleaner Vacuum-Bag Curing

An improvement upon recommended procedures saves time and expense.

Marshall Space Flight Center, Alabama

A caul plate used in vacuum-bag curing can become more easily reusable by a simple extra step in setting up the bag. Ordinarily, a caul, which covers and protects a laminated composite panel during curing, is coated with resin when removed from the bag. Removing the coating is nearly impossible; it is more economical to discard the caul, even though a new plate must then be prepared for the next cure. Moreover, the resin on the caul also sticks to the composite panel and delays removal of the panel.

The problem is eliminated by covering the face and edges of the caul plate with adhesive-backed polytetrafluoroethylene sheet (see figure). (Interestingly, documents spelling out the procedure for vacuum-bag curing recommend a polytetrafluoroethylene cover for the lower press platen but not for the caul plate.) The added polytetrafluoroethylene sheet has a smooth surface, to which the resin will not adhere. This enables the caul plate to be reused and shortens the time needed to remove the panel from the curing assembly. The extra step in no way detracts from the properties of the cured panel.

This work was done by Johnny M. Clemons, Benjamin G. Penn, Frank E. Ledbetter, III, and Julia G. Daniels of **Marshall Space Flight Center**. *No further documentation is available.*

Inquiries concerning rights for the commercial use of this invention should be addressed to the Patent Counsel, Marshall Space Flight Center [see page 23]. Refer to MFS-28071.

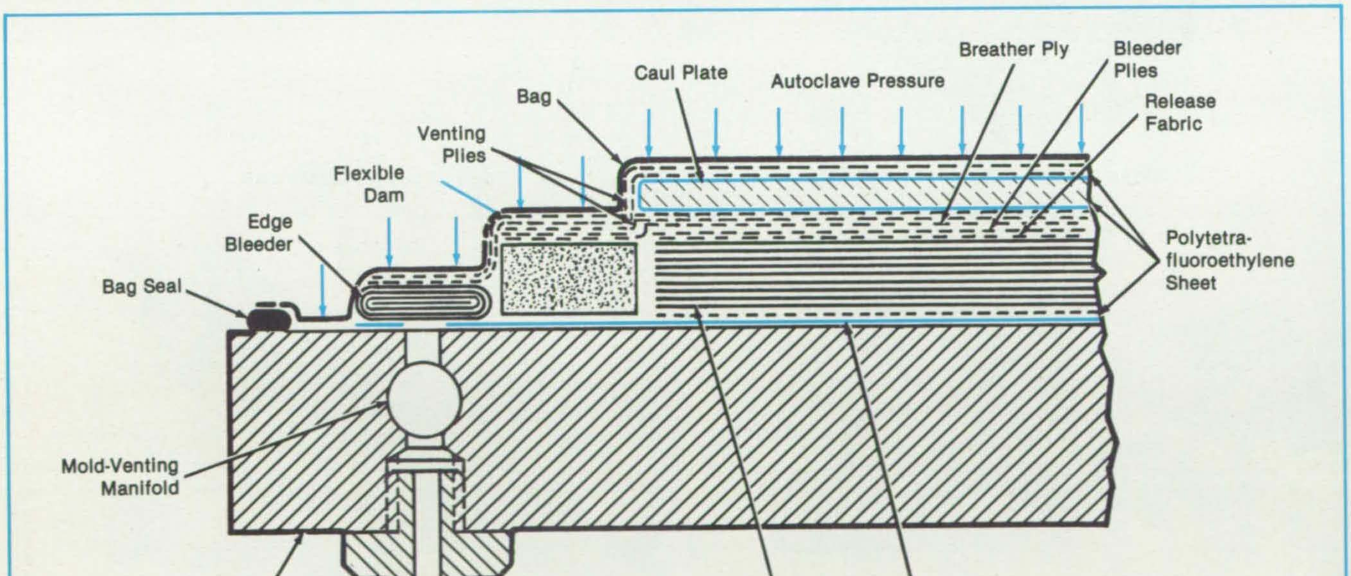

Autoclave Molding in a vacuum bag is cleaner if an adhesive-backed covering (color) is placed around the caul plate as well as on the mold plate. The covering is easy to remove after curing and leaves the caul plate free of resin deposits.

Mobile Platform for Large Structures

A proposed platform would move forward and in reverse, turn left and right, and change planes.

Lyndon B. Johnson Space Center, Houston, Texas

A mobile-platform concept is proposed to move remote manipulators, workers, or other loads over truss panels on large structures. Such a platform would move at a constant speed so that it does not cause a swinging motion in hanging loads and therefore overstress remote-manipulator arms. The platform could be transferred around corners to adjacent panels.

The platform would ride on sprocketed guide pins extending from the structure at truss joints (see figure). A set of orthogonal tracks under the platform slides on the pins, which have enlarged heads to interlock with the tracks. At least three tracks engage at least three pins at any position on the panel so that the platform is adequately and stably supported.

The platform can travel longitudinally and transversely on the panel, in both for-

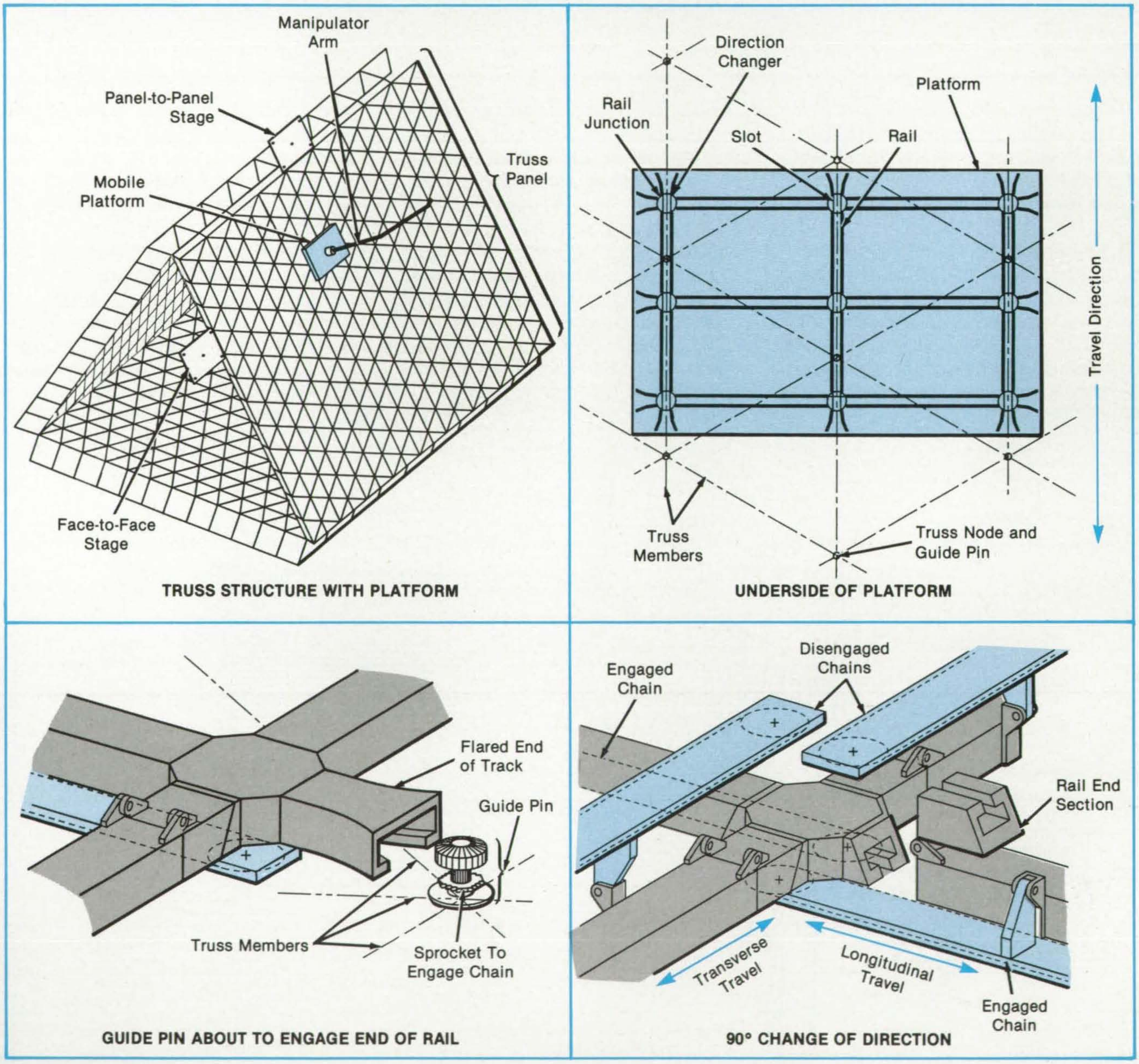

Tracks Slide on Pins on a truss panel. Although a truss member joins other members at angles of 0°, 120°, and 240°, the pin arrangement allows the platform to travel at angles of 0° and 90° with a truss edge. The rails are flared at their outer ends so that the pins engage them smoothly. The drive chains under the platform engage sprockets on the guide pins. The drive chains are shown in position for longitudinal travel, with a rail end section opened for a change to transverse travel.

ward and reverse directions. To get from one point to another, the platform moves in a series of straight lines, making left and right turns as necessary.

Two sets of chain drives under the platform — one for longitudinal motion, the other for transverse motion — propel it by engaging the guide-pin sprockets. Electric motors turn the chain drives.

To change from longitudinal to transverse motion, the platform comes to a complete stop and goes through a brief series of events. First, direction changers — slotted disks at each rail junction — rotate 90°. The slots in the direction changers ensure that the platform does not slip sideways. When the disks have all turned 90° from the longitudinal direction, they permit transverse movement and prevent longitudinal slippage.

Next, the end sections of the rails pivot upward. This provides clearance for the previously-engaged drive chains (for longitudinal motion) to disengage and rotate upward into the platform base and for the previously disengaged drive chains (for transverse motion) to rotate downward into engagement with the guide-pin sprockets. After drive-chain rotation, the end sections resume their original positions. To change from transverse to longitudinal motion, the platform goes through a similar sequence.

The platform transfers to adjacent truss panels on flaplike stages at the panel edges. The platform drives onto a stage, the stage pivots first at the near edge and then at the far edge to align with the plane of the adjacent panel, and the platform drives off onto the new panel. To transfer to the opposite face of a panel, the platform uses a stage that pivots about an axis near its center; the stage does a complete flip-flop, thereby aligning the platform with the plane of the opposite panel face.

This work was done by Clarence J. Wesselski and William C. Schneider of **Johnson Space Center**. *For further information, Circle 15 on the TSP Request Card.*

Inquiries concerning rights for the commercial use of this invention should be addressed to the Patent Counsel, Johnson Space Center *[see page 23].* *Refer to MSC-20985.*

Preventing Cracks in Silicon-Reactor Liners

Correct placement may help to prevent contamination while eliminating crack-causing deposits.

NASA's Jet Propulsion Laboratory, Pasadena, California

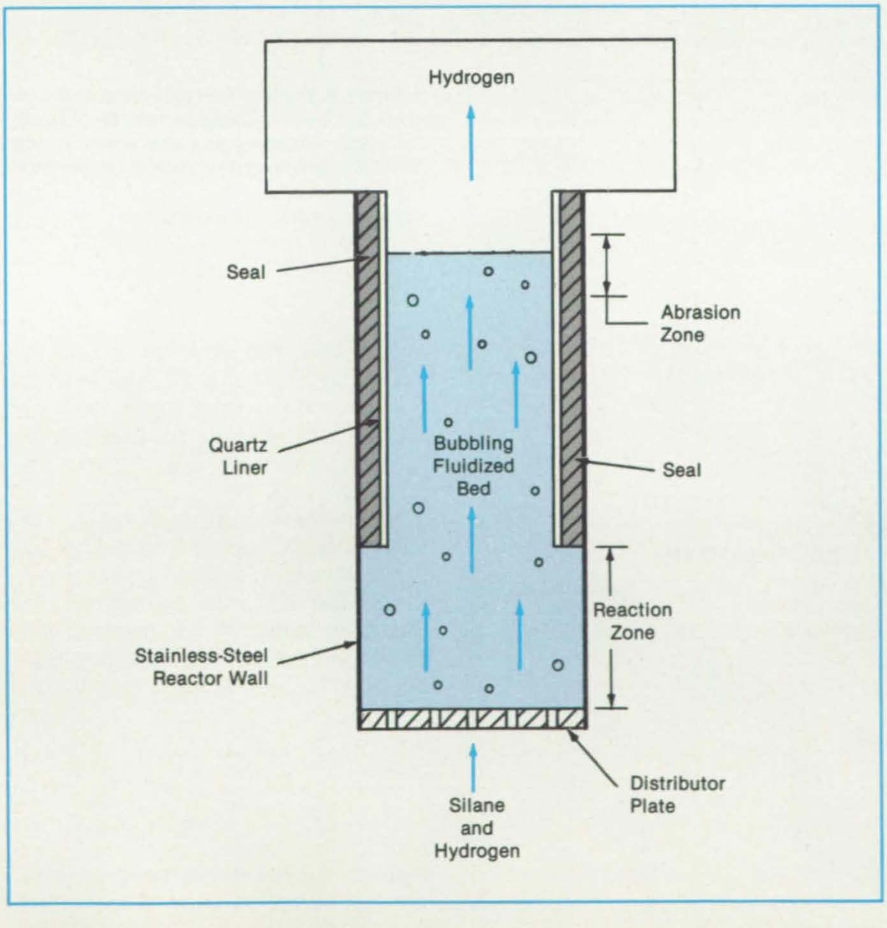

The **Bottom of the Quartz Liner** is raised above the reaction zone. The liner still covers the abrasion zone at the top of the fluidized bed.

Repositioning the quartz liner in a silicon fluidized-bed reactor prevents cracking of the liner when it cools. The liner protects the stainless-steel walls of the reactor from abrasion by the particles in the fluidized bed. It thus prevents contamination of the newly formed silicon by material abraded from the wall and ensures a high-quality product.

However, silicon tends to deposit on the liner as it decomposes from the silane flowing with hydrogen through the bed. When the quartz cools, the difference in contraction between it and the accumulated silicon layer tends to crack the liner. A costly replacement is then necessary before the reactor can be used again.

If the liner is positioned so that it covers the abrasion zone at the top of the bed but not the reaction zone at the bottom, the problem is avoided (see figure). The liner still protects the reactor wall but is not exposed to deposition of significant amounts of silicon.

This work was done by Ralph Lutwack of Caltech for **NASA's Jet Propulsion Laboratory**. *For further information, Circle 41 on the TSP Request Card.*
NPO-16708

Reinforced Masks for Ion Plating of Solar Cells

Long fingers would be held more rigidly.

NASA's Jet Propulsion Laboratory, Pasadena, California

A proposed mask for the ion plating of surface electrodes on silicon solar cells would be reinforced to hold its shape better during handling. The need for reinforcement arises in a typical conventional mask (see Figure 1), because it includes long fingers that are unsupported at their ends.

The fabrication process for the improved mask would be similar to that of a conventional mask. However, additional cuts and bends would be made in the wide diametral strip (see Figure 2) to form bridges between pairs of mask fingers facing each other across this strip. The bridges would be high enough not to act as masks so that the entire strip area would still be plated.

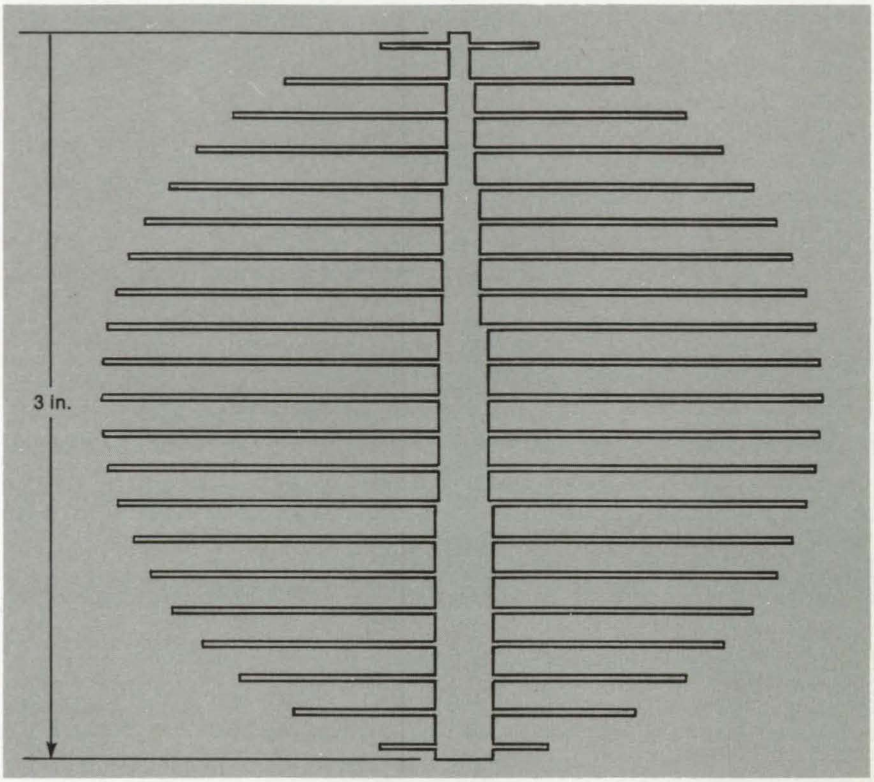

Figure 1. A **Typical Conventional Mask** is made from a thin sheet of steel by cutting out parallel narrow grooves and a wider perpendicular strip. The ends of the remaining metal strips at the edge of the wide cutout strip are unsupported.

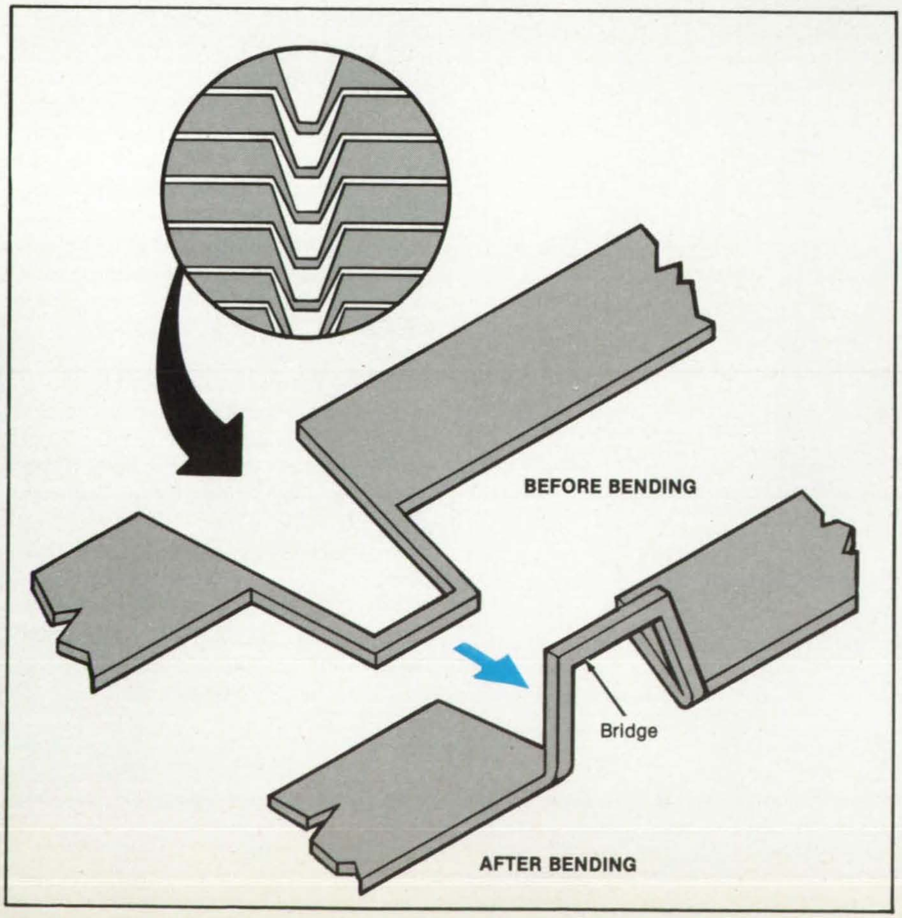

Figure 2. The **Reinforced Mask** is cut so that nesting bridges of metal are formed across the wide cutout strip, connecting the ends of the remaining metal strips. The bridges are then bent out of the mask plane.

This work was done by William R. Conley, E. Grant Swick, and Jack C. Volkers of Illinois Tool Works, Inc., for **NASA's Jet Propulsion Laboratory.** *For further information, Circle 153 on the TSP Request Card.*

This invention is owned by NASA, and a patent application has been filed. Inquiries concerning nonexclusive or exclusive license for its commercial development should be addressed to the Patent Counsel, NASA Resident Office-JPL [see page 23]. Refer to NPO-16417.

Fast-Response Heating of Silicon Melts

Heating would be confined to a small mass near the growing crystal.

NASA's Jet Propulsion Laboratory, Pasadena, California

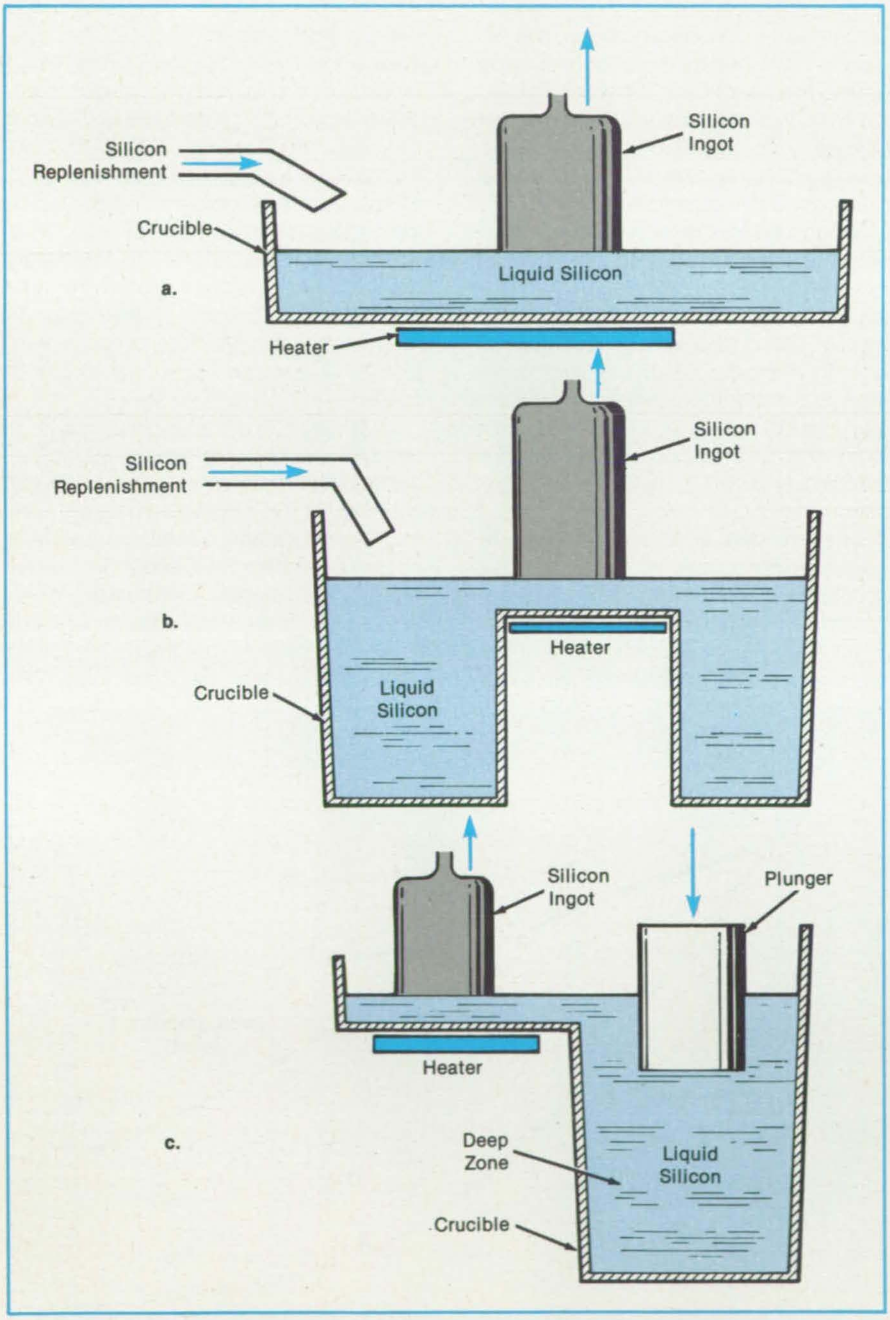

In versions b and c, a **Deep Zone Adjoins a Shallow Zone** of molten silicon. A heater can raise the temperature of the shallow zone quickly. In all three versions, the melt level is maintained by replenishment with silicon (top and middle) or by immersing a plunger in the liquid (bottom).

A proposed improvement for silicon crystal growing would enable rapid heating of the melt in the vicinity of the liquid-solid interface to compensate for decreases in melt temperature, to ensure a uniform diameter and composition in the ingot. The improvement is intended for growing large silicon ingots by the Czochralski process, in which a cylindrical single-crystal ingot is pulled from molten silicon.

At present, it is impossible to respond quickly to sudden drops in melt temperature by boosting the power to the electrical heating elements that surround the melt crucible, because the melt is too massive to heat up quickly enough. Instead, an industrial crystal grower automatically raises the pulling rate to compensate and thereby maintain a constant ingot diameter. However, this practice is not entirely satisfactory: Rapid changes in the pulling rate cause changes in the solidification rate and in the inclusion of impurities and defects. (These effects were previously masked by the effects of convection currents but will become increasingly important as controlled convection furnaces are developed.)

For the purpose of effecting a rapid heating of the melt in the vicinity of the interface, a shallow melt would underlie the growing ingot (see figure). A heater under the shallow zone would provide heat when the melt cooled. With a relatively small mass of molten silicon above it, the heater can rapidly raise the melt temperature to the proper level. At the same time, there is ample liquid silicon in the deep zone adjacent to the shallow center to replace the material consumed by the growing ingot.

This work was done by Andrew D. Morrison of Caltech for **NASA's Jet Propulsion Laboratory**. *For further information, Circle 96 on the TSP Request Card. NPO-16730*

Mathematics & Information Services

Hardware, Techniques, and Processes

Books and Reports

Maximum-Likelihood Decoder on a Hypercube Multiprocessor

Efficient parallel processing is used to implement complex decoders.

NASA's Jet Propulsion Laboratory, Pasadena, California

A hypercube multiprocessor connection scheme makes it practical to decode long convolutional codes with efficient use of hardware. The hypercube design reduces both the communication time among processors and the space needed for their interconnection. This decoding concept is applicable to concurrent processing of digital signals using convolutional codes for error correction.

A convolutional code produces encoded symbol sequences based on the input information bits and on the state of a finite-state machine with m memory cells. The task of the decoding algorithm (Viterbi algorithm) is to search among all possible received symbol sequences, which are corrupted by errors, and select the most likely transmitted sequence. Such a machine is called a maximum-likelihood decoder.

The complexity of the decoder increases exponentially with m, because it is necessary to compare the likelihoods of all possible 2^m sequences. For long codes ($m > 10$), a single microprocessor is inadequate as a maximum-likelihood decoder.

A multiple-microprocessor system can be used to decode long codes. In a concurrent formulation, it is necessary to divide the algorithm into equal parts, to share equally the resources available in each processor, and to minimize the communication among the processors so that only nearest neighbors need to exchange messages. The hypercube configuration arises from topological considerations concerning the equivalence of networks: it turns out that a maximum-likelihood decoder can be constructed by connecting the processors to their nearest neighbors as though each processor was located at a vertex of an m-dimensional cube.

Each processor, at a given stage k, receives the surviving sequence and the accumulated metric (the measure of the likelihood of the surviving sequence) from its neighbor along dimension k of the hypercube. In practice, about 5m stages are required to obtain performance close to optimum. This corresponds to using the m dimensions of the hypercube five times. To minimize internode communications,

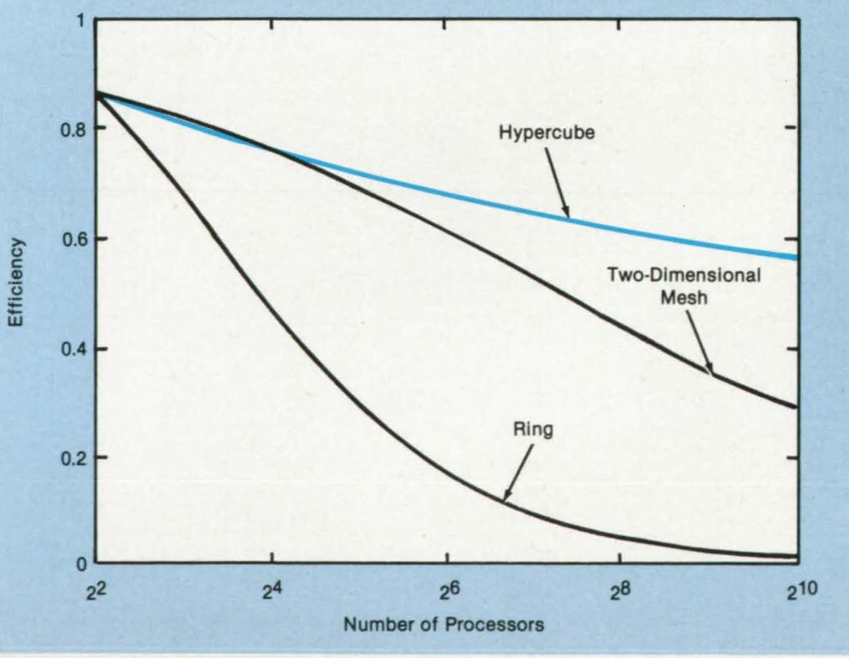

The **Efficiencies of Different Decoder Configurations** are shown as functions of the number of processors. The hypercube configuration gives the greatest speedup for maximum-likelihood decoding of long convolutional codes.

the number of stages is increased slightly, enabling the input/output operations to be simplified and the decoded bits to be read out at node zero (the origin of the cube coordinate system).

The decoding operation requires that blocks of data be loaded into every processor. In the hypercube network, data from the host processor are inserted only through node zero. These data are then broadcast throughout the hypercube by transmission between neighboring nodes.

In general, when the number of available processors 2^n is less than the number of states in the decoder 2^m, 2^{m-n} states can be assigned to each processor.

The efficiency, η, of a parallel architecture is related to the speedup factor, s, and to the number of processors, N, by $s = \eta N$. The figure compares the efficiencies of 2^{13}-state decoders having different interconnection configurations; each decoder has a communication time equal to the time for one operation. The hypercube configuration exhibits the greatest efficiency for large decoders. Decoders for m up to 14 have been tested successfully on a 64-node hypercube multiprocessor.

This work was done by Fabrizio Pollara of Caltech for **NASA's Jet Propulsion Laboratory**. *For further information Circle 132 on the TSP Request Card.*

This is the invention of a NASA employee, and a patent application has been filed. Inquiries concerning license for its commercial development may be addressed to the inventor, Mr. Edward Ansell (CIT Waiver), Director of Patents and Licensing, California Institute of Technology, Pasadena, CA 91125. Refer to NPO-16724.

Solving Finite-Element Problems on a Concurrent Processor

By use of the "conjugate gradients" technique, the concurrent efficiency is greater than 90 percent.

NASA's Jet Propulsion Laboratory, Pasadena, California

An algorithm applies the method of conjugate gradients to the iterative solution of finite-element problems on a concurrent processor. With the algorithm, iteration rates are nearly proportional to the number of processors. For sufficiently large problems, the fraction of proportional speedup achieved, called the concurrent efficiency, exceeds 90 percent. These results indicate that future application of this and related algorithms to large finite-element problems will depend primarily upon the applicability of iterative techniques, not upon issues of concurrency or efficiency.

Most finite-element applications involve solving matrix elliptic partial differential equations of the form $A\mathbf{x} = \mathbf{b}$. In such an equation, $\mathbf{x}$ is a vector of unknown quantities, to be solved for at each node in the problem domain (see Figure 1). A is the "stiffness" matrix, which contains the terms that determine the interaction among the different unknown degrees of freedom in $\mathbf{x}$. The forcing terms or boundary values are introduced through the vector $\mathbf{b}$.

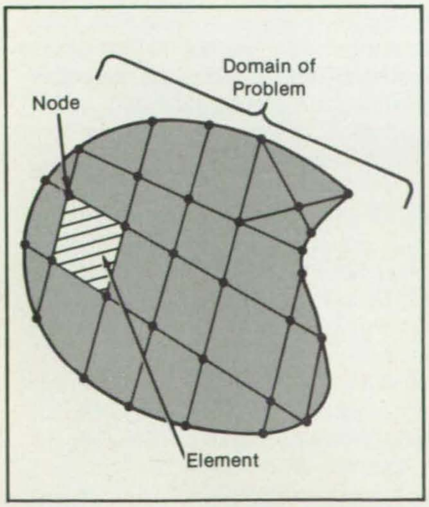

Figure 1. A **Typical Finite Element Application** involves solving a matrix equation of the form $A\mathbf{x} = \mathbf{b}$. Vector $\mathbf{x}$ is to be solved for at each node within the problem domain.

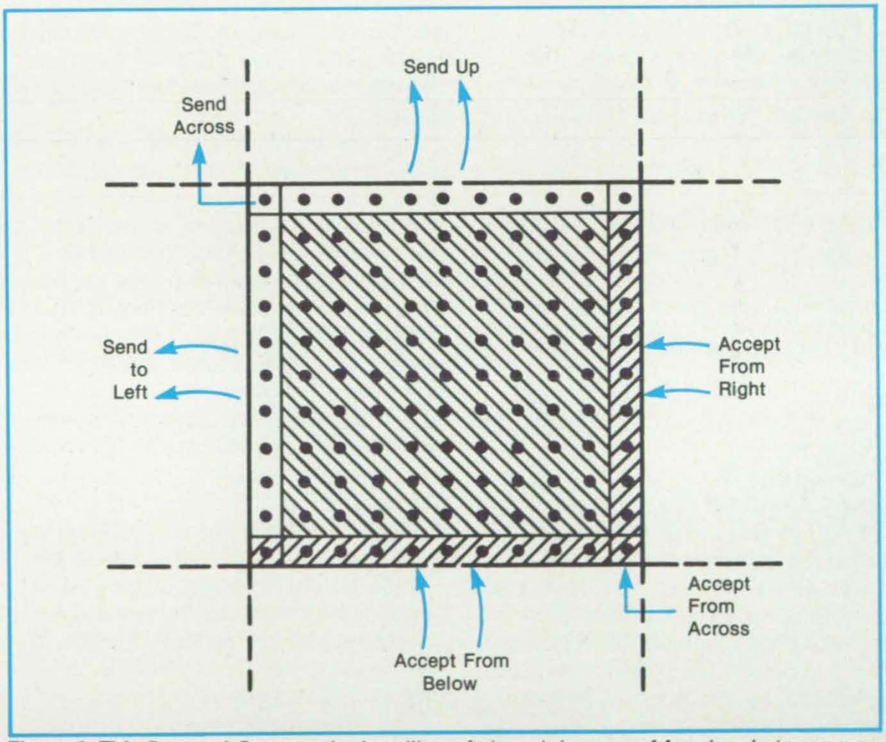

Figure 2. **This Protocol Governs** the handling of shared degrees of freedom between processors in the two-dimensional case.

Each entry of A is computed by performing integrals over the elements that include the node in question. The stiffness matrix therefore consists of an assembly of individual element matrices, which are mapped into the "global" matrix A through a master-equation bookkeeping scheme.

The conjugate-gradient solution method is a technique for iteratively searching the space of vectors $\mathbf{x}$ in such a way as to minimize a function of the residual errors. The method involves a six-step algorithm that involves two basic kinds of operations: the vector inner product and the matrix-vector product. Both operations are done in parallel by decomposing the problem into regions corresponding to the physical domain of the problem. A given "global" vector is spread out among the processors of a concurrent

ensemble, with concurrent operations being performed on the various "pieces" of the vectors in each processor. The only need for information from outside a given processor occurs when nodes on the boundary between the "jurisdictions" of the two processors are computed.

Figure 2 illustrates schematically the protocol for handling shared degrees of freedom between processors in a two-dimensional finite-element grid. Each processor obeys a convention by which it accumulates contributions to global vector quantities from neighboring processors along the right and lower edges of its region. Contributions arising from degrees of freedom along the left and upper edges are sent to the neighboring processor for accumulation. (The lower-right and upper-left corner degrees of freedom are passed twice in reaching their destinations.) Final up-to-down and left-to-right shifts redistribute the final sums of all contributions to all the neighboring processors.

The scheme is applicable to any multiple-instruction, multiple-data computer that supports the global broadcast of data from a designated controlling process or processor to the concurrent array, the transmission of unique data messages between array elements and the control process, and element-to-element data transmission between nearest neighbors. A finite-element/conjugate-gradient program was tested on a series of two-dimensional plane/strain elasticity problems. In these tests, the Mark II hypercube computer was used in configurations from one node (0-dimensional cube) through the full 32 nodes (5-dimensional hypercube). The problems were formulated as rectangular arrays of elements with boundary displacements imposed to produce a simple shear-field solution. The problems were solved using 1, 2, 4, 8, 16, and 32 processors. Concurrent efficiencies ranged from 76 to 98 percent.

This work was done by Gregory A. Lyzenga, Arthur Raefsky, and Bradford H. Hager of Caltech for **NASA's Jet Propulsion Laboratory**. *For further information, Circle 123 on the TSP Request Card. NPO-16745*

Books and Reports

These reports, studies, and handbooks are available from NASA as Technical Support Packages (TSP's) when a Request Card number is cited; otherwise they are available from the National Technical Information Service.

Theory of Periodic-Binary-Sequence Generators

Algorithms yield feedback shift registers with maximum regularity.

A report provides an extensive mathematical treatment of new and previous results related to the generation of pseudonoise binary sequences by feedback shift registers. The generator architectures are amenable to efficient implementation in very-large-scale integrated (VLSI) circuits. The report includes literature references to applications of such sequences in random-number generation, radar, VLSI testing, data encryption and decryption, algebraic error-detection and error-correction encoding and decoding, and feedback-shift-register synthesis of sequential machines.

Polynomials of degree r over a Galois field characteristic 2 [GF(2)] represent the behavior of shift registers with linear feedback. The object of the report is the algorithmic determination of the trinomial of lowest degree, when it exists, that contains a given irreducible polynomial over GF(2) as a factor. This corresponds to embedding the behavior of an r-stage shift register with linear-logic feedback into that of an n-stage shift register (n usually > r) with a single two-input exclusive OR gate in its feedback loop. The architecture of such feedback shift registers has maximum regularity (i.e., identical cells), with intercell communications serialized to a maximum degree.

Sections 1 and 2 of the report contain a thorough exposition of background material on Galois-field algebra, including cyclotomic theory. Section 3 develops logical-circuit theory of feedback shift registers. Two types of feedback shift registers are considered. The state behavior of shift registers with linear-logic feedback to a single stage is related to the mathematical properties of the characteristic polynomial of a linear recurrence relationship between the bit being fed back and the content of stages contributing to the feedback. The state behavior of shift registers with interstage linear-logic feedback is related to successive powers of the inverse of the root of the characteristic polynomial. A one-to-one correspondence between the successive states of two types of feedback shift registers associated with the same characteristic polynomial is derived.

The extensive collection of theorems and lemmas on the properties of classes of polynomials over GF(2), contained in Section 4, are the principal contributions of the report. The fruit of this work, presented in Appendixes B and C, is the compilation of polynomials (primitive and irreducible nonprimitive) and trinomials of lowest degree that, respectively, contain the foregoing polynomials as factors. The trinomials characterize feedback shift registers of maximum regularity and linear-logic feedback circuitry of minimum complexity for generating periodic binary sequences associated with the polynomial factors.

Number-theoretic functions including the Euler phi function and the Mobius function are briefly discussed in Appendix A because of their applicability to feedback shift-register theory. Appendix B exhaustively considers primitive polynomials over GF(2) through degree 12. It is proven in Section 4 that trinomials exist that contain any given primitive polynomial as a factor. Furthermore the trinomial of lowest degree is square free; i.e., its irreducible factors are distinct. Irreducible factors, determined by Berlekamp's factorization algorithm, of each (lowest degree) trinomial of degree less than 70 containing a given primitive polynomial as a factor are listed. Within the list are factors having degrees as high as 52. Also noted are the results of testing each additional factor to ascertain if the lowest-degree trinomial that contains a given primitive polynomial (of degree 12 or less) is also the lowest-degree trinomial that contains the factor in question. This leads to the extension of the table to a partial listing of primitive polynomials of degree 13 through 19 and of the respective trinomial that contains each as a factor. Appendix C deals with irreducible nonprimitive polynomials over GF(2) through degree 12. In contrast to primitive polynomials, there are many irreducible nonprimitive polynomials that are not a factor of existing trinomials.

In Section 4, a sufficient but nonnecessary condition is proved that guarantees the existence of one or more trinomials containing a given irreducible nonprimitive polynomial as a factor. Of these trinomials, those of lowest degree are square free. As in Appendix B, the irreducible factors of each (lowest degree) trinomial of degree less than 70 are listed. Among these are factors whose degrees are as high as 56. Also noted are the results of testing each additional factor to determine if the trino-

mial of lowest degree containing a given irreducible nonprimitive polynomial (of degree 12 or less) is also the lowest degree trinomial to contain the factor in question. The tables in Appendixes B and C enable one to design a feedback shift register with a single two-input exclusive OR gate in its feedback to generate periodic binary sequences. The structure and period of the sequence are governed by the mathematical properties of the characteristic polynomial selected from the tables.

This work was done by Marvin Perlman of Caltech for **NASA's Jet Propulsion Laboratory**. *Further information may be found in NASA-CR-175649 [N85-22886/NSP], "Periodic Binary Sequence Generators: Very Large Scale Integrated (VLSI) Circuits Considerations."*

Copies may be purchased [prepayment required] from the National Technical Information Service, Springfield, Virginia 22161, Telephone No. (703) 487-4650. Rush orders may be placed for an extra fee by calling (800) 336-4700.
NPO-16628

Structural Error and Identifiability in Mathematical Models

Errors and previously implicit assumptions are treated explicitly.

A paper discusses the errors in mathematical models of physical systems and the problem of identifying a model from the system input and output. This problem is approached by explicitly taking account of erroneous choices of model structure ("structural error"); for example, the neglect of nonlinearities or small effects, or the representation of a higher-order system by a lower-order model.

In this specialized context, "system identification" denotes the determination of a mathematical model that represents the physical system as closely as possible under the prescribed experimental conditions. In practice, system identification is often divided into the following three phases:

1. Selection of a model structure;
2. Testing of the structure to ensure that a unique solution for its parameters is possible (the identifiability test); and
3. Parameter estimation.

Structural error can affect both the identifiability of a model and the final values of the parameter estimates.

The paper is concerned specifically with linear or weakly nonlinear models. Two different sets of model equations represent the relationships among the system state, input, output, and model parameters; one of these sets describes the basic assumed (and somewhat erroneous) model while the other represents an ideal model that would completely and accurately describe the system. Included in the ideal model are an additive error term that specifies the structural error and a set of the "true" parameter values, which are generally not known.

The identifiability problem is then reformulated on the basis of equivalence and near equivalence between model and system. "Near equivalence" would be established if a model-dependent criterion function is less than the acceptable maximum modeling error and if the absolute magnitude of the difference between model and true outputs is less than the maximum acceptable output error.

The practical identification problem then is to determine the parameters of a nearly equivalent model from observations of the inputs and outputs of the system and model. The paper derives a number of theorems concerning necessary and sufficient conditions for near equivalence and the identifiability of parameters.

This work was done by Fred Y. Hadaegh of **NASA's Jet Propulsion Laboratory** *and George A. Bekey of The University of Southern California. To obtain a copy of the report, "Structural Error and Identifiability," Circle 12 on the TSP Request Card.*
NPO-16661

Near Identifiability of Dynamical Systems

Concepts regarding approximate mathematical models are treated rigorously.

A paper presents new results in the analysis of structural identifiability, equivalence, and near equivalence between mathematical models and the physical processes they represent. The paper helps to establish a rigorous mathematical basis for concepts related to structural indentifiability and equivalence by revealing fundamental requirements, tacit assumptions, and sources of error. "Structural identifiability," as used by workers in this field, can be loosely translated as meaning the ability to specify a unique mathematical model and a set of model parameters that accurately predict the behavior of the corresponding physical system.

Previous work on structural identifiability was based on the assumption that the structures of physical systems were completely known (at least in principle), enabling the model structures to be specified exactly. In practice, mathematical models and physical systems agree only approximately and over restricted ranges of inputs for restricted intervals of time. This gives rise to the need for a concept of near (that is, approximate) identification.

The "true model" of a system is the model that exactly represents the input/output behavior of the system under the limited circumstances in which it is observed. For purposes of the analysis, the difference in the state vectors between a given model and the true model is expressed as an additive error term called the "structural error." Lacking an exact representation of the structural error, the difference in behavior between the true model and the class of models under study may be characterized by some norm of the difference between the outputs of the system and the model. The near-equivalence problem is concerned with determining whether the model parameters stay in the neighborhood of the true parameters when the model and system outputs stay within given bounds.

Once the model structure is defined (except for the parameters) the problem is to determine a set of unknown parameters. The question of near identifiability is posed as follows: If two distinct parameter sets are in the neighborhood of the true parameter set and the model outputs of both sets stay within the given bounds, are the outputs distinguishable?

The practical identification problem consists of the determination of a parameter set of a model that is nearly equivalent to the system within the limits on the difference in outputs as measured by a scalar criterion function. If such a parameter set can be found, the system is termed "practically identifiable" or "nearly identifiable."

Bounds on the output error are derived precisely as a function of the structural error. Sufficient conditions for near equivalence are then obtained for given bounds on the output error. This enables the definition of near identifiability in terms of the modeling error and gives rise to two theorems expressing sufficient conditions for near-identifiability. An example illustrates the concepts introduced in the paper.

This work was done by Fred Y. Hadaegh of **NASA's Jet Propulsion Laboratory** *and George A. Bekey of The University of Southern California. To obtain a copy of the report, "Near-Identifiability of Dynamical Systems," Circle 11 on the TSP Request Card.*
NPO-16785

Life Sciences

Hardware, Techniques, and Processes

Cutting Head for Ultrasonic Lithotripsy

Kidney stones are disintegrated safely and efficiently.

Goddard Space Flight Center, Greenbelt, Maryland

Kidney stones lodged in the urinary tract are disintegrated with increased safety and efficiency by a cutting head attached to the end of a vibrated wire probe. The cutting head aligns the probe with the stone and enables the probe to vibrate long enough (typically less than one minute) to disintegrate the stone. The design of this cutting head reduces the risk of metal-fatigue-induced breakage of the probe tip that could leave metal fragments in the urinary tract.

In a recent alternative to the surgical removal of kidney stones lodged in the upper two thirds of the ureter, an ultrasonically vibrated wire probe disintegrates a stone into small fragments that the patient can then pass spontaneously. In this procedure, a catheter is placed cystoscopically at the site of the stone. A long wire probe is then passed through a lumen of the catheter until it touches the stone. The wire probe is attached to the ultrasonic transducer that sets the wire probe into stone-fragmenting lateral and longitudinal vibrations.

This apparatus is limited in effectiveness by the slippage of the thin wire probe off the kidney stone and its lodgment between the stone and urinary tract. Attempts to prevent this slippage by providing a wider tip with a cutting surface have resulted in the dangerous breakage of the wire probe at the tip after only 10 to 20 seconds of operation.

The new cutting-head design prevents premature breakage and assures the seating of the stone on the head (see figure). Constructed of stainless steel, the head has a cutting tip and an elongated collar that relieves the stress on the wire. The wire is inserted in a central circular hole in the rear of the head. At locations shortly behind its cutting teeth, the head is swaged onto the wire. Swaging is used to avoid detempering problems associated with soldering and to minimize stress raisers.

The cutting teeth are machined into the end of the cutting tip and are provided with flat ends to prevent them from scraping the urethra. The teeth form a cup-shaped receptacle that seats a kidney stone. Even if the stone is highly irregular

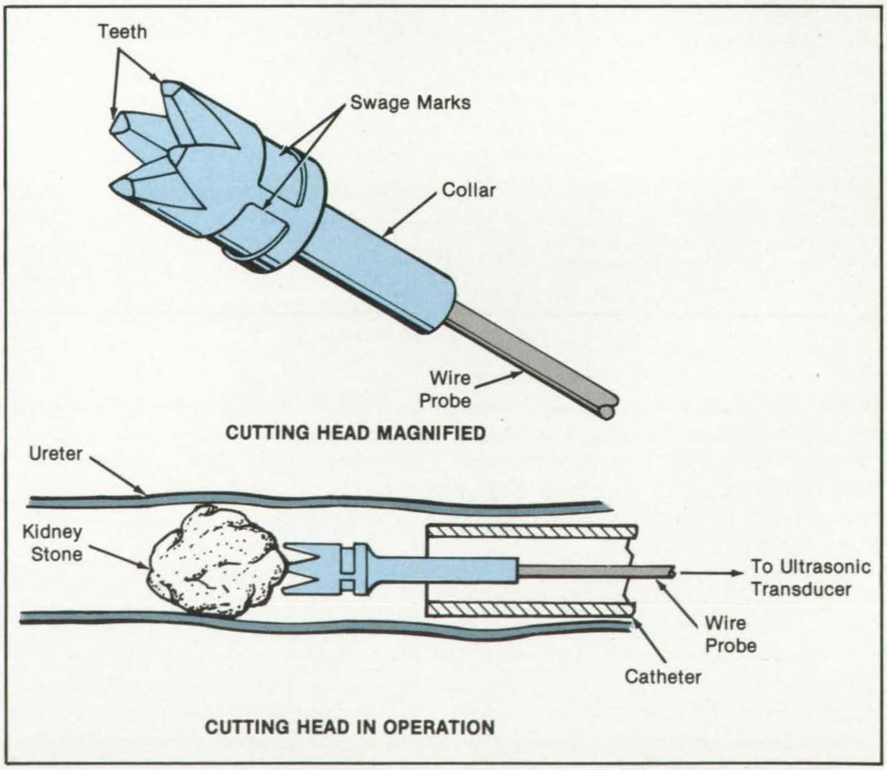

The **Teeth of the Cutting Head** both seat and fragment the kidney stone, while the extension of the collar into the catheter lessens mechanical strain in the probe wire, increasing probe life and lessening the danger of in situ probe breakage.

in shape and even if the tip and the stone are aligned imperfectly, the stone will fragment when contacted by any portion of the cutting tip.

Because part of the collar stays within the catheter while the cutting tip is extended against the stone, the mechanical bending loads imposed on the probe wire by the vibration of the head are diminished. When vibrating at the typical operating frequency of 20 kHz, the assembly lasts more than four minutes before the wire breaks off the head; this provides ample time to disintegrate the kidney stone.

This work was done by Earl D. Angulo of **Goddard Space Flight Center** *and Roger Goodfriend of F.A.C.S. For further information, Circle 44 on the TSP Request Card.*

This invention is owned by NASA, and a patent application has been filed. Inquiries concerning nonexclusive or exclusive license for its commercial development should be addressed to the Patent Counsel, Goddard Space Flight Center *[see page 23].* *Refer to GSC-12944.*

Transformation Aids Crop Analysis From Spectral Data

Most data variability is captured in three spectral features.

Lyndon B. Johnson Space Center, Houston, Texas

Crop analysis could be aided by a mathematical transformation that optimizes the perspective of the six-dimensional (six-band) spectral data taken from a spacecraft or aircraft. This transformation can be applied to any temperate-climate vegetated scene, providing a direct view of the regions of data concentration resulting from band correlations and fundamental reflectance properties of scene classes. Almost all of the data variability is captured in three spectral features, thus reducing by a factor of 2 the number of spectral features that must be carried, while incurring a minimal loss of important information.

An analysis of both simulated and actual data in the six reflective bands (which do not include the thermal band) revealed that the data from vegetation and soils occupy primarily three dimensions, defining two planes, as illustrated in the figure. The transformation rotates the data to bring the coordinate axes into alignment with these planes. This rotation preserves all of the Euclidean data relationships, changing only the viewing perspective.

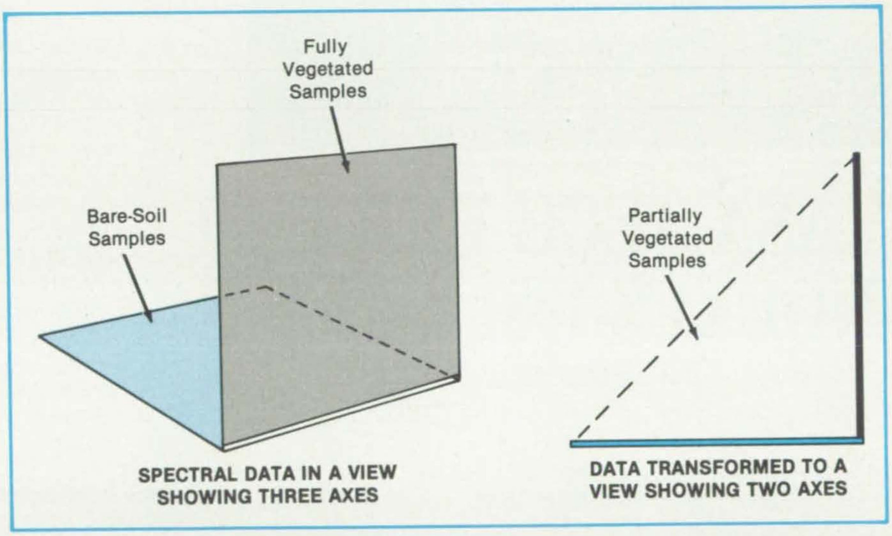

A **Three-Dimensional Representation** with two principal planes retains about 95 percent of the six-dimensional spectral data that can be used to distinguish among scenes containing green plants and bare soil with varying degrees of moisture.

The transformation matrix expresses the relationships among the intensities in each of the six spectral bands and the coordinates along each of six axes in the transformed space. Three of the transformed coordinates, namely, "brightness," "greenness," and "wetness" contain 95 percent of the total data variability. "Brightness," a weighted sum of all six bands, is related to total reflectance and defines the intersection of the two planes in the figure. "Greenness," primarily a contrast between the near-infrared band and the sum of the visible bands, indicates the density of green vegetation. "Wetness," a contrast between the weighted sum of intensities at the four shortest wavelengths and those of the two longest wavelengths, indicates the amount of moisture in nonvegetated soil.

As presented, the transformation matrix represents an adjustment of simulation-based results, using data from three actual scenes to fine tune the simulated-data coefficients to obtain the correct alignment of the coordinate axes and the data planes.

Because of the small number of scenes analyzed to date, the transformation must be considered preliminary, and its direct applicability to other scenes should be tested before it can truly be declared to be invariant; for example, atmospheric and illumination differences will affect the orientation of the data, and thus the consistency of the transformation, and should therefore be taken into account. However, any adjustments indicated by analysis of more scenes are expected to fall into the category of fine tunings rather than radical changes.

This work was done by Eric P. Crist and Richard C. Cicone of Environmental Research Institute of Michigan for **Johnson Space Center**. *For further information, Circle 19 on the TSP Request Card.*
MSC-20859

Letters

The "Letters" column is designed to encourage a wide exchange of ideas among *NASA Tech Briefs* readers. To contribute a request for information or to respond to such a request, use the feedback cards in this issue, or write or call: Manager/Technology Transfer Division, P.O. Box 8757, Baltimore/Washington International Airport, MD 21240; (301) 859-5300. While we can print only a small number of letters, we will endeavor to select those that are of varied and wide interest.

Our Good Fortune

NASA Tech Briefs is the best magazine, without a doubt. We in the public sector (i.e. not working for NASA) are very fortunate indeed to get NASA Tech Briefs—how else could we so easily benefit from progress being made at NASA? No other publication comes close. Keep up the good work. Don't let the politicians cut your budget—we need you!

Gioacchino V. Sarno
PhD Staff Scientist
Alcoa Defense Systems
San Diego, CA

It's Beneficial

Your program is of great benefit to our business and we salute NASA for it. It's too bad the rest of the federal government can't get off its duff so that we all can have a strong economy and a great way of life.

William Hyde
Automotive Research Corp.
Idaho Falls, ID

Read It In NASA Tech Briefs First

I am responsible for manufacturing projects that are so new and innovative very little is published on them. The state of microwave technology is such that outside of technical bulletins, NASA Tech Briefs is the sole source available to me that features related articles and presentation of microwave reception and transmission equipment.

David S. Thurston
Manufacturing Engineer
Microwave Assembly Division
General Dynamics
Pomona, CA

Time Well Spent

NASA Tech Briefs delivers the most up-to-date data on new developments throughout science. I find myself waiting for new issues to arrive as I pore over previous ones for the 10th time. I wish NASA Tech Briefs was a monthly publication.

Scott J. Crane
Polymer Engineer
Hewlett Packard
San Jose, CA

[NTB will be published 10 times in 1987, starting with this issue. July/August and November /December will be combined issues.]

Silver Threads Among the Gold

If in the past a NASA Tech Briefs issue was not immediately useful, I read the introduction and put it in a box with the others. Approximately 80% of them have subsequently been pulled out for various projects, where they provided invaluable help. I think NASA Tech Briefs is a very good program.

S. P. Hotaling
Syracuse Research Corp.
Defense Electrical Engineering Division
Syracuse, NY

Subject Index

Advertiser's Index

***RAC** stands for **Reader Action Card.** For further information on these advertisers, please circle the RAC number on the Reader Action Card elsewhere in this issue. This index has been compiled as a service to our readers and advertisers. Every precaution is taken to ensure its accuracy, but the publisher assumes no liability for errors or omissions.

By distilling the control of a steering wheel, brake and accelerator into an easily-operated joystick, the Unistik Vehicle Controller System requires only small movements of one hand to control a car.

Mission Accomplished

Through the technology transfer process, many of the systems, methods and products pioneered by NASA are re-applied in the private sector, obviating duplicate research and making a broad range of new products and services available to the public.

Last summer an engineer named Jerry Polson drove an experimental vehicle 3000 miles through the Rocky Mountains from Boulder to Vancouver, using only a joystick to start, accelerate, steer and stop the vehicle.

The trip really began in 1972 when a paraplegic named Tom Wertz saw Apollo astronauts driving the Lunar Rover with one hand...using a T bar. Three years later Wertz was driving one himself, at the Johnson Space Center's test range. He realized that if this technology could be adapted to automobiles, it would let handicapped people become more independent.

NASA and the Veteran's Administration agreed, and in 1981 contracted Johnson Engineering (Boulder, CO) to implement Wertz's idea. Seven months later Johnson installed a prototype system, the Unistik Vehicle Controller, in a Ford van.

Johnson came up with a two-axis joystick design that controls high-torque electric motors actuating the vehicle's steering wheel, brake and accelerator pedals. Essentially a remote manipulator using fly-by-wire like techniques, Unistik allows the driver to control the vehicle through small, low force hand motions—from any position.

The Unistik Controller was designed for C-5 quadriplegics, such as Wertz, who have spinal cord lesions at the fifth cervical vertebra. Persons with such severe injuries have very limited use of their upper extremeties, able to move their hands only a few inches to either side. The joystick thus has a control resistance of less than eight ounces, and mounts on an armrest for the forearm.

Simple, but Effective

Unistick driving is simple. Moving the stick forward accelerates the vehicle, to the rear slows it down, and left or right turns the steering wheel in the proper direction. Moving the joystick to the two o'clock position, for instance, will give an accelerating turn to the right. Polson mentions that during his trip "it was interesting to see how easy it was to operate, and how techniques evolved to make optimal use of the system."

Normal driving controls such as steering wheel and pedals are still operable—and still move—when the Unistik operates. A push of a button deactivates the Unistik, returning the van to normal operation. Thus, both handicapped and able-bodied people can use the same vehicle.

"The 1981 prototype has gone through an evolutionary development," says John Bernstein, Director of the Corporate Business Divison at Johnson. "We're in the final throes of the field engineering and testing phases for a phase II design." This streamlined version has a number of improvements. Taking another tip from the aerospace industry, redundant circuits automatically engage if critical systems such as steering and braking fail. The system performs a self check before allowing the driver to switch to go into gear. Another joystick controls turn signals and headlights.

Phase III, currently pending NASA approval, will place the system in a newer van, and may include a voice control system. The voice system will operate standard automobile features such as lights, window wipers, turn signals and automatic windows.

Why Now?

The logic of this design seems obvious, raising the question of why this sort of system hasn't been on the market for years. According to Bernstein, "previous automotive controllers were mostly mechanical." Tom Wertz adds, "they worked well at low speeds, but had severe problems at greater velocities."

"The Unistik represents the first integrated technical approach," says Bernstein. "It's the first time microprocessors have been used in conjunction with the mechanical elements." Polson elaborates: "A redundant system like ours, with reasonable size and cost, requires computer technology that has only recently been available."

NASA's wide ranging technology transfer achievements pale in comparision to when they're able to assist the handicapped. The Unistik superbly performs that role. According to Wertz: "There are a lot of higher injury and Multiple Sclerosis people who will be able to use the Unistik, partly because the controller can easily be changed; you'll be able to get a T-bar handle. This will help disabled people get around by themselves. Their job market will expand, and they'll become more independent." □

ABOUT THE NASA TECHNOLOGY UTILIZATION PROGRAM

This document was prepared under the sponsorship of the National Aeronautics and Space Administration. NASA Tech Briefs is published ten times a year and is free to engineers in U.S. industry and to other domestic technology transfer agents. It is both a current-awareness medium and a problem-solving tool. Potential products...industrial processes...basic and applied research... shop and lab techniques...computer software...new sources of technical data...concepts...can be found here. The short section on New Product Ideas highlights a few of the potential new products contained in this issue. The remainder of the volume is organized by technical category to help you quickly review new developments in your areas of interest. Finally, a subject index makes each issue a convenient reference file.

Further information on innovations—Although some new technology announcements are complete in themselves, most are backed up by Technical Support Packages (TSP's). TSP's are available without charge and may be ordered by simply completing a TSP Request Card, found at the back of this volume. Further information on some innovations is available for a nominal fee from other sources, as indicated. In addition, Technology Utilization Officers at NASA Field Centers will often be able to lend necessary guidance and assistance.

Patent Licenses—Patents have been issued to NASA on some of the inventions described, and patent applications have been submitted on others. Each announcement indicates patent status and availability of patent licenses if applicable.

Other Technology Utilization Services—To assist engineers, industrial researchers, business executives, Government officials, and other potential users in applying space technology to their problems, NASA sponsors Industrial Applications Centers. Their services are described on pages 22-23. In addition, an extensive library of computer programs is available through COSMIC, the Technology Utilization Program's outlet for NASA-developed software. See special section on computer programs on page 44.

Applications Program—NASA conducts applications engineering projects to help solve public-sector problems in such areas as safety, health, transportation, and environmental protection. Two applications teams, staffed by professionals from a variety of disciplines, assist in this effort by working with Federal agencies and health organizations to identify critical problems amenable to solution by the application of existing NASA technology.

Reader Feedback—We hope you find the information in *NASA Tech Briefs* useful. A reader-feedback card has been included because we want your comments and suggestions on how we can further help you apply NASA innovations and technology to your needs. Please use it; or if you need more space, write to the Manager, Technology Transfer Division, P.O. Box 8757, Baltimore/Washington International Airport, Maryland 21240.

Advertising Reader Service—Reader Action Card (RAC): For further information on the advertisers, please circle the RAC number on the separate Reader Action Card in this issue.

Change of Address—If you wish to have *NASA Tech Briefs* forwarded to your new address, use the Subscription Card enclosed at the back of this volume of *NASA Tech Briefs*. Be sure to check the appropriate box indicating change of address, and also fill in your identification number (T number) in the space indicated.

But when it is, call BEI. We offer you the most complete line of accurate, high-reliability motion control components and systems anywhere in the world.

Standard and custom motion components from BEI are applied to advanced products in a broad variety of markets and industries. These include computer and office automation machines, light and heavy-duty industrial equipment, and the world's most accurate, high-resolution, and reliable components for space and military systems.

BEI Divisions are dedicated to being the best in their respective motion component specialties. Look to BEI for:

- Optical Rotary Encoders
- Brushless Motors, Actuators, Commutators and Drive Electronics
- Precision Servo Drives for Controlling Rate, Position, and Instrumentation Indexing
- Integrated Drive or Motion Control Assemblies

When accurate, reliable motion components are essential to your product or program, call BEI at (619) 931-1500. Or write to us at the address below.

BEI Motion Systems Company
2111 Palomar Airport Road • Suite 250 • Carlsbad, CA 92008

BEI

When reliable motion control is essential.

Circle Reader Action No. 337